

GALENA LEAD ISOTOPE STUDY OF MINERAL DEPOSITS IN THE
EAGLE BAY FORMATION, SOUTHEASTERN BRITISH COLUMBIA

by

FRANCOISE MELANIE GOUTIER

B.Sc UNIVERSITE DE MONTREAL, 1982

A THESIS SUBMITTED IN PARTIAL FULFILMENT OF

THE REQUIREMENTS FOR THE DEGREE OF

MASTERS OF SCIENCE

in

THE FACULTY OF GRADUATE STUDIES

DEPARTMENT OF GEOLOGICAL SCIENCES

We accept this thesis as conforming
to the required standard

THE UNIVERSITY OF BRITISH COLUMBIA

OCTOBER, 1986

@ Francoise Melanie Goutier, 1986

In presenting this thesis in partial fulfilment of the requirements for an advanced degree at the University of British Columbia, I agree that the Library shall make it freely available for reference and study. I further agree that permission for extensive copying of this thesis for scholarly purposes may be granted by the head of my department or by his or her representatives. It is understood that copying or publication of this thesis for financial gain shall not be allowed without my written permission.

Department of GEOLOGICAL SCIENCES

The University of British Columbia
1956 Main Mall
Vancouver, Canada
V6T 1Y3

Date Oct. 1988

ABSTRACT

The Eagle Bay Formation in the Adams Plateau-Clearwater area, 35km northeast of Kamloops, hosts several economic and sub-economic mineralized occurrences. The age and genesis of these mineral deposits can be estimated by using a specific growth curve which depicts the lead evolution for the Eagle Bay Formation. This curve, named the remodeled curve, represents a local deviation from the average 'shale' curve of Godwin and Sinclair (1982) for the autochthonous part of the Canadian Cordillera. This remodeled curve is specifically applicable to the Adams Plateau-Clearwater area. The lead isotope data from the deposits of the Eagle Bay Formation plot in three distinct clusters along the curve indicating that the lead isotopic signature of the Eagle Bay Formation is upper crustal, and that three periods of mineralization can be recognized or 'fingerprinted'. Accordingly, mineralization cogenetic with Devonian volcanism, and veins related to Cretaceous magmatism can be distinguished by location of galena-lead isotope values within clusters 1 or 3 respectively. Cluster 2 reflects a Late Triassic pulse of mineralization and includes epigenetic veins and stratiform deposits. These deposits are either replacement or cogenetic with their host. The Triassic model age for mineralization that is apparently stratiform and cogenetic raises questions about the currently assigned Cambrian age of

associated host rock. To accommodate the lead isotope data a new Upper Triassic unit (T-EBG) within the Eagle Bay Formation is defined.

The distinctive lead isotopic signature between deposits hosted by the Eagle Bay Formation is valuable as a guide for future mineral exploration programs in the Adams Plateau-Clearwater area. Recognition of lead isotopic fields that fingerprint types of mineral deposits, provides a useful and practical framework for the classification and evaluation of new mineralized prospects in the area.

Table of Contents

ABSTRACT	ii
LIST OF TABLES	vii
LIST OF FIGURES	viii
ACKNOWLEDGMENTS	ix
1. GENERAL INTRODUCTION	1
2. GENERAL GEOLOGY OF THE ADAMS PLATEAU- CLEARWATER AREA	4
2.1 INTRODUCTION	4
2.2 STRATIGRAPHY	9
2.3 INTRUSIONS	13
2.3.1 DEVONIAN INTRUSIONS	13
2.3.2 CRETACEOUS INTRUSIONS	14
2.3.3 LAMPROPHYRE DYKES	17
2.4 STRUCTURE	17
2.4.1 PRE-JURASSIC STRUCTURES	18
2.4.2 JURASSIC STRUCTURES	18
2.4.3 CRETACEOUS STRUCTURES	19
2.4.4 TERTIARY STRUCTURES	20
3. LEAD ISOTOPE SYSTEMATICS	22
3.1 HISTORY OF LEAD ISOTOPE INTERPRETATION	22
3.2 BASIC PRINCIPLES AND EQUATIONS	26
3.3 ANALYTICAL PROCEDURES	31

3.3.1	SAMPLE DESCRIPTION	31
3.3.2	ANALYTICAL PRECISION	31
3.3.3	CALCULATION OF AVERAGE VALUES FOR THE DEPOSITS	34
3.4	THE REMODELED CURVE FOR THE EAGLE BAY FORMATION	39
3.4.1	DEPARTURE TIME, INITIAL COMPOSITION AND U VALUE	47
3.4.2	W VALUE	51
3.4.3	SUMMARY	52
3.5	MODEL AGE DETERMINATION	53
4.	LEAD ISOTOPES, MINERAL DEPOSITS AND STRATIGRAPHY	55
4.1	INTRODUCTION	55
4.2	CLUSTER 1: DEVONIAN COGENETIC DEPOSITS	58
4.3	LEAD DATA BETWEEN CLUSTER 1 & 2	63
4.4	CLUSTER 2: TRIASSIC STRATIFORM AND VEIN DEPOSITS	64
4.4.1	DEPOSITS GEOLOGY	64
4.4.2	MULTIPLE INTERPRETATION OF LEAD DATA	70
4.4.3	SUMMARY	80
4.5	LEAD DATA BETWEEN CLUSTER 2 & 3	80
4.6	CLUSTER 3: CRETACEOUS VEINS	83

4.7	LEAD DATA BEYOND CLUSTER 3	87
4.8	SUMMARY	88
5.	CONCLUSIONS	90
REFERENCES CITED		93
APPENDIX A		103
APPENDIX B		147
APPENDIX C		149

LIST OF TABLES

TABLE 3.0 Equations used in lead isotopic model calculation	28
TABLE 3.1 Statistics related to the calculation of mass fractionation factors using Broken Hill Standard (BHS:UBC1)	33
TABLE 3.2 Representative calculation of average galena lead isotopic values for a given deposit	35
TABLE 3.3 Average galena lead isotope values for ore deposits in the Eagle Bay Formation	37
TABLE 3.4 Lead isotope values for the remodeled shale curve.....	48
TABLE 4.0 Classification and name of deposits within discrete clusters of data defined in Figures 3.3 to 3.5	56
TABLE A.1 Mineral deposits in the Adams Plateau area described in appendix A	104

LIST OF FIGURES

FIGURE 1.0 Generalized tectonic map of the Canadian Cordillera	2
FIGURE 2.0 Regional geologic map of the Adams Plateau-Clearwater area	5
FIGURE 2.1 Geology of the Eagle Bay Formation showing major rock units and faults	10
FIGURE 3.0 Model evolution of lead with time. A: Diagram $^{207}\text{Pb}/^{204}\text{Pb}$ vs. $^{206}\text{Pb}/^{204}\text{Pb}$ B: Diagram $^{208}\text{Pb}/^{204}\text{Pb}$ vs. $^{206}\text{Pb}/^{204}\text{Pb}$	23
FIGURE 3.1 Schematic evolution of the lead in galena from the Eagle Bay Formation	29
FIGURE 3.2 $^{207}\text{Pb}/^{204}\text{Pb}$ vs. $^{206}\text{Pb}/^{204}\text{Pb}$ diagram showing the isotopic distribution of all analyses from the Birk Creek area	36
FIGURE 3.3 $^{207}\text{Pb}/^{204}\text{Pb}$ vs. $^{206}\text{Pb}/^{204}\text{Pb}$ diagram for deposits hosted by the Eagle Bay Formation using data from Table 3.3	41
FIGURE 3.4 $^{208}\text{Pb}/^{204}\text{Pb}$ vs. $^{206}\text{Pb}/^{204}\text{Pb}$ diagram for deposits hosted by the Eagle Bay Formation using data from Table 3.3	43
FIGURE 3.5 $^{206}\text{Pb}/^{208}\text{Pb}$ vs. $^{206}\text{Pb}/^{207}\text{Pb}$ diagram for deposits hosted by the Eagle Bay Formation using data from Table 3.3	45
FIGURE 4.0 Geology of the Eagle Bay Formation with location of the sampled mineral deposits	59
FIGURE 4.1 Folded mineralized layers, Lucky Coon deposit	67
FIGURE A.1 Map of the Homestake property	121
FIGURE A.2 Lower hemisphere equal area projection of structural elements, Homestake deposit area	123
FIGURE A.3 Vertical section (97+00) through the RG 8 sulphide barite lens, Rea Gold deposit	126
FIGURE A.4 Equal area projections onto lower hemisphere of structural elements Rea Gold deposit	128
FIGURE A.5 Detailed sections A-A' and B-B' from the north side of Birk Creek area	131

ACKNOWLEDGEMENTS

I acknowledge the British Columbia Ministry of Energy, Mines and Petroleum Resources for financial support of field work. Many from the Ministry were helpful. I am particularly grateful to Trygve Hoy, with whom it was a pleasure to work, for his encouragement and supportive attitude, and to Paul Schiarizza for ideas and critical discussions which influenced my thinking throughout this research.

Sincere thanks are extended to my advisor Dr. C.I. Godwin for his direction, encouragement and supervision of my thesis, and to Dr. R.L. Armstrong for providing access to his Geochronological Laboratory at The University of British Columbia. I wish to thank all students, faculty and staff members in the department of Geological Sciences who contributed by their knowledge and friendship to the completion of this thesis.

I also thank Alex Davidson and Ian Pirie of Corporation Falconbridge Copper and Glen Shevchenko of Noranda Exploration Co. Ltd. for their availability and for discussing some aspects of this project with me. The information and galena samples they provided are greatly appreciated.

1. GENERAL INTRODUCTION

The Eagle Bay Formation is in the Adams Plateau-Clearwater area, centred 35km northeast of Kamloops in southeastern British Columbia (Fig. 1.0). The formation is a multiply-deformed sequence of low-grade meta-sediments and volcanic rocks stacked as imbricated slices on the southwestern flank of the Shuswap Metamorphic Complex. It hosts several economic and sub-economic lead-zinc-silver-gold occurrences of various types and affinities that were intermittently in production during the first half of the century. Recent discovery of the polymetallic Rea Gold deposit, a gold-arsenopyrite-rich volcanogenic Kuroko type deposit near Johnson Lake, regenerated interest in the area by providing evidence of potentially significant economic mineralization.

This thesis was initiated to assess whether galena lead isotope studies would aid interpretations of the nature and age of the different deposits occurring within the Eagle Bay Formation. It also was intended to provide a practical and useful framework for guiding exploration programs in the Adams Plateau-Clearwater area. Observations (and in some cases detailed mapping) were made on 37 mineralized occurrences which were sampled for this study (Appendix A). Field work was conducted over the summers of 1984 and 1985. Remains from past

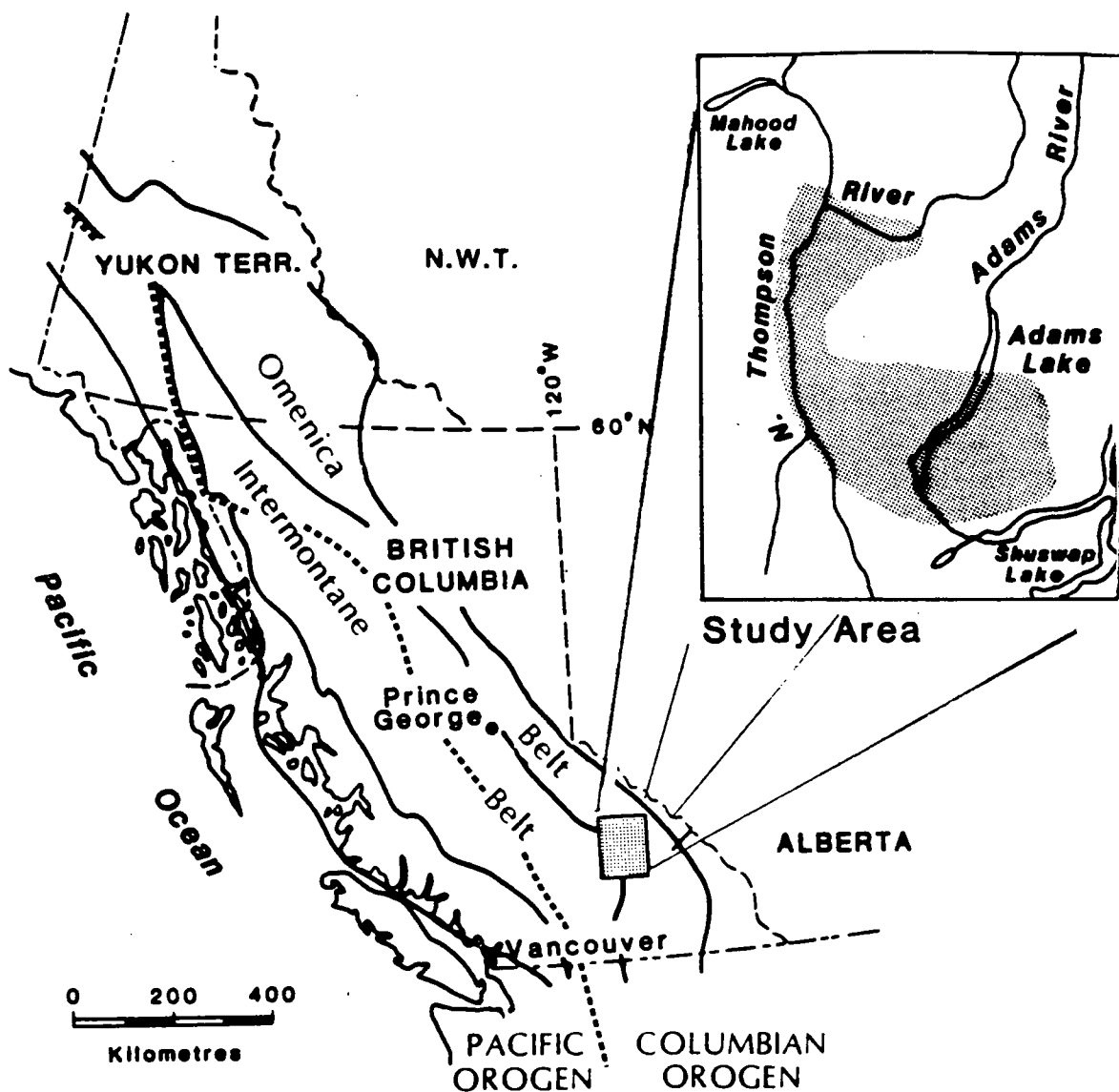


Figure 1.0. Generalized tectonic map of the Canadian Cordillera showing the major structural divisions and location of the study area (after Wheeler and Gabrielse, 1972).

mining activities and logging roads in the area facilitated access to the visited properties.

The first part of this study presents an overview of the geology of the Eagle Bay Formation and of adjacent areas. The second part outlines the basic principles which govern uses of the common lead method for model age determinations. A remodeled version of the 'shale' growth curve of Godwin and Sinclair (1982) is used to interpret the lead isotopic data from deposits hosted by the Eagle Bay Formation. The third part of this thesis interprets galena lead model ages of deposits defined by the remodeled curve. Implications of the clustering of the data into three distinct groups (Devonian, Triassic and mid-Cretaceous) are presented. The discrepancy between Triassic lead model age obtained for several stratiform deposits and their geological setting is discussed, and leads to the interpretation that if the mineralization is not of Triassic replacement type, but rather cogenetic with its host then the stratigraphy of the Eagle Bay Formation should include a Triassic unit. The results are fundamental to geological understanding and to mineral exploration in the Adams Plateau-Clearwater area.

2. GENERAL GEOLOGY OF THE ADAMS PLATEAU-CLEARWATER AREA

2.1 INTRODUCTION

Mineral deposits and occurrences in the Adams Plateau-Clearwater area are hosted by the Eagle Bay Formation, which is composed of a multiply deformed sequence of low-grade meta-sediments and volcanic rocks. The Eagle Bay Formation lies within Kootenay Terrane (Monger, 1985) along the western flank of the Monashee Terrane in the Omineca Belt (Fig. 2.0). The Eagle Bay Formation ranges in age from Cambrian to Permian (Schiarizza and Preto, 1984). However, as defined in this thesis it contains rocks that may be as young as Upper Triassic.

Much of the area adjacent to and east of the Eagle Bay Formation is called the Northwestern Shuswap Complex (Okulitch, 1984). This complex, along with the Monashee Complex (Read and Brown, 1981) and the Okanagan Plutonic and Metamorphic Complex, is part of the larger Shuswap Metamorphic Complex that currently is included in Monashee Terrane (Monger, 1985). The boundary between the Eagle Bay Formation and the Northwestern Shuswap Complex now is recognized to be a low angle detachment fault rather than a metamorphic or intrusive contact (Brock, 1934; Fyson, 1970). This fault, named the Eagle River fault in recent

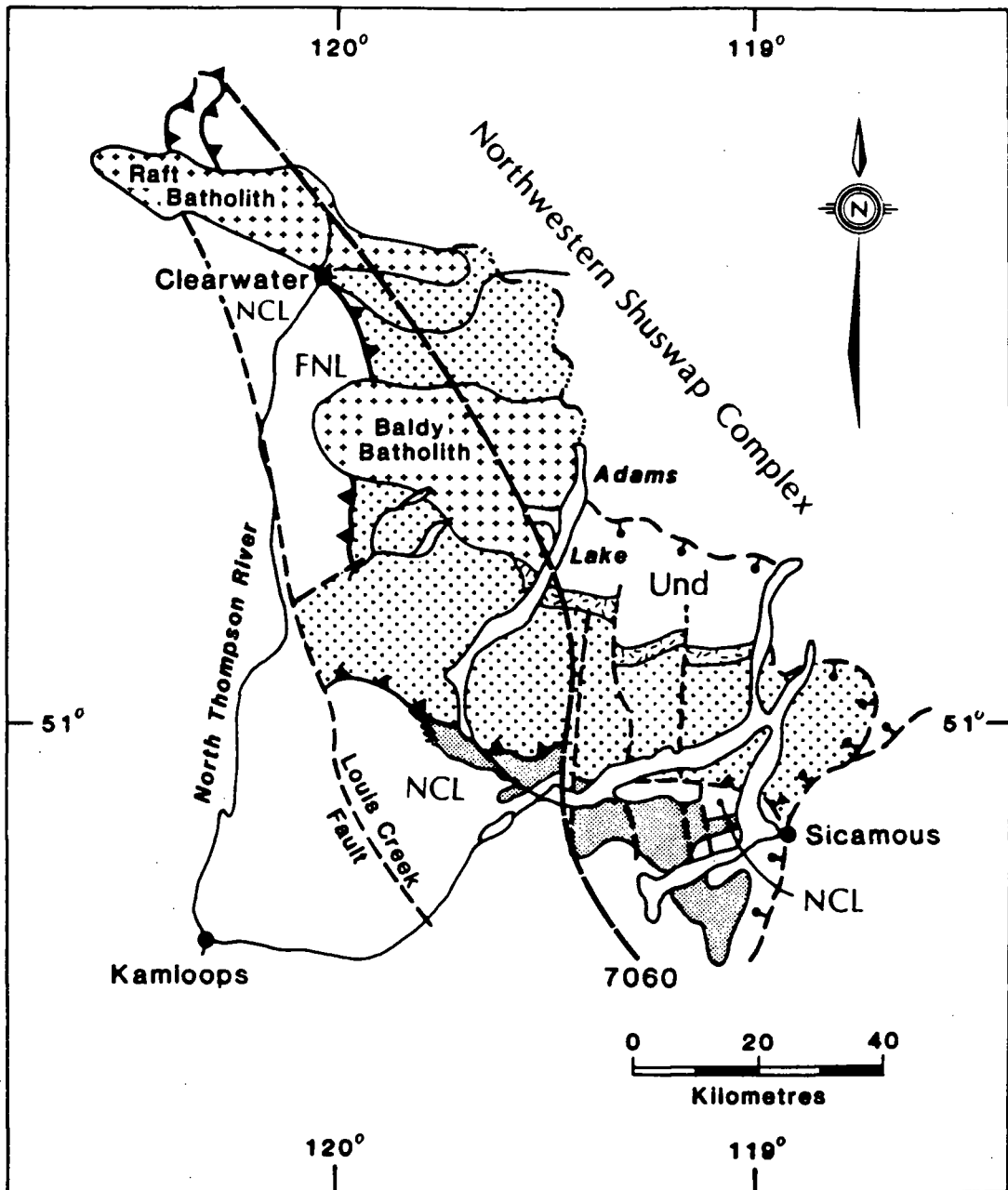


Figure 2.0 Regional geologic map of the Adams Plateau-Clearwater area showing the location of the Eagle Bay Formation relative to other major formations and groups, majors intrusions, and regionally important faults (modified: from Okulitch and Cameron, 1976; Journeay, 1986; Jung, 1986).

LEGEND

Jurassic & Cretaceous



Granitic rocks

Upper Triassic



Undiff. Nicola Group rocks

Upper Triassic and older



Eagle Bay Formation



Fennell Formation

Undetermined age



Sicamous Formation



Undiff. Paleozoic rocks



Undiff. Paleoz. intrusives

SYMBOLS



High angle faults



Eagle River Detachment



Quesnel Lake thrust



0.7060 initial $^{87}\text{Sr}/^{86}\text{Sr}$
ratio, isotopic contour line

mapping (Journey, 1986; Fig. 2.0), is interpreted as the break-away zone for the southern Okanagan detachment (Journey, 1986) and therefore is part of the major extensional fault system related to the Eocene thermal event identified in south-central British Columbia (Ross, 1974; Journey, 1986; Coney, 1980; Tempelman-Kluit, 1984; Bardoux, 1984; Parkinson, 1985; Parrish, 1985).

The Eagle Bay Formation is bordered on the west by the Fennell Formation of the Slide Mountain Group (Campbell and Tipper, 1971). The Fennell Formation is composed of an oceanic assemblage of pillowed basalts, diorite and ribbon cherts (Uglow, 1922). These two formations are separated by an easterly directed thrust fault (Okulitch, 1979; Schiarizza and Preto, 1984). To the south the formation is inferred to be in fault contact with the Upper Triassic(?) Sicamous Formation (Okulitch, 1984; Daughtry in Preto et al., 1985; see section 4.4.3). The formation is truncated to the north by the Raft batholith (Fig. 2.0).

Monashee Terrane (Monger, 1986) is exposed in a series of domal metamorphic complexes. Each is characterized by a core of older metamorphic plutonic basement, which either crops out or is covered by polydeformed and regionally metamorphosed mixed sequences of sedimentary and volcanic rocks (Brown and Read,

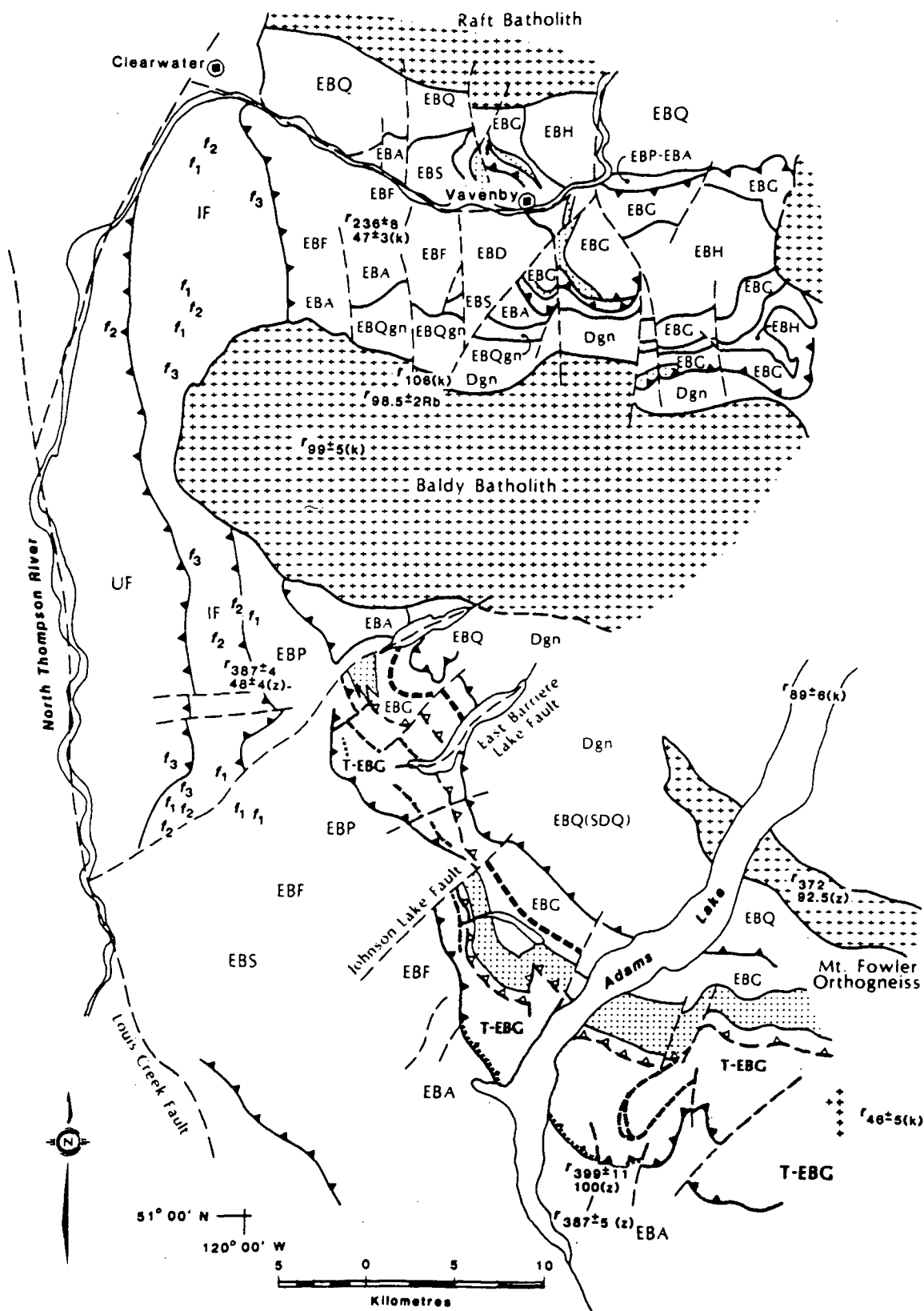
1983; Coney, 1980). Rocks within the complexes range in age from possibly Archean to earliest Jurassic (Duncan, 1982; Okulitch, 1984). The Shuswap Metamorphic Complex is regarded as the core zone of the Columbian Orogeny which caused major deformation in the Omineca Belt--and in the Eagle Bay Formation--during Jurassic time (Reesor and Moore, 1970; Okulitch, 1984). Unambiguous evidence for pre-Jurassic deformation in the belt is lacking, although some of the structures may have been generated in previous orogenies such as Kenoran, the Hudsonian, or the East Kootenay (Okulitch, 1979).

Evidence of a major Eocene thermal and extensional event is widespread throughout the Intermontane and Omineca Belts. Parrish (1985) argues that the unroofing of metamorphic core complexes is primarily a result of Tertiary extensional tectonics, rather than of Mesozoic compression as suggested by Brown and Read (1983). Thus, the Eagle Bay and the Fennell Formations, as well as the Raft and the Baldy batholiths, would have been located above the Monashee Complex at the time of their formation and would have slid off the metamorphic complex approximately 50Ma ago. The Eagle River detachment fault zone (Journeay, 1986; Fig. 2.0), and numerous normal faults of Tertiary age and related Tertiary volcanic rocks (Schiarizza, 1985; Hickson, 1986) are also attributed to the Eocene thermal and deformational event. However problems arise when the

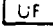
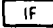
initial $^{87}\text{Sr}/^{86}\text{Sr}$ ratios of the Raft and the Baldy batholiths are taken into account. Values considerably higher than those present, ranging from 0.7083 to 0.7101, are to be expected from intrusions that pass through the Monashee Complex during their ascent. Therefore, Jung (1986) argues that the present position of the Raft and Baldy batholiths correspond to their original emplacement position, and that it is improbable that they ever were located over the Monashee Complex. This argument is also in agreement with the interpretation of Okulitch (1979) that the roots of the batholiths are in the Northwestern Shuswap Complex.

2.2 STRATIGRAPHY

The Eagle Bay Formation was first mapped by Dawson (1898) as the Adams Lake and Nisconlith Series. Subsequently Daly (1915) divided the Adams Lake Series into three informal formations called the Adams Lake greenstone, the Tshinakin limestone, and the Bastion schists. Rice and Jones (1948) and Jones (1959) renamed many of the rocks previously included in the above series, and defined the Mount Ida Group within which the Eagle Bay Formation was the youngest conformable member. The Eagle Bay formation then included much of Dawson's Adams Lake Series and Daly's (1915) greenstone formation; it contained three members: a thick basal succession of chloritic schist, a mixed sedimentary sequence including the prominent Tshinakin



Devonian to Permian**Fennell Formation**

-  **UF** Upper structural division: pillowed and massive meta-basalt, minor chert
-  **IF** Lower structural division: pillowed and massive meta-basalt and ribbon chert, limestone, diorite, gabbro, quartzfeldspar, porphyry, rhyolite

Mississippian

-  **EBP** Phyllite and slate with interbedded sandstone and grits


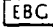





Devonian and/or Mississippian

-  **EBF** Feldspathic phyllite (intermediate to felsic tuff)



Devonian

-  **EBA** Sericite-quartz-phyllite and schist (intermediate to felsic volcanics and volcanoclastics)

Devonian and/or older

-  **EBS** Mixed meta-sedimentary sequence (phyllites)
-  **EBC** Calcareous chlorite-schist, fragmental schist (mafic to intermediate volcanics)
-  Tshinak limestone
-  mixed phyllite (EBCp)
-  quartzite (EBCq)
-  polymictic conglomerate (EBCcg)
-  T-EBG (? Triassic)

Lower Cambrian and/or older

-  **EBQ** Chlorite-muscovite quartzite, chlorite-muscovite-quartz schist and minor meta-sediments (SDQ)
-  **EBH** Quartzite, grit and chlorite-sericite-quartz schist

Intrusives**Jurassic & Cretaceous**

-  Raft batholith, Baldy batholith, Scotch Creek plug

Late Devonian


-  **Dgn** Granite and granodiorite orthogneiss

f₁, 2, 3 Fossil locality: Mississippian, Pennsylvanian, Permian

f Cambrian

k, z, Rb Isotopic date: K/Ar, uranium-lead, Rb/Sr

 Faults

 Thrust fault (this study)


 Thrust fault (Schiarizza et al, 1984)

Figure 2.1 Geology of the Eagle Bay Formation showing major rock units and faults (modified from Schiarizza and Preto, 1984).

Limestone, and an upper sequence of chloritic schist. Subsequent work by Campbell and Tipper (1971), Okulitch (1979), Schiarizza and Preto (1984), Preto and Schiarizza (1985), and Schiarizza (1986, 1986b) refined the understanding of the stratigraphy of both the Eagle Bay Formation and the adjacent Fennell Formation. Recent work by Preto and Schiarizza (1985) indicates that the Eagle Bay Formation is exposed in four imbricated slices separated by southwesterly directed thrust faults (Fig. 2.1; Schiarizza and Preto, 1984; Schiarizza, 1986b). Stratigraphic ages and/or contact relationships established by Schiarizza and Preto (1984) have been modified to accommodate results obtained from the lead isotope investigation of mineral deposits occurring throughout the Eagle Bay Formation. Discussion of the lead isotopic composition from these deposits, and their implications on the interpretation of the stratigraphy of the Eagle Bay Formation are presented in Chapter 4.

Eagle Bay Formation is directly correlative with other stratigraphic sequence occurring on the edge of the Shuswap Metamorphic Complex. Okulitch (1979) has correlated the Formation partly with the Cambrian to Ordovician Lardeau Group, and partly with the younger Milford Group of the Kootenay Arc. Struik (1986), based on lithologic, structural and age similarities, correlates the Eagle Bay Formation with both the Barkerville and the Kootenay Arc Terranes. Similarly, Ross and

Fillipone (in press) suggest that some parts of the Eagle Bay Formation, notably the basal quartzite and the prominent meta-volcanic carbonate succession, are directly correlated with similar rocks in the Snowshoe Group near Crooked Lake (100km east of Williams Lake). Struik (1986) proposed that all three successions were deposited in a similar geological setting. Accordingly, the Eagle Bay Formation is now included by Monger (1985) in the Kootenay Terrane under "variably metamorphosed Lower Paleozoic strata comprising pellicite, quartzite, grits, basic acidic rocks and Devonian and (?) older intrusions."

2.3 INTRUSIONS

The Eagle Bay Formation has been intruded repeatedly. Magmatism and/or volcanism affected the area in Devonian, Cretaceous and Eocene time.

2.3.1 Devonian Intrusions

Meta-biotite granodiorite, correlated with the Mount Fowler orthogneiss (Fig. 2.1), intrudes Devonian volcanic rocks of the Eagle Bay Formation. Zircons from the batholith yielded upper and lower intercept dates on concordia diagrams of Devonian and of mid-Cretaceous ages (372 ± 6 Ma and 92.5Ma: Okulitch, 1975). Similar bodies of intermediate to felsic composition, ranging in age from Late Devonian to mid-

Mississippian (Mortensen et al., in press), occur throughout the Snowshoe meta-sediments in the Barkerville Terrane. The presence of these intrusions in both the Eagle Bay Formation and the Snowshoe Group do not prove, but support correlations between these two successions in regionally distinct areas.

An extrusive phase of similar composition (meta-rhyolite) found on the Beca property also yielded zircon dates of Devonian age, 399 ± 11 Ma, from the upper intercept on a concordia diagram (Preto and Schiarizza, 1985). The similarities in age and rock type between the Mt Fowler orthogneiss, the felsic intrusions, and some of the meta-volcanics (e.g. unit EBA, Fig. 2.1) suggest that they are cogenetic and of Devonian age. The occurrence of these volcanic and intrusive rocks of felsic affinities on the western margin of the Shuswap Complex and the presence of volcanogenic deposits within the Devonian volcanic units (Rea Gold and Homestake deposits, Appendix A), provides evidence for subduction related processes during the Devonian.

2.3.2 Cretaceous Intrusions

The Raft and Baldy batholiths are elongated bodies that intrude the Eagle Bay Formation (Fig. 2.1). In several localities, both batholiths are surrounded by a structural and metamorphic hornfelsic aureole in which regional structures are rotated parallel to the westward trend of the intrusions

(Campbell and Tipper, 1971).

Small intrusive bodies, such as the Scotch Creek and the Deep Creek plutons as well as quartz porphyry dykes or sills, occur throughout the area (Fig. 2.1). They are inferred to be cogenetic with the Cretaceous Baldy batholith.

Both intrusions, are equigranular granodiorite to quartz monzonite and are similar chemically. They contain chloritized biotite as the only mafic mineral. Widespread minor concentrations of sulphide minerals within the intrusions include the galena-sphalerite rich quartz veins of the Leemac property (Appendix A), and several molybdenite occurrences in the Barriere Lake area reported in unpublished provincial open file reports available at the British Columbia Ministry of Energy, Mines and Petroleum Resources.

Cretaceous Rb/Sr dates were obtained for the two batholiths by Jung (1986) with a five point whole rock and mineral separate isochron. A mid-Cretaceous date of 104Ma with an initial $^{87}\text{Sr}/^{86}\text{Sr}$ ratio of 0.7060 was obtained from a sample from the western part of the Raft batholith. A mid-Cretaceous date of 98.5 ± 2.2 Ma with initial $^{87}\text{Sr}/^{86}\text{Sr}$ ratio of 0.7054 was obtained for the Baldy batholith. These similar dates and initial ratios, plus the similarity in texture and composition

indicate that the two batholiths are probably cogenetic. Furthermore two K-Ar mid-Cretaceous dates of 99 ± 5 Ma and 82 ± 6 Ma were obtained by Wanless et al. (1966) for the Baldy batholith. Since the K-Ar dates are concordant with the Rb-Sr dates, the batholiths were probably not substantially affected by any later thermal events. However, incomplete new uranium-lead data on zircons from the Raft batholith indicates some uncertainty in its assigned mid-Cretaceous crystallization age (Jung, pers. comm., 1986).

The initial $^{87}\text{Sr}/^{86}\text{Sr}$ ratios of about 0.7060 for the Raft and Baldy batholiths are higher than those below 0.7040 from batholiths located to the west in the Intermontane Belt. Values comparatively greater than 0.7060 are reported to the east in the Shuswap Metamorphic Complex (Jung, 1986). The initial strontium isotope ratio of 0.7060 passes through the Eagle Bay Formation as shown on Figure 2.0. This line probably represents a transition at depth corresponding to the western limit of Precambrian basement rocks (Armstrong, in Jung, 1986). The relatively high initial $^{87}\text{Sr}/^{86}\text{Sr}$ ratios for the Raft and Baldy batholiths emphasize a genetic link between the magma and the old crustal material from which these batholiths were derived. The high ratios apparently reflect the addition of radiogenic ^{87}Sr from magma generated in, or contaminated by, a Precambrian basement underlying the Eagle Bay Formation. The initial

strontium ratios are in general agreement with the lead isotopic signature of the deposits in the Eagle Bay Formation--both indicate the presence of upper crustal material beneath the formation.

2.3.3 Lamprophyre Dykes

Lamprophyre dykes are widely distributed in the Adams Plateau-Clearwater area, and commonly are noted on properties where sulphide mineralization is reported (see description in Appendix A for Mosquito King, Crowfoot Mountain, and Rexspar). These dykes commonly occur along northerly trending faults and several have yielded mid-Eocene dates (dates by the Geological Survey of Canada are summarized in Jung, 1986). The relationship between these dykes and sulphide mineralization is discussed in Chapter 4.

2.4 STRUCTURE

The Eagle Bay Formation is complexly deformed. Timing relationships often are neither clear nor consistent, although it is generally agreed that all the stratified units were deformed (or re-deformed) during the Jurassic folding event related to the Columbian Orogeny (Campbell, 1973). This orogeny, associated with the accretion of a western allochthonous terrane against the Omineca belt and the craton (Monger et al., 1982), produced a pervasive foliation and

southwesterly directed thrust faults. The Eagle Bay Formation subsequently was deformed and refolded by northwesterly trending folds associated to the intrusion of the Raft and Baldy batholiths in the mid-Cretaceous. Later northeasterly trending strike-slip faults, as well as northerly striking normal faults, cut through the major units and structures of the formation.

2.4.1 Pre-Jurassic Structures

The first deformation of the Eagle Bay Formation may be as old as Early Devonian as indicated by the presence of an early metamorphic foliation, which is axial planar to very rare, small isoclinal folds (Schiarizza, 1986). However, direct evidence of such a deformational event has been masked by subsequent deformation and regional metamorphism.

Juxtaposition of the Fennell and the Eagle Bay Formations resulted from easterly directed thrusts. This thrusting event was post mid-Permian, since conodont bearing strata of mid-Permian age are repeated by the thrusts. Thrusting was also earlier than Jurassic because the thrusts are folded by structures related to the Jurassic Columbian Orogeny (Schiarizza and Preto, 1984).

2.4.2 Jurassic Structures

Units of the Eagle Bay Formation exhibit evidence of syn-metamorphic deformation characterized by: 1) pervasive shistosity sub-parallel to the original bedding and axial planar to isoclinal folds that verge westward, and 2) lack of continuity of the units along strike due to shearing that caused transposition of the layering and disruptions of isoclinal folds (Dickie, 1985). The Nikwikaia Lake synform on the Adams Plateau (Fig. 2.1) is a large westerly trending fold related to this deformation. Redistribution of sulphide masses in the crests of folds in deposits in the synform area (Appendix A: Lucky Coon, Elsie, King Tut) is probably related to this event (Fig. 4.1).

A southwesterly directed thrusting event established the present configuration of the units by creating major imbricated panels within the Eagle Bay Formation (Fig. 2.1). This thrusting probably occurred near the end of the Colombian Orogeny

2.4.3 Cretaceous Structures

A prominent upright, easterly oriented set of folds, well exposed in the vicinity of the Raft and the Baldy batholiths, is related to the presence of the mid-Cretaceous intrusions. The best examples of this phase of folding are exposed in the Clearwater area where intrusions locally change

the predominantly northerly dip direction of bedding and shistosity (Schiarizza, 1986). On the Adams Plateau, outcrop scale folds have the same easterly orientation; these folds probably were generated during or soon after the intrusive event.

Northeasterly trending strike-slip faults, such as the Barriere Lakes and Johnson Creek fault (Fig. 2.1), cut the Eagle Bay Formation and the Fennell Formation and account for some major stratigraphic truncations. In the Scotch Creek area, some of these faults were intruded by Cretaceous porphyry dykes and plugs. However, in other places similar faults extend into the Baldy batholith indicating that this faulting is Cretaceous or younger.

2.4.4 Tertiary Structures

The youngest phase of deformation, affecting both the Eagle Bay Formation and the adjacent Fennell Formation, is of Eocene age and is characterized by open, northerly plunging folds with upright axial planes. This deformation is responsible for regional warping of previous structures, such as the folding of the axial surface trace of the Nikwikaia Lake synform. The orientation of this set of folds is similar to the orientation of a set of normal faults that cut all units of the Eagle Bay Formation. These faults do not cut the overlying

Miocene basalts; they locally are intruded by Tertiary basaltic and/or lamprophyre dykes. These structures probably are related to the Tertiary extensional and thermal event.

3. LEAD ISOTOPE SYSTEMATICS

3.1 HISTORY OF LEAD ISOTOPE INTERPRETATION

Houtermans (1946) and Holmes (1946) were among the first to tackle the concept of addition of radiogenic lead, derived from radioactive decay of uranium and thorium, to primeval lead and independantly derived the fundamental equations which govern the increase of radiogenic lead over time. The evolution of lead with time in source regions characterized by different uranium and thorium contents are depicted in Figure 3.0. With the increase of available data inadequacies in the model were highlighted and the term 'anomalous lead' was introduced to categorize ore lead data which gave negative or excess model ages. Nevertheless, aside from anomalous lead, the isotopic composition of lead from several conformable ore deposits of various ages were used to construct a growth curve for conformable ore lead. Stanton and Russell (1959), therefore proposed that this curve represented the development of isotopic composition of deposits derived from a nearly homogenous source, the upper mantle, which had maintained an almost constant U/Pb and Th/Pb ratio since the formation of the earth. A summary paper (Kanasecwich, 1968) reviewed the the principles and the applicability of lead isotope models as known in the late 1960's.

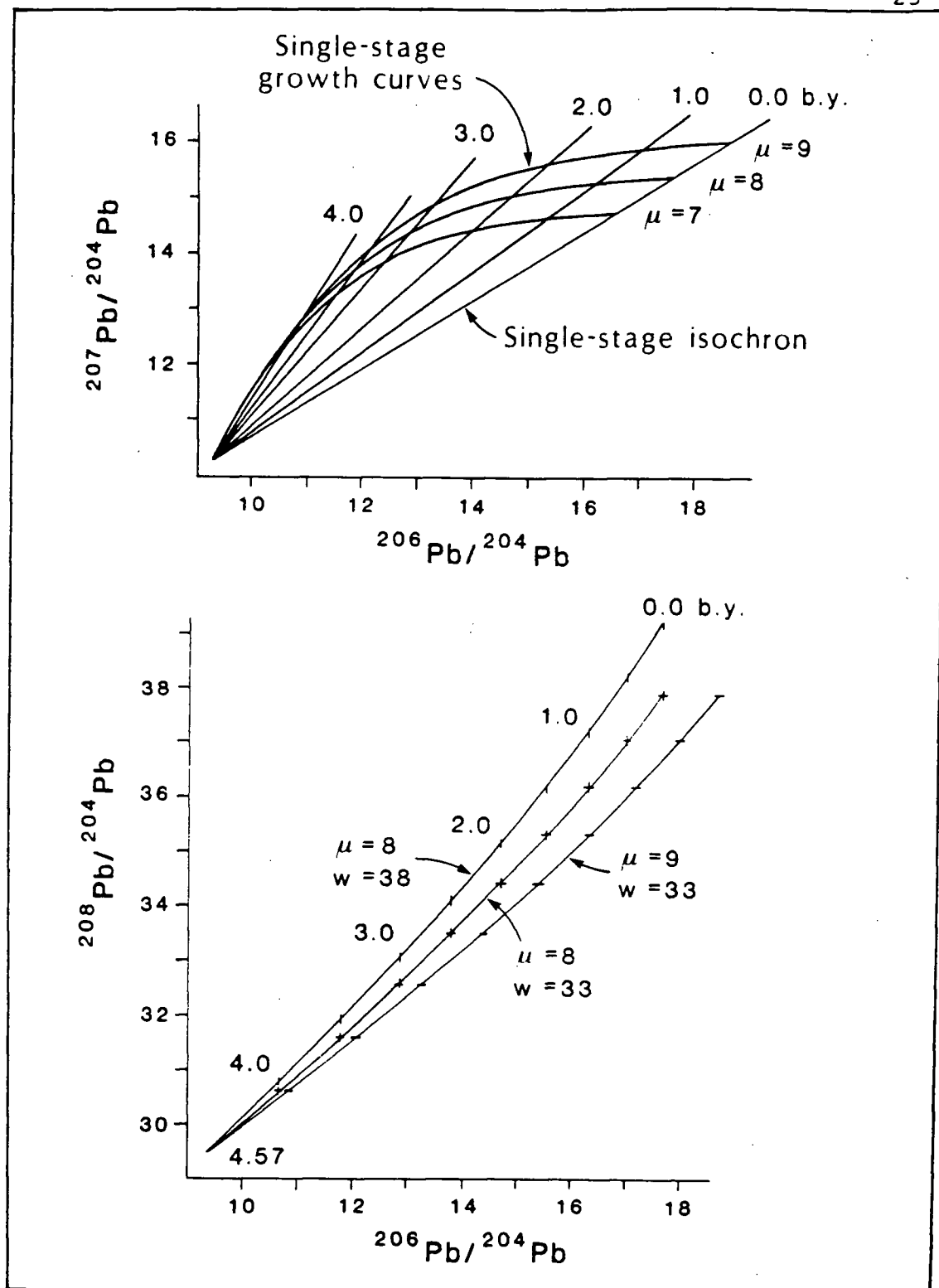


Figure 3.0 Model evolution of lead with time (from Koppel and Grunefelder, 1979). A: Diagram $^{207}\text{Pb}/^{204}\text{Pb}$ vs. $^{206}\text{Pb}/^{204}\text{Pb}$ showing single-stage growth curves with μ as a parameter and single-stage isochrons. B: Diagram $^{208}\text{Pb}/^{204}\text{Pb}$ vs. $^{206}\text{Pb}/^{204}\text{Pb}$ showing single-stage growth curves with μ and w as parameters.

Refinements of the parameters used to calculate the growth curve (decay constants for U and Th, isotopic composition of primeval lead, etc.) as well as improvement in lead chemistry and analytical methods, resulted in the recalibration of the curve in the late 1960's (Stacey et al., 1969, Cooper et al., 1969). The effects of new decay constants on calculated model ages were reviewed by Oversby (1974). These modifications emphasized the deviations of the data from a single stage curve, and demonstrated the inadequacy of such curve in characterizing the evolution of ore lead through time.

Several mathematical models, involving mixing of different environments and multi-stage growth, were then devised to simulate average lead isotope evolution curves that fitted the data more closely. Doe and Stacey (1974) changed the parameters related to the age of the earth used in their calculations and explained the departure from single stage conditions by the mixing of several isotopic heterogeneous source materials. Stacey and Kramers (1975) established a two-stage model in which the departure of the second stage curve at 3.7Ga corresponded apparently to a time of major crustal differentiation, and generation of an uranium-enriched and of an uranium-depleted environment. Cumming and Richards (1975) gave an alternative interpretation to the sudden episodic model espoused by Stacey

and Kramers (1975) by presenting a continuous evolution model in which U/Pb and Th/Pb ratios constantly increased in the source material for conformable ore.

Following development of these empirical models, Doe and Zartman (1979), following Armstrong (1968) and Armstrong and Hein (1973), presented the plumbotectonic model that incorporated, by means of computer modeling, geological processes related to plate tectonic concepts with lead evolution systematics. Their idealized model furnished a more global approach to lead evolution by simulating mixing between various distinct environments--each characterized by different concentrations and proportions of U, Th and Pb. These environments existed long enough to produce marked differences in lead evolution with time.

Subsequently, Godwin and Sinclair (1982) constructed the 'shale' growth curve that was specifically applicable to the autochthonous portion of the Canadian Cordillera characterized by high U/Pb and Th/Pb ratios. This part of the Cordillera is upper crustal in lead isotope character as defined by Doe and Zartman (ibid.).

This study used a remodeled 'shale' growth curve (cf. Godwin and Sinclair (1981; 1982) to obtain a better fit with the

lead data on galena from deposits in the Eagle Bay Formation. The reasons for these changes are discussed in section 3.4.

3.2 BASIC PRINCIPLES AND EQUATIONS

The wide range in lead isotopic ratios related to time and geological setting and geochemical cycles of lead, uranium and thorium provide a useful method for estimations of the age and conditions of formation for ore material. The common lead method is based upon measurement of lead that has evolved through time in one or in successively closed systems or environments. It is assumed that these environments, characterized by distinct U/Pb and Th/Pb contents, and broadly corresponding to a major source or reservoir for magma generation (e.g. upper mantle or crust), have undergone an isolated evolution for a sufficient length of time to acquire a specific isotopic signature before mixing occurs between them. The transfer of lead from one system to another generally implies active geological processes (orogenic episodes, formation of new crustal segments, etc.) characterized by a change in the U/Pb and the Th/Pb ratio due to the preferential affinities of uranium and thorium to upper crustal rocks compared to depletion in environments involving mantle and/or lower crustal materials.

Age determinations on galena using the common lead method rely on the measurement of lead produced from uranium isotopes (^{206}Pb , ^{207}Pb), and from the thorium isotope (^{208}Pb) decay. Galena is used because after crystallization its lead isotopic composition is 'frozen' due to the absence of radioactive elements in its structure. The amount of radiogenic component of a sample is computed and expressed as the ratio of the radiogenic lead over ^{204}Pb , whose natural abundance does not change with time. The $^{206}\text{Pb}/^{204}\text{Pb}$, $^{207}\text{Pb}/^{204}\text{Pb}$, $^{208}\text{Pb}/^{204}\text{Pb}$ ratios will therefore increase with time from their initial ratios from the decay of uranium and thorium.

The rate of decay and production of the radiogenic isotope is governed by the half-life of each parent isotope and the parent abundance. The time taken for the ^{238}U to decay into ^{206}Pb is about the same as the age of the earth; thus about half of the ^{238}U isotope has decayed since the earth formed. The half-life of ^{235}U is considerably shorter; accordingly about 75% of the primordial ^{235}U isotope had decayed to ^{207}Pb by 3.0Ga (Doe, 1970); and subsequent generation of ^{207}Pb is small. This difference in the rate of isotopic production of lead from these two isotopes over time is reflected by the smooth flattening of the isotopic growth curve toward younger ages (Fig. 3.0).

Model ages can be calculated from measured isotopic ratios

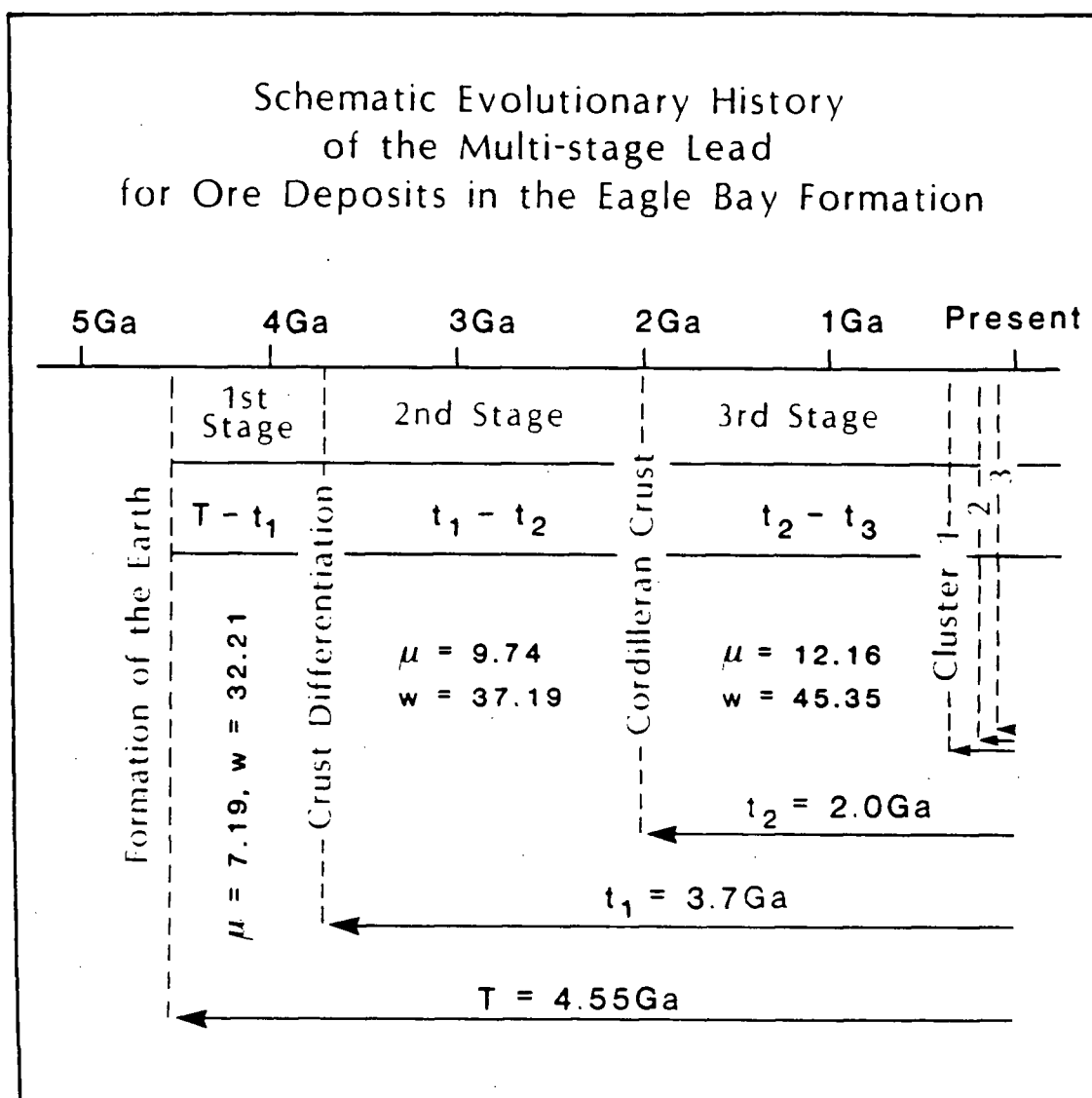


Figure 3.1 Schematic evolution of the lead in galena from the Eagle Bay Formation is as follows (modified from Faure, 1977): system 1 starts T years ago and exists for a period of time equal to $T - t_1$. At t_1 the lead is transferred to system 2 and continues to evolve during interval $t_1 - t_2$. At time t_2 the lead is transferred to system 3 and resides there for $t_2 - t_3$ years. At t_3 the lead is withdrawn and fixed in galena--an environment containing no uranium or thorium--so that between t_3 and present no further isotopic evolution occurs.

Table 3.0 Equations used in lead isotope model calculation.

$$\begin{aligned}
 1 \quad & ({}^{206}\text{Pb}/{}^{204}\text{Pb})_t = ({}^{206}\text{Pb}/{}^{204}\text{Pb})_0 + \mu (e^{\lambda_8 T} - e^{\lambda_8 t}) \\
 2 \quad & ({}^{207}\text{Pb}/{}^{204}\text{Pb})_t = ({}^{207}\text{Pb}/{}^{204}\text{Pb})_0 + \frac{\mu}{137.88} (e^{\lambda_5 T} - e^{\lambda_5 t}) \\
 3 \quad & ({}^{208}\text{Pb}/{}^{204}\text{Pb})_t = ({}^{208}\text{Pb}/{}^{204}\text{Pb})_0 + W (e^{\lambda_2 T} - e^{\lambda_2 t}) \\
 & ({}^{206}\text{Pb}/{}^{204}\text{Pb})_0 = a_0 = 9.307 \quad \text{primordial lead (= Pb isotopic composition)} \\
 & ({}^{207}\text{Pb}/{}^{204}\text{Pb})_0 = b_0 = 10.294 \quad \text{at time T)} \\
 & ({}^{208}\text{Pb}/{}^{204}\text{Pb})_0 = c_0 = 29.479 \quad (\text{Tatsumoto et al., 1973})
 \end{aligned}$$

T = age of the Earth (calculated with the new decay constants) = 4.57 b.y. (Tilton, 1973).

$$\frac{({}^{207}\text{Pb}/{}^{204}\text{Pb})_t - b_0}{({}^{206}\text{Pb}/{}^{204}\text{Pb})_t - a_0} = \frac{1}{137.88} \times \frac{(e^{\lambda_5 T} - e^{\lambda_5 t})}{(e^{\lambda_8 T} - e^{\lambda_8 t})}$$

This is the equation of a straight line, the so-called isochron.

$$\frac{{}^{207}\text{Pb}}{{}^{204}\text{Pb}_t} = b_0 + \frac{1}{137.88} \times \frac{(e^{\lambda_5 T} - e^{\lambda_5 t})}{(e^{\lambda_8 T} - e^{\lambda_8 t})} \times \left[\frac{{}^{206}\text{Pb}}{{}^{204}\text{Pb}_t} - a_0 \right]$$

$$\begin{aligned}
 \mu &= {}^{238}\text{U}/{}^{204}\text{Pb} \\
 W &= {}^{232}\text{Th}/{}^{204}\text{Pb}
 \end{aligned}$$

$\lambda_8, \lambda_5, \lambda_2$: decay constants of ${}^{238}\text{U}$, ${}^{235}\text{U}$, and ${}^{232}\text{Th}$ respectively.

(see Steiger and Jäger, 1977: Sub-commission on Geochronology: Convention on the use of uniform decay constants in geo- and cosmochronology; EPSL, 36, 359-362).

The recommended constants are:

$$\begin{aligned}
 \text{Uranium:} \quad & \lambda ({}^{238}\text{U}) = 1.55125 \times 10^{-10}/\text{y} \\
 & \lambda ({}^{235}\text{U}) = 9.8485 \times 10^{-10}/\text{y} \\
 & \text{atomic ratio } {}^{238}\text{U}/{}^{235}\text{U} = 137.88
 \end{aligned}$$

$$\text{Thorium:} \quad \lambda ({}^{232}\text{Th}) = 4.9475 \times 10^{-11}/\text{y}$$

of galena by solving equations 1 to 3 for t_2 in Table 3.0. To use these equations the number, and characteristics of each successive environment from which lead was derived must be known or approximated. Change of U/Pb and Th/Pb, due to fractionation in the environment from which galena was generated, is assumed to be negligible. Furthermore any model age should be interpreted within a known geologic and tectonic framework. This is because the isotopic composition of galena is directly related to the time and type of mineralizing process which formed the galena. In some cases the lead system can also be disturbed by subsequent events; marked radiogenic enrichment in vein deposits has been observed (Russell and Farquhar, 1960; Watson, 1981), and signs of re-equilibration of the isotopic composition of galena due to metamorphism have been reported in several studies (Cumming and Gurchurdis, 1973; Richards, 1981; Brevart et al., 1982).

Evolution of the lead in the deposits hosted by the Eagle Bay Formation follows a multi-stage history schematically depicted in Figure 3.1. The first two stages of the lead evolution are assumed to have followed the Stacey and Kramers (1975) model, in which the lead developed initially from a primeval composition (inferred to be that of troilite lead, Tatsumoto et al., 1973) at time T established at 4.57Ga, followed by a second stage that started at 3.7Ga with higher u

and w values--departure of the second stage corresponds to the approximate age for the isolation of the lower mantle from the mixing system. The last stage of the lead evolution for the deposits of the Eagle Bay Formation is approximated by the 'shale' curve of Godwin and Sinclair (1982). This last stage, however, appears to more closely model the lead evolution in the Eagle Bay Formation when it is anchored to the Stacey and Kramers (1975) curve at 2.0Ga. Construction of the remodeled curve is developed in section 3.4.

3.3 ANALYTICAL PROCEDURES

3.3.1 Sample Description

Ore samples were collected from 37 deposits and mineralized occurrences listed in Table 4.1 and described in Appendices A and C. All samples were selected from sulphide rich horizons and/or from cross-cutting mineralized structures. In several deposits both massive ore and vein mineralization were sampled to determine the effects of different types of occurrence on isotopic composition. All the lead analysed was extracted from hand picked galena and prepared according to the methods described in Appendix B.

3.3.2 Analytical Precision

Lead isotopic ratios were measured on a VG Isomass 54R

solid source mass spectrometer interfaced with a HP-85 computer in the Geochronology Laboratory of R. L. Armstrong at The University of British Columbia. Several blocks of data were routinely taken for each sample load. The reported results (Appendix C) represent the normalized mean of these data. Within run precision, expressed as the percentage standard deviation, is usually better than 0.05%. Repeated measurement of Broken Hill Standard (BHS-UBC1) and analyses of duplicates (Appendix C) monitored the analytical precision of the runs. Thirteen determinations of BHS-UBC1, made during the course of this study, were added to 35 previously obtained values to compute the average ratio given in Table 3.1. An empirical mass fractionation correction factor was calculated using accepted values for BHS-UBC1 established by Richards (1981). This factor was used to normalize the isotopic ratios of all analyses.

The maximum variation observed in duplicate analysis is less than 1.0%. The averaged differences between the two sets of values are 0.023, 0.019 and 0.054 for the $^{206}\text{Pb}/^{204}\text{Pb}$, $^{207}\text{Pb}/^{204}\text{Pb}$ and $^{208}\text{Pb}/^{204}\text{Pb}$ ratios respectively. Paired-t test conducted on the duplicate analyses established with 95% confidence that no systematic bias exists between the different sets of duplicate analysis. However, even under optimal conditions errors arise from fractionation processes (which

TABLE 3.1: Statistics related to the calculation of mass fractionation factors
using Broken Hill Standard (BH6-UBC1).

	Lead Isotope Ratios									
	206/204	abs ±	207/204	abs ±	208/204	abs ±	206/207	abs ±	206/208	abs ±
Maximum	15.962	0.007	15.324	0.005	35.453	0.056	1.042307	0.020002	0.490814	0.000705
Minimum	15.941	0.001	15.300	0.000	35.369	0.002	1.041436	0.000014	0.448946	0.000009
Average (n=46)	15.950	0.003	15.311	0.002	35.413	0.010	1.041732	0.001330	0.490409	0.000089
Std. Dev.	0.0053		0.0060		0.0021		0.000019		0.000017	
% Std. Dev.	0.033		0.039		0.005		0.002		0.004	
BH6-UBC1	16.004		15.390		35.651		1.039886		0.448907	
Error	0.001		0.007		0.007		0.007		0.018	
Corr. Fact	1.003377		1.005149		1.006734		0.998237		0.996661	
Precision	0.000112		0.000205		0.000121		0.000013		0.000061	

1. BH6-UBC standard values from double spike analyses reported by Richards 1981.

cause preferential depletion of elements), and from error in the measurement of the low intensity ^{204}Pb peak. The combination of these errors generates a spread in the values. Isotopic fractionation, the main source of variations in single filament isotopic determinations (Cooper and Richards, 1966; Ozard and Russell, 1970), is mass-dependent and results in the displacement of a point from its true value along a line with slopes that correspond to the product of coordinate ratio times the ratio of the respective mass difference--e.g. a slope of $3Y/2X$ on the $^{207}\text{Pb}/^{204}\text{Pb}$ vs. $^{206}\text{Pb}/^{204}\text{Pb}$ diagram (Ozard and Russell, 1970; Richards et al., 1981). The ^{204}Pb error causes the spread of the values along a slope equal to the $^{207}\text{Pb}/^{206}\text{Pb}$ and $^{208}\text{Pb}/^{206}\text{Pb}$ values since for each of the ratios ($^{206}\text{Pb}/^{204}\text{Pb}$, $^{207}\text{Pb}/^{204}\text{Pb}$ and $^{208}\text{Pb}/^{204}\text{Pb}$) the error is related to the ^{204}Pb measurement (York, 1969). The slopes of the corresponding errors is depicted on each diagram (Figs. 3.3 to 3.5).

3.3.3 Calculation of Average Values for the Deposits

The average isotopic composition for each deposit (Table 3.3) are presented on conventional $^{207}\text{Pb}/^{204}\text{Pb}$ vs. $^{206}\text{Pb}/^{204}\text{Pb}$, $^{208}\text{Pb}/^{204}\text{Pb}$ vs. $^{206}\text{Pb}/^{204}\text{Pb}$, and $^{206}\text{Pb}/^{207}\text{Pb}$ vs. $^{206}\text{Pb}/^{208}\text{Pb}$ diagrams (Figs. 3.3 to 3.5). The plotted average values were obtained from the computation of repeated analyses of various samples collected at the deposit site (Table 3.2; Appendix C).

TABLE 3.2: Representative calculation of average galena lead isotopic values¹ for a given deposits.

Sample Number ²	Lead Isotope Ratios		
	206/204 \pm	207/204 \pm	208/204 \pm
BIRK CREEK			
30508-001	18.948 (0.02)	15.718 (0.02)	38.861 (0.03)
30508-001D	18.947 (0.08)	15.741 (0.08)	38.856 (0.08)
30508-002	18.904 (0.03)	15.710 (0.01)	38.791 (0.03)
30508-002D	18.882 (0.03)	15.699 (0.03)	38.751 (0.03)
30508-003	18.901 (0.02)	15.691 (0.01)	38.744 (0.02)
(30508-003D	19.026 (0.30)	15.798 (0.30)	39.027 (0.30)) ³
30508-004	18.896 (0.02)	15.705 (0.01)	38.755 (0.02)
30508-004D	18.949 (0.14)	15.741 (0.05)	38.987 (0.16)
30508-005	18.893 (0.01)	15.721 (0.01)	38.829 (0.01)
30508-506	18.878 (0.06)	15.708 (0.13)	38.893 (0.18)
30508-506D	18.869 (0.08)	15.722 (0.10)	38.834 (0.18)
Mean (n=11)	18.927	15.723	38.848
Rejection level			
at ± 2 st. dev.	0.098	0.059	0.186
Mean (n=10)	18.907	15.716	38.848
Std. Error ⁴	0.01	0.005	0.03

1. Similar calculation has been made apply to all deposits (Appendix C).
2. 30508 represents the number given to the deposit; 001, 002, etc. defines different samples taken from the deposit; D, indicates duplicate analyses of the same sample.
3. Data from this run was rejected on the basis of more than 2 standard deviations from the mean.
4. Standard error = standard deviation / square root of number of samples (n).

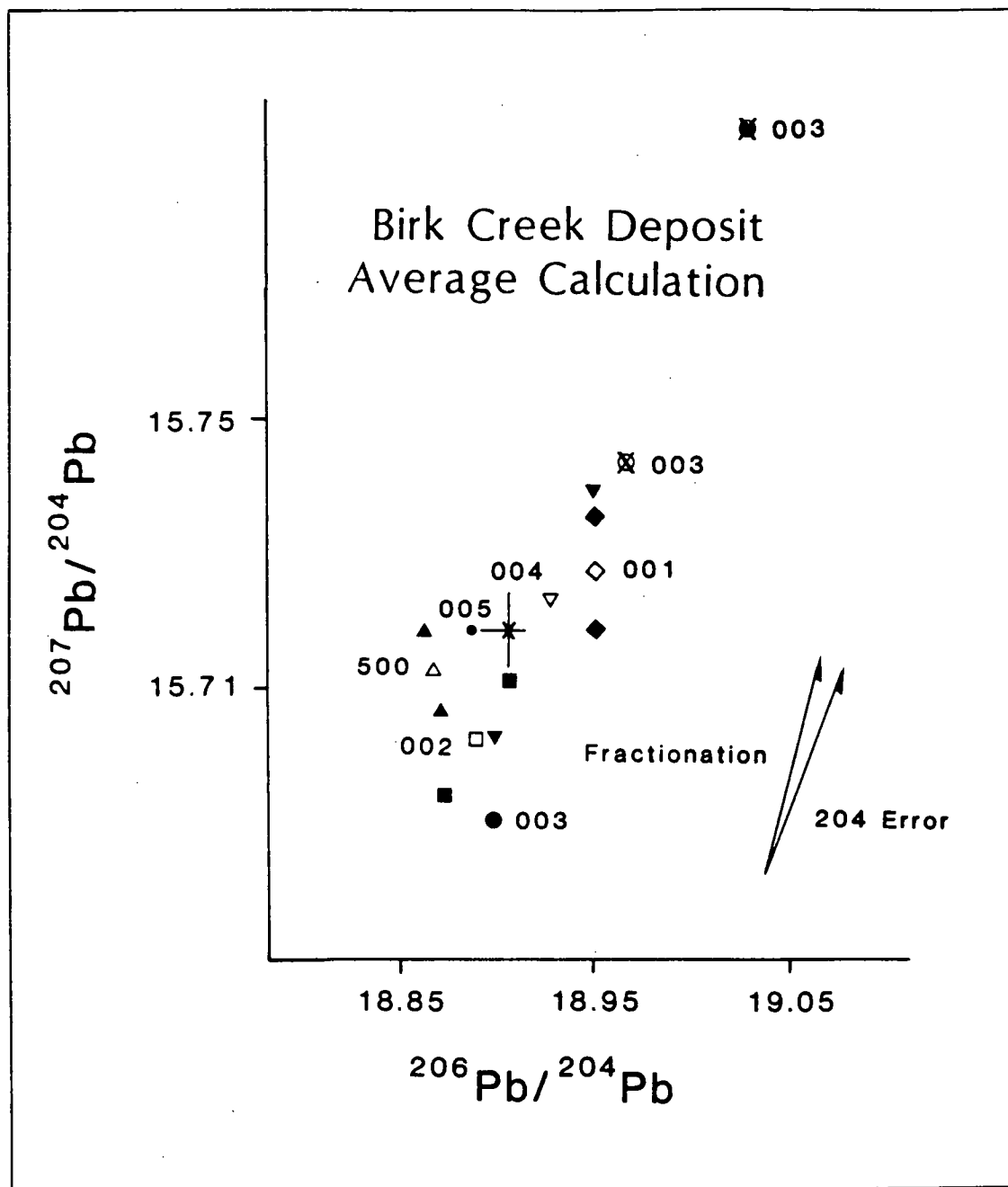


Figure 3.2 $^{207}\text{Pb}/^{204}\text{Pb}$ vs. $^{206}\text{Pb}/^{204}\text{Pb}$ diagram showing the isotopic distribution of all analyses from the Birk Creek area. Filled symbols represent individual analyses and open symbols define their average. Crossed symbols identify deleted analysis. The average value for the Birk Creek area is depicted with its associated standard error (Table 3.2).

TABLE 3.3: Average galena lead isotope values from ore deposits in the Eagle Bay Formation.

Deposit Name	Map No2	Lead Isotope Ratios ¹				
		206/204	207/204	208/204	206/207	206/208
<u>Cluster 1 Devonian</u>						
Birk Creek	508	18.907	15.716	38.848	1.20304	0.48699
Homestake	511	18.854	15.700	38.626	1.20085	0.48845
Rea Gold	515	18.869	15.699	38.755	1.20192	0.48688
Ford	538	18.883	15.698	38.676	1.20289	0.48823
Average (n=4)		18.887	15.703	38.720	1.20211	0.48767
Std. Error Mean		± 0.010	± 0.004	± 0.216	$\pm .00047$	$\pm .00039$
<u>Between cluster 1 & 2</u>						
Art	517	19.060	15.737	39.147	1.21110	0.48687
Twin Mountain	519	19.027	15.704	38.832	1.21164	0.49027
<u>Cluster 2 Triassic</u>						
Agate Bay	506	19.143	15.701	38.909	1.21922	0.49200
Lucky Coon	518	19.142	15.694	38.900	1.21968	0.49208
King Tut	523	19.045	15.688	38.835	1.21718	0.49255
Elsie	524	19.142	15.700	38.975	1.21925	0.49197
Mosquito King	525	19.090	15.693	38.846	1.21648	0.49142
Pet	526	19.126	15.732	38.980	1.21575	0.49151
Spar	527	19.130	15.690	38.881	1.21927	0.49201
Red Top	531	19.146	15.721	38.939	1.21779	0.49170
Red Mineral 2	534	19.131	15.714	38.069	1.21747	0.48966
Silver King A	536	19.081	15.708	38.899	1.21471	0.49052
Orell SP	537	19.128	15.692	38.885	1.21902	0.49191
Sunrise	541	19.105	15.696	38.849	1.21716	0.49176
Enargite	504	19.096	15.690	38.987	1.21704	0.48979
Fortuna	513	19.125	15.721	39.018	1.21650	0.49016
White Rock	528	19.151	15.722	39.048	1.21810	0.49046
Vaverby	542	19.191	15.703	38.846	1.21574	0.49145
Silver King-Queen	545	19.104	15.684	38.978	1.21807	0.49012
PS-85-175	548	19.177	15.721	38.962	1.21987	0.49220
Average (n=18)		19.125	15.701	38.936	1.21775	0.49138
Std. Error Mean		± 0.007	± 0.003	± 0.016	$\pm .00365$	$\pm .00023$

TABLE 3.3 (continued)

Deposit Name	Map No2	Lead Isotope Ratios ¹				
		206/204	207/204	208/204	206/207	206/208
<u>Between cluster 2 & 3</u>						
Fluke	532	19.223	15.703	39.361	1.22416	0.48838
Mt McClennan	539	19.269	15.698	38.967	1.22747	0.49448
Foghorn	505	19.208	15.711	39.138	1.22258	0.49076
Rexspar	516	19.177	15.916	38.986	1.20528	0.49273
Birch Island	540	19.335	15.820	39.235	1.22200	0.49364
Tindal	543	19.251	15.714	39.080	1.22509	0.49261
Rouge	547	19.260	15.744	39.156	1.22330	0.49188
<u>Cluster 3</u>						
Leemac	546	19.391	15.729	39.336	1.23279	0.49294
Red Mineral 1	533	19.345	15.699	39.360	1.23229	0.49149
Red Mineral 3	535	19.354	15.706	39.383	1.23228	0.49142
Sonja	544	19.356	15.691	39.251	1.23353	0.49313
Beca	507	19.339	15.680	39.016	1.23338	0.49567
Average (n=5)		19.357	15.701	39.264	1.23285	0.49293
Std. Error Mean		<u>+0.040</u>	<u>+0.008</u>	<u>+0.055</u>	<u>+0.00026</u>	<u>+0.00077</u>
<u>Beside cluster 3</u>						
June	521	19.461	15.719	39.504	1.23809	0.49263

1. Lead isotopic ratios represent calculated average values from data in Appendix C (calculation of average value is described in section 3.3.2).
2. Map no. in Appendix C is prefixed by 30 and suffixed by analytical sample number.

Figure 3.2 represents an example of such data collected from the Birk Creek area. In the average value calculation, data falling outside two standard deviations from the mean were deleted (as were outlier values obtained from runs with poor precision. Thus means representing only the 'best' values are presented in Tables 3.2 and 3.3. Consistency between samples from massive ore and from cross-cutting structures was observed in all deposits where both types of samples were collected. This indicates that mineral showings of different habit can be cogenetic and formed from similar and/or interactive hydrothermal systems. In many cases veins may represent feeder zones to massive ore.

3.4 THE REMODELED CURVE FOR THE EAGLE BAY FORMATION

The average lead isotopic composition obtained from deposits in the Eagle Bay Formation (Table 3.3) forms a coherent series of clusters characterized by high $^{206}\text{Pb}/^{204}\text{Pb}$, $^{207}\text{Pb}/^{204}\text{Pb}$, and $^{208}\text{Pb}/^{204}\text{Pb}$ values. The isotopic uniformity displayed by the set of data as a whole is best explained by the presence of a common ultimate source for the lead in all the deposits. Because the data plot above the average 'orogene' curve of Doe and Zartman (1979), a growth curve representing the evolution in an upper crustal environment is used to determine the model ages for the various deposits clustered along it.

Figure 3.3

$^{207}\text{Pb}/^{204}\text{Pb}$ vs $^{206}\text{Pb}/^{204}\text{Pb}$ diagram for deposits hosted by the Eagle Bay Formation using data from Table 3.3. Filled symbols denote deposits grouped in specific clusters; open symbols are outliers. Deposits in cluster 1 to 3 are plotted with different symbols. Bars represent ± 1 standard error around the mean of the cluster. The average growth curves shown are the 'shale' curve of Godwin and Sinclair (1982) and the remodeled shale curve ($t_2 = 2.0\text{Ga}$, $u = 12.16 \pm .08$).

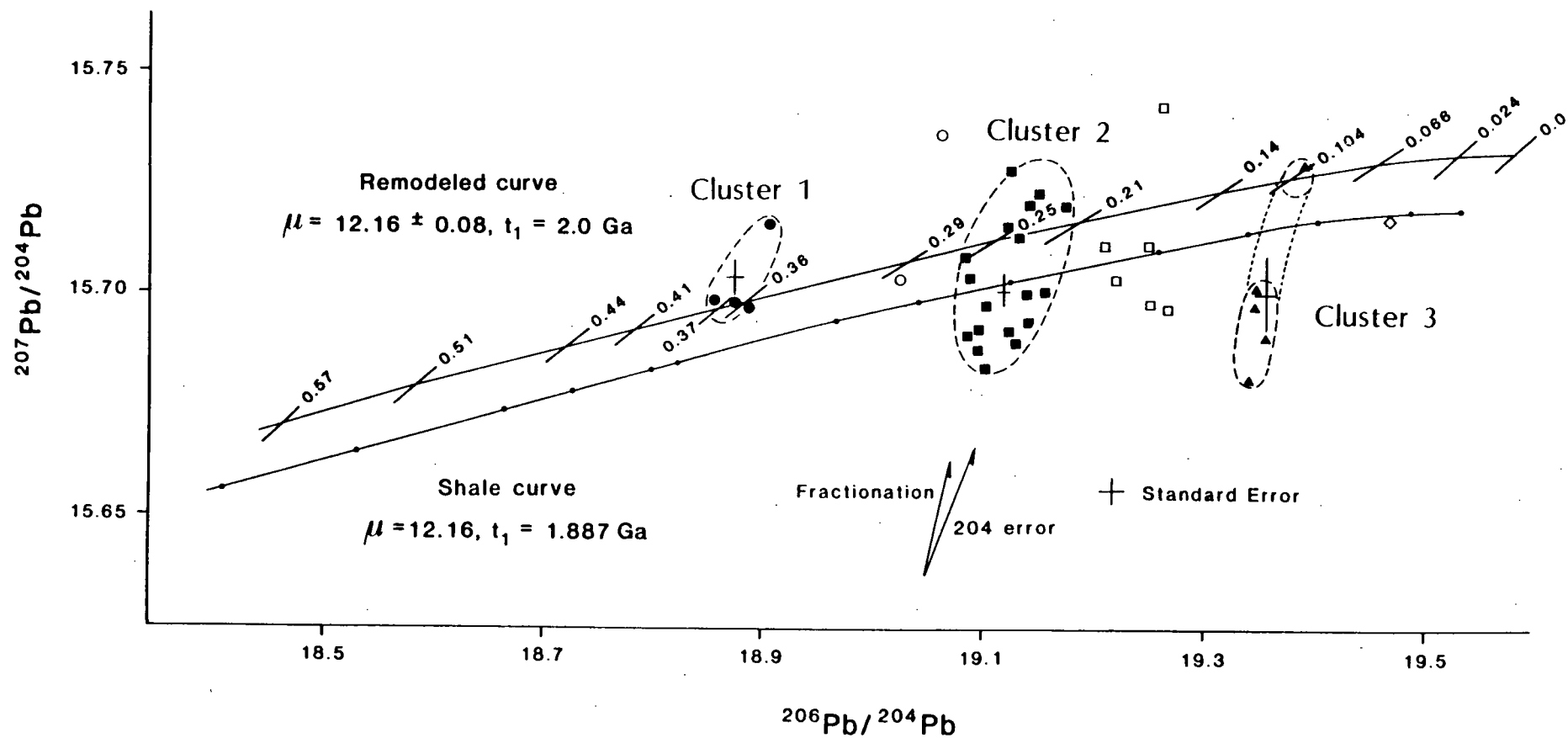


Figure 3.4

208pb/204pb vs 206Pb/204Pb diagram for deposits hosted by the Eagle Bay Formation using data from Table 3.3. Filled symbols denote deposits grouped in specific clusters; open symbols are outliers. Deposits in cluster 1 to 3 are plotted with different symbols. Bars represent ± 1 standard error around the mean of the cluster. The average growth curves shown are the 'shale' curve of Godwin and Sinclair (1982) and the remodeled shale curve ($t_2 = 2.0\text{Ga}$, $w = 45.35$).

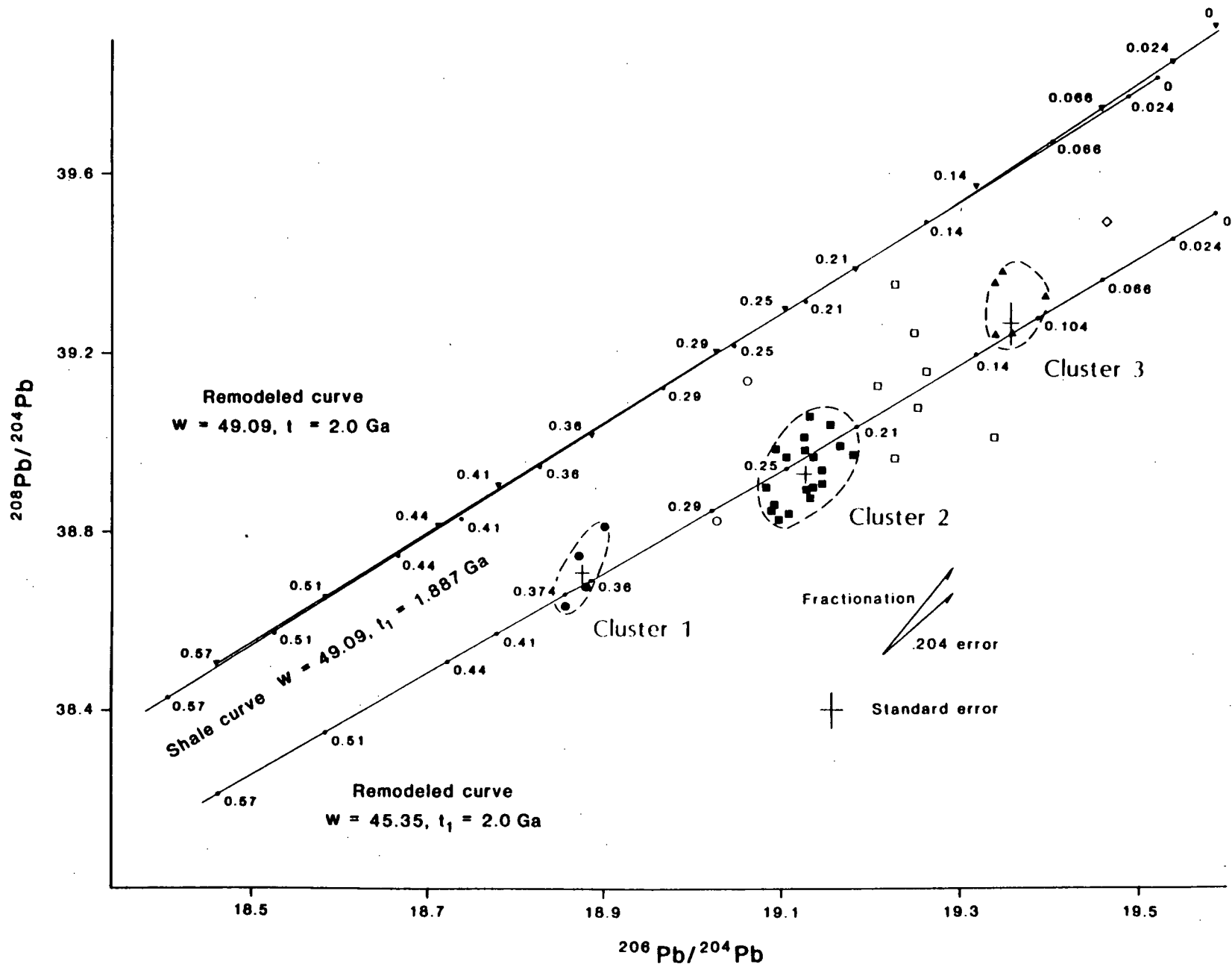
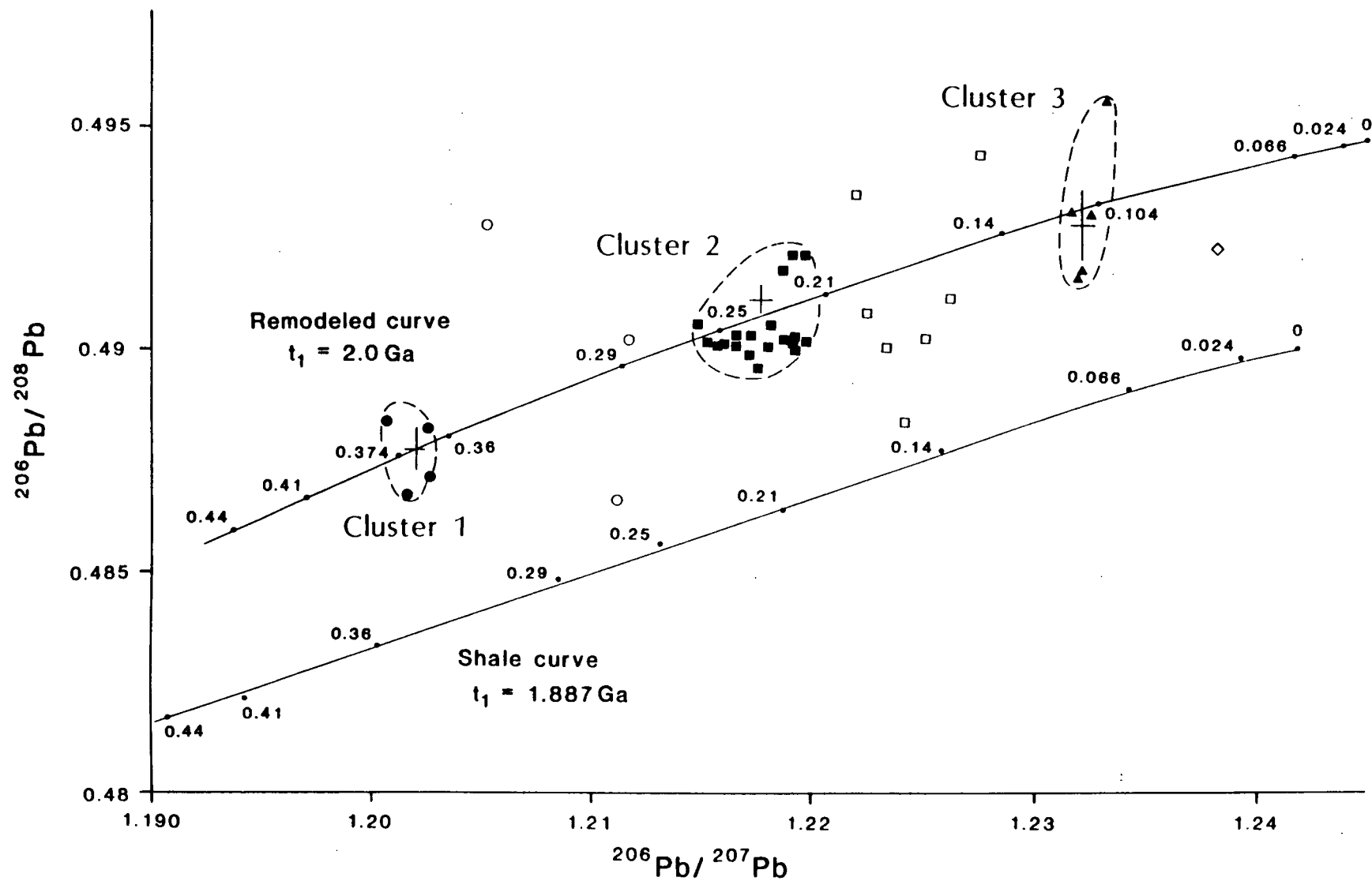


Figure 3.5

$^{206}\text{Pb}/^{208}\text{Pb}$ vs $^{206}\text{Pb}/^{207}\text{Pb}$ diagram for deposits hosted by the Eagle Bay Formation using data from Table 3.3. Filled symbols denote deposits grouped in specific clusters; open symbols are outliers. Deposits in cluster 1 to 3 are plotted with different symbols. Bars represent ± 1 standard error around the mean of the cluster. The average growth curves shown are the 'shale' curve of Godwin and Sinclair (1982) and the remodeled shale curve ($t_2 = 2.0\text{Ga}$, $u = 12.16 \pm .08$).



The approximate coincidence of the data from the deposits of the Eagle Bay Formation with the 'shale' curve of Godwin and Sinclair (1982) supports the utilization of such a curve for model age estimation, and indicates that the lead in the deposits of the Eagle Bay Formation evolved in an upper crustal environment characterized by high u and w values. The curve is consistent with the active continental margin setting assigned to deposition of the Eagle Bay Formation, and implies that there was a significant contribution of material from recycled and homogenized Precambrian crust to constituent rock units of the formation.

However, the high $^{207}\text{Pb}/^{204}\text{Pb}$ isotopic signature of the galena from the Eagle Bay Formation resulted in the data plotting above the average 'shale' curve on the $^{207}\text{Pb}/^{204}\text{Pb}$ vs. $^{206}\text{Pb}/^{204}\text{Pb}$ diagram (Fig. 3.3). Similarly the plotted $^{208}\text{Pb}/^{204}\text{Pb}$ ratios are shifted below the 'shale' curve on the $^{208}\text{Pb}/^{204}\text{Pb}$ vs. $^{206}\text{Pb}/^{204}\text{Pb}$ diagram (Fig. 3.4). Presentation of the data on a $^{206}\text{Pb}/^{207}\text{Pb}$ vs. $^{206}\text{Pb}/^{208}\text{Pb}$ diagram (Fig. 3.5) reveals that the slight but systematic discrepancy between the data set and the 'shale' curve is real and not due to analytical error of ^{204}Pb (this diagram minimizes the effect of this error by eliminating the ^{204}Pb measurement errors). Consequently the 'shale' curve represents an approximation of the average lead

behavior, but does not fit the data closely enough to permit model age determinations. Remodeling of the curve (Table 3.4), by changing the parameters used to define it, resulted in a better coincidence with the data from deposits hosted in the Eagle Bay Formation--especially $^{208}\text{Pb}/^{204}\text{Pb}$ vs. $^{206}\text{Pb}/^{204}\text{Pb}$ and $^{206}\text{Pb}/^{208}\text{Pb}$ vs. $^{206}\text{Pb}/^{207}\text{Pb}$ (Figs. 3.4 and 3.5). The remodeled curve as defined here applies specifically only to the deposits in the Eagle Bay Formation. It does not detract from the general validity of the 'shale' curve--especially as applied east of the Adams Plateau. The remodeled curve represent a local variation from the average 'shale' curve due to the specific geological setting characteristic of the Eagle Bay Formation. The following discussion reviews the changes in parameters made to obtain the remodeled curve.

3.4.1 Departure Time, Initial Composition, and u Values

The remodeled curve is anchored to the Stacey and Kramers (1975) curve at 2.0Ga. This date has been favored because it is close to Rb/Sr whole rock dates from granitic gneiss of the Shuswap Complex (2.0 to 2.25Ga: Duncan, 1982), and to the determined age of the basement by the common lead method from three groups of stratabound deposits in terrane correlated with the Eagle Bay Formation (Duncan, 1982). The 2.0Ga date is slightly older than the homogenization time of the continental

TABLE 3.4: Lead isotope values for the remodeled curve.

Parameters: $u = 12.16$, $w = 45.35$, $t_2 = 2.0\text{Ga}$

Age ¹	Time Ga ¹	Lead Isotope Ratios				
		206/204	207/204	208/204	206/207	206/208
Present	0.0	19.582	15.736	39.515	1.24440	0.49556
Neogene	0.024	19.537	15.734	39.461	1.24171	0.49510
Paleogene	0.066	19.457	15.730	39.366	1.23693	0.49426
Cretaceous	0.14	19.315	15.723	39.198	1.22846	0.49275
Jurassic	0.21	19.180	15.716	39.044	1.22041	0.49124
Triassic	0.25	19.102	15.711	38.953	1.21584	0.49039
Permian	0.29	19.023	15.707	38.858	1.21112	0.48955
Carboniferous	0.36	18.884	15.698	38.699	1.20296	0.48797
Devonian	0.41	18.784	15.692	38.586	1.19704	0.48681
Silurian	0.44	18.723	15.688	38.518	1.19346	0.48608
Ordovician	0.51	18.581	15.678	38.354	1.18516	0.48446
Cambrian	0.57	18.458	15.670	38.218	1.17792	0.48297
Anchor point ²	2.0	15.159	15.192	34.799	0.99783	0.43562

1. Time boundaries from DNAG Geologic Time Scale (Palmer, 1983).

2. Calculated from stage 2 of Stacey and Kramers (1975) $u = 9.74$, $w = 37.19$, $t_1 = 3.7\text{Ga}$.

basement by the Hudsonian orogeny. It was chosen as the departure point for the model related to galena lead isotopes in the Eagle Bay Formation. Nevertheless this starting point represents an estimated parameter which is required by the multi-stage model adopted in this study.

Estimation of the initial ratio at 2.0Ga is not unambiguous. However, here it is simply assumed that the environment from which the basement was generated evolved along an average curve similar to the secondary growth curve of Stacey and Kramers (1975) starting at 3.7Ga (a similar assumption was made in the construction of the 'shale' curve). The initial ratios therefore correspond to the empirical data calculated by Stacey and Kramers (1975, p. 216) and are: $^{206}\text{Pb}/^{204}\text{Pb} = 15.159$, $^{207}\text{Pb}/^{204}\text{Pb} = 15.192$, and $^{208}\text{Pb}/^{204}\text{Pb} = 34.799$.

The u value of 12.16 was used to calculate the remodeled curve because it represents the average U/Pb value for the Omineca Belt calculated for the 'shale' curve (Godwin and Sinclair, 1982). The calculated u values for the data from the Eagle Bay Formation (using equations in Table 3.0) coincidentally covered a range centered around a u of 12.0. Isotopic compositions on the remodeled curve were also calculated with $u = 12.08$ and 12.24 (Fig. 3.3) to display the effect of a variation of u on the position of the remodeled curve.

Utilization of 2.0Ga as a departure point generates a curve which plots above the 'shale' curve (Figs. 3.3 and 3.4). Consequently, any isotopic composition associated with any model age on the remodeled curve will be greater in both $^{207}\text{Pb}/^{204}\text{Pb}$ and $^{206}\text{Pb}/^{204}\text{Pb}$ ratios relative to the 'shale' curve. The upward displacement of the curve's position increases the coincidence between the curve and clusters 1 and 3. This aspect is significant because these two clusters, containing deposits of known Devonian and Cretaceous age, fall appropriately on the remodeled curve at 375Ma and 100Ma respectively. This better fit of the data with the remodeled curve supports the use of 2.0Ga rather than 1.887Ga as the anchor point for the remodeled curve. On the other hand, the variations caused by the utilization of different u values are less significant (Fig. 3.3), and it does not appear to be advantageous to change the u value to accommodate the data.

3.4.2 w Value

Utilization of a w value equal to 49.09 (value used for the 'shale' curve: Godwin and Sinclair, 1982) to remodel the thorium curve (on the $^{208}\text{Pb}/^{204}\text{Pb}$ vs. $^{206}\text{Pb}/^{204}\text{Pb}$ diagram; Fig. 3.5) is inadequate. Compared to the uranogenic curve (above section) the change resulting from the utilization of t_2 equal to 2.0Ga rather than 1.887Ga does not sensibly affect the

position of the remodeled curve relative to the distribution of the data set, since it only displaces the isochron intersections upward and to the right (depicted as points and crosses in Figure 3.4). A closer fit of the remodeled curve to the data is obtained when the w value is lowered to 45.35. This value is markedly lower than the 49.09 value used for the 'shale' curve; however this value is higher than the estimated value of 41.86 used by Doe and Zartman (1979) to characterize the upper crustal environment for their plumbotectonic model. The geochemical behavior of thorium during the fractionation process is not as well understood as uranium and, the Th/Pb ratio is considered less specific in discriminating among various source materials (Zartman, 1974). Therefore, although a slightly lower value is required to fit the data from the deposits of the Eagle Bay Formation, it does not imply any major difference in the composition of the protolith for these rocks.

3.4.3 Summary

Uniformity within deposits and the range of the lead isotopic compositions obtained on galena from the deposits hosted by the Eagle Bay Formation indicates that the protolith for the lead has an average upper crustal signature. This emphasizes the involvement of old crustal basement beneath the Eagle Bay Formation and/or sediment sources for the Eagle Bay rocks. Lead from the deposits hosted by the Eagle Bay Formation

has generally similar isotopic compositions to the lead in the Cariboo Gold veins (Andrew, 1982), and is significantly different (mainly higher $^{207}\text{Pb}/^{204}\text{Pb}$ values) from the lead in the Intermontane Belt (Andrew, 1982) and the Slide Mountain Group (Aggarwal and Nesbitt, 1984). In addition this similarity in the lead isotopic signature of deposits in the Eagle Bay Formation and in the Barkerville Terrane supports the correlations established by Struik (1986).

Proximity of the data to the 'shale' curve indicates that this curve is a possible approximation to the average behavior of the lead. But the distinct remodeled curve more closely fits the data from the Eagle Bay Formation. This remodeled curve is used throughout the following discussion to assign model ages to the pulses of mineralization in the Eagle Bay Formation mainly represented by three distinct clusters of data with Devonian, Upper Triassic, and Cretaceous model ages.

3.5 MODEL AGE DETERMINATIONS

Using the multi-stage model depicted in Figure 3.1, model ages for the mineralization can be derived from the measured isotopic ratios of the deposits. By combining equation 1 and 2 of Table 3.0, the equation of a family of straight lines (isochrons) passing through the anchor point of the remodeled

shale curve at 2.0Ga on Stacey and Kramers' (1975) curve can be obtained. The slope of the appropriate isochron on which the lead isotopic composition lies can be used to determine a value of t_3 and to assign a model age for the galena. Since the above equation is transcendental, t_3 cannot be directly calculated by conventional algebraic methods, and computer programs use an iterative calculation to approximate the best value for t_3 . Calculation of the slope m , and t_3 determinations were made using the average isotopic values (Table 3.3.) for each deposit. Because the $^{207}\text{Pb}/^{204}\text{Pb}$, $^{206}\text{Pb}/^{204}\text{Pb}$ slope model ages are very sensitive to small changes in m , variations in the $^{207}\text{Pb}/^{204}\text{Pb}$ intercept of 0.1% (comparable to experimental error) resulted in large variations in the calculated model ages (differences of 100Ma were obtained for some of the deposits in cluster 1). Consequently, the slope model ages obtained for each deposit were not used. Instead, ages of the clustered groups of deposits were determined by where they plot along the remodeled curve.

Table 3.3 lists the mean values for each cluster (calculated in the same way as averages for each deposit in section 3.3.3). These means with their associated standard error are plotted on the lead diagrams (Figs. 3.3 to 3.5). Model age for the clusters were then established from the age on the remodeled curve at which the clusters--around their mean

values--intersected the curve. These model ages are primarily controlled by the $^{206}\text{Pb}/^{204}\text{Pb}$ ratios as it is these ratios that exhibit greater variations. The model ages for clusters 1, 2 and 3 were determined from each diagram (Fig. 3.3 to 3.5) as being respectively Late Devonian, Late Triassic, and mid-Cretaceous. These model ages of corresponding clusters of deposits are discussed in Chapter 4.

4. LEAD ISOTOPES, MINERAL DEPOSITS AND STRATIGRAPHY

4.1 INTRODUCTION

The dominant influence of an upper crustal component on the lead isotope composition in galena of deposits hosted by the Eagle Bay Formation was established in Chapter 3. This chapter focuses on the differences between these deposits as defined by the clustering of the lead data into three main groups along the remodeled curve (deposits in each cluster are in Table 4.0). Deposits sharing similar lead isotope signatures define genetic links; difference in isotopic composition between the distinct clusters allow model ages to be assigned and sometimes permits distinctions between deposits that are cogenetic with, or are markedly younger than their host rocks.

Stratigraphic correlation and construction of composite stratigraphic successions within the Eagle Bay Formation has been hampered by intense deformation and metamorphism, which commonly obscures contact relationships among the units. Lead isotope data are consistent with the Devonian age for the unit EBA established by other criteria (see section 2.3.1). However lead data suggest an Upper Triassic age for the structurally lower part of unit EBG, which is considered to be Cambrian by

TABLE 4.0: Classification and name of deposits within discrete clusters of data defined in Figures 3.3 to 3.5

Deposit Classification	Host Unit1	Deposit Name	Map No1
<u>Cluster 1 Devonian</u>			
Volcanogenic Cogenetic with host rocks	EBA	Birk Creek	508
		Homestake	511
		Ford	538
	EBF	Rea Gold	515
<u>Between cluster 1 & 2</u>			
Veins	EBS	Art	517
	EBG	Twin Mountain	519
<u>Cluster 2 Triassic</u>			
Stratiform Cogenetic with host rocks	EBG	Agate Bay	506
		Lucky Coon	518
		King Tut	523
		Elsie	524
		Mosquito King	525
		Pet	526
		Spar	527
		Red Mineral 2	534
		Silver King A	536
		Orell SP	537
Replacement	EBQ	Red Top	531
		Sunrise	541
Veins	EBA	Enargite	504
		Fortuna	513
	EBG	White Rock	528
		Vaverby	542
		Silver King-Queen	545
		PS-85-175	548

TABLE 4.0 (continued)

Deposit Classification	Host Unit ¹	Deposit Name	Map No ¹
<u>Between cluster 2 & 3</u>			
Stratiform	EBG	Fluke	532
Replacement	EBQ	Mt McClennan	539
Uranium (volcanogenic) Vein	EBA	Rexspar	516
		Foghorn	505
		Birch Island	540
		Tindal	543
		Rouge	547
Cluster 3			
Vein	Baldy	Leemac	546
	EBG	Red Mineral 1	533
		Red Mineral 3	535
	EBA	Sonja	544
Replacement(?)	EBA	Beca	507
<u>Beyond cluster 3</u>			
Vein		June	521

1. Host Unit and Map No. are on Figure 4.0. Map no. in Appendix C is prefixed by 30 and suffixed by analytical sample number.

Schiarizza (1986). Interpretations proposed here, although not completely unambiguous, are constrained substantially by available geological data.

4.2 CLUSTER 1: DEVONIAN COGENETIC DEPOSITS

Two mineralized deposits, Rea Gold and Homestake, and two mineralized showings, Birk Creek and Ford, (Table 4.0, Fig. 4.0, Appendix A) are enclosed by cluster 1 around the Devonian isochron on the remodeled curve (Fig. 3.3 to 3.5). These four occurrences are hosted by Devonian volcanic units (EBA and EBF) of the Eagle Bay Formation. These units form a conformable succession (locally separated by orthogneiss bodies) composed of strongly foliated quartz-sericite-phyllite, chloritic phyllite, and sericite schist, within which quartz and plagioclase phenocrysts and relict igneous textures are locally visible. This succession was interpreted by Preto (1981) as a deformed and recrystallized felsic to intermediate volcanic sequence metamorphosed to greenschist facies. Units EBA and EBF are partly interlayered with, but mostly overlain by, a turbidite sequence composed of phyllites, argillite, sandstone, grit and minor carbonates (unit EBP). Zircons from the metavolcanic rocks (Fig. 4.0) yielded a Devonian, 372 ± 11 Ma date (Preto and Schiarizza, 1985). Conodonts found in two limestone beds of unit EBP yielded a mid-Mississippian age (Osagien to early

Devonian to Permian**Fennell Formation**

- UF** Upper structural division: pillowed and massive meta-basalt, minor chert
- IF** Lower structural division: pillowed and massive meta-basalt and ribbon chert, limestone, diorite, gabbro, quartzfeldspar, porphyry, rhyolite

Mississippian

- EBP** Phyllite and slate with interbedded sandstone and grits




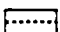

Devonian and/or Mississippian

- EBF** Feldspathic phyllite (intermediate to felsic tuff)

Devonian

- EBA** Sericite-quartz-phyllite and schist (intermediate to felsic volcanics and volcanoclastics)

Devonian and/or older

- EBS** Mixed meta-sedimentary sequence (phyllites)
- EBG** Calcareous chlorite-schist, fragmental schist (mafic to intermediate volcanics)
-  Tshinakian limestone
-  mixed phyllite (EBGp)
-  quartzite (EBGq)
-  polymictic conglomerate (EBGcg)
-  T-EBG (? Triassic)

Lower Cambrian and/or older

- EBQ** Chlorite-muscovite quartzite, chlorite-muscovite-quartz schist and minor meta-sediments (SDQ)
- EBH** Quartzite, grit and chlorite-sericite-quartz schist

Intrusives**Jurassic & Cretaceous**

-  Raft batholith, Baldy batholith, Scotch Creek plug

Late Devonian

- Dgn** Granite and granodiorite orthogneiss

Symbols**Mineral occurrences**

- ○ Cluster 1 (Devonian) ▲ △ Cluster 3 (Cretaceous)
- □ Cluster 2 (Triassic) ◇ Cluster 4 (Tertiary)
- X Outliers




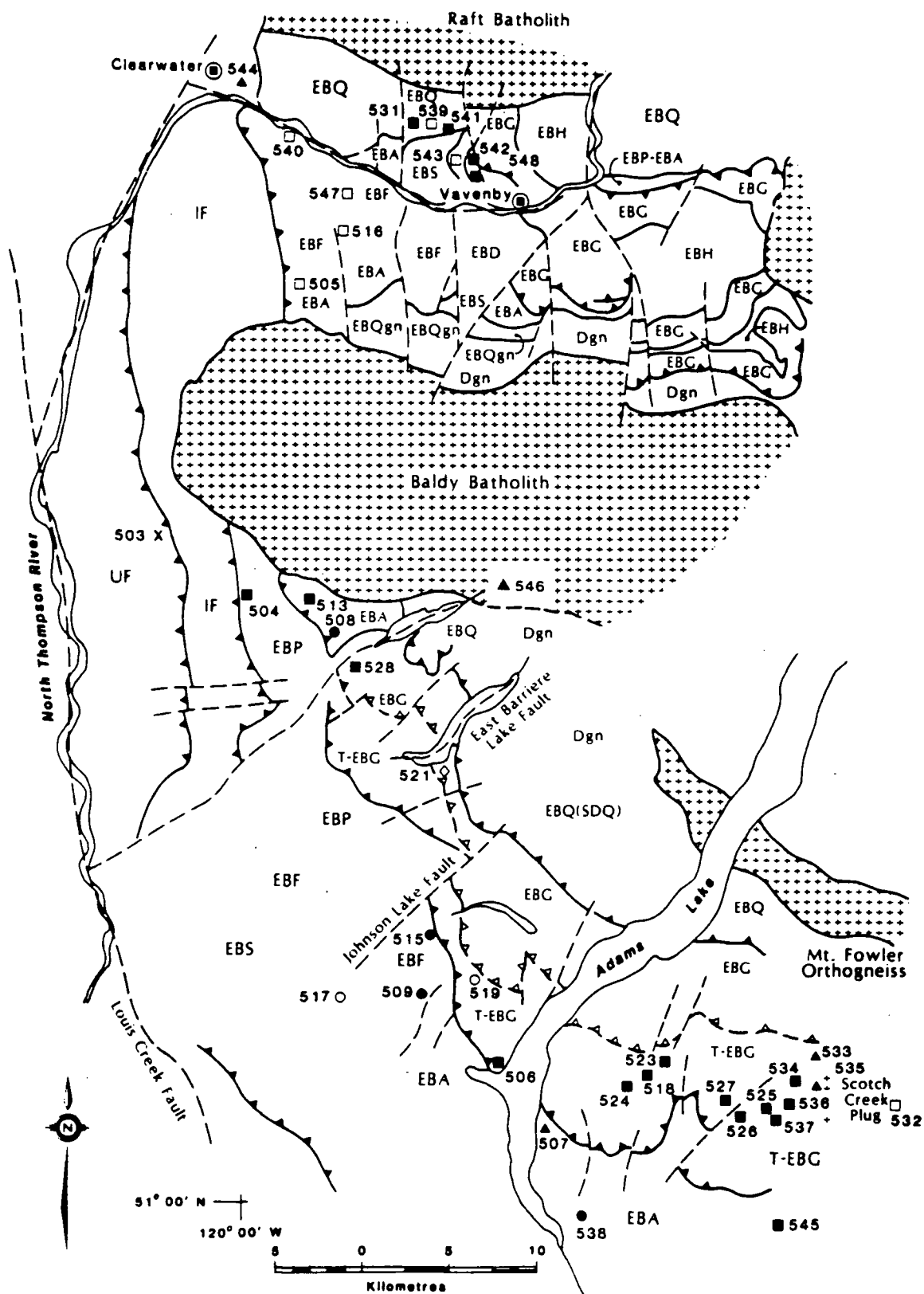
-  Faults
-  Thrust fault (this study)
-  Thrust fault (Schiarizza et al, 1984)

Figure 4.0 Geology of the Eagle Bay Formation showing the location of the sampled mineral deposits within the major thrust units (modified from Schiarizza and Preto, 1984).



Meramecien: Okulitch and Cameron, 1976). Based on these age determinations, a bracketed Devono-Mississippian age has been assigned to these units.

Rea Gold and Homestake deposits, located on the limbs of a major overturned and northwesterly trending syncline similarly occur within or near the top of a felsic pyroclastic sequence included in a thicker more mafic pile of tuffs and minor flows. Deformation has affected the deposits and is marked by a well defined penetrative foliation. Definite folds are difficult to outline due the shistosity developed in the rocks. Both deposits, composed of massive sulphide lenses and associated barite, exhibit extensive footwall alteration zones characterized by silicification, sericitization and pyrite development. These deposits are similar in many respects to the syngenetic volcanogenic polymetallic Kuroko deposits (Hoy and Goutier, 1986; Appendix A).

A Devono-Mississippian lead model age for the deposits is coincident with other age determinations from their host units (EBA and EBF), and consequently, the mineralizing solutions probably were cogenetic with the formation of the host rocks. The lead isotopic signature of cluster 1 can therefore be used to fingerprint deposits which formed under similar conditions. Thus, although the silicified pyrite-pyrrhotite rich occurrences

of the Birk Creek area and the stratiform massive sulphide zones mineralized with Pb-Zn-Cu of the Ford property (Table 4.0, Fig. 4.0, Appendix A) are not conclusively volcanogenic in origin, their lead isotopic composition suggests such an interpretation.

The cogenetic and volcanogenic mineralization probably was deposited either from solutions associated with the volcanism or concentrated from the volcanic pile by circulating solutions in a convective cell soon after, or during the formation of the Devonian units EBA and EBF (Hutchison, 1973; Solomon, 1976; Lydon, 1985). The probable presence of an underlying larger intrusive mass, which may have set up the convective cell, is indicated by the occurrence of quartz porphyry intrusive bodies considered to be cogenetic with the volcanics (Preto, 1981; Goutier et al., 1985).

The observed isotopic ratios represent an average of the lead leached by the mineralizing solutions from the source rocks. The lead isotopic compositions from veins associated with the deposits are statistically indistinguishable from the lead extracted from the massive deposit. This suggests that formation of the veins was contemporaneous with the formation of the massive ore; they may represent feeders to massive ore bearing horizons. Compared to Kuroko type deposits (Lambert and

Sato, 1974; Sato and Sasaki, 1976; Sato et al., 1980), the lead data of cluster 1 are markedly radiogenic. This enrichment in radiogenic lead suggests that the ultimate source of Devonian intrusives is underlying Precambrian basement, a conclusion in agreement with the interpretation of Armstrong (in Jung, 1986) on the western position of the basement boundary (Fig. 2.0; see section 2.3.2).

4.3 LEAD DATA BETWEEN CLUSTER 1 & 2

Two mineralized veins (Twin Mountain and Art; Table 4.0, Figure 4.0, Appendix A) have their lead isotopic compositions plotting distinctively to the right of cluster 1. The Twin Mountain vein has a lead model age of mid-Pennsylvanian, and occurs in the Cambrian unit EBG (Schiarizza and Preto, 1984). The high barite content of some of the veins at Twin Mountain makes them mineralogically more similar to the nearby Rea Gold and Homestake deposit (hosted by the Devono-Mississippian units EBA and EBF) than to any deposits of the Cambrian unit EBG. The major thrust inferred by Schiarizza and Preto (1984) which isolate Twin Mountain from the Devono-Mississippian units has not been confirmed by detailed mapping by Corporation Falconbridge (see Hoy and Goutier, 1986) or by White (1985). The mid-Pennsylvanian model age determined for the Twin Mountain vein might indicate that the inferred thrust actually represents

an unconformity between separated volcanic and volcanoclastic sequences, and that the host unit could be younger than Cambrian as currently interpreted. However, the mid-Pennsylvanian lead model age by itself does not refute the Cambrian age assigned to the unit EBG.

4.4 CLUSTER 2: TRIASSIC STRATIFORM AND VEIN DEPOSITS

Cluster 2 represents galena lead with an Upper Triassic model age (Fig. 3.3 to 3.5). Several remobilized stratiform deposits hosted by the unit EBG, and veins randomly distributed through the Eagle Bay Formation have lead isotopic compositions that plot in this cluster. The form of the stratiform deposits suggests that they could be cogenetic with their host unit. Unit EBG, however, has been defined as Cambrian (Schiavizza, 1986b). Consequently, a major discrepancy exists between the Triassic model age for apparently cogenetic mineralization and the assigned Cambrian age of the host. The following constitutes a brief geological description of the deposits of cluster 2 and provides a framework for the discussion of the lead isotope interpretations in section 4.2.2.

4.4.1 Deposit geology

Stratiform deposits

Remobilized stratiform deposits are represented by the Lucky Coon, Elsie, King Tut, Mosquito King and Spar deposits on

the Adams Plateau, and by the Sunrise and Red Top deposits in the Clearwater area (Table 4.0, Fig. 4.0, Appendix A). The term stratiform is used here to characterized sulphides rich layers conformable with the surrounding rocks (cf. Glossary of Geology, American Geological Institute, 1979). These deposits on the Adams Plateau are hosted by unit EBG which consists mainly of massive and fragmental greenschist, of intermediate and mafic volcanic affinities, associated with sedimentary units represented by graphitic and siliceous phyllite containing layers of phyllitic limestone, calc-silicate, and phyllitic quartzites. The gangue of these deposits is siliceous; pyrite, the most abundant sulphide, occurs with dark 'black jack' sphalerite and galena. Small amounts of arsenopyrite (absent in the Mosquito King deposit) and chalcopyrite also occur. None of these deposits exhibit clear mineral zonation, and the ratios of the different sulphides are highly variable between, as well as within, the deposits. However, the overall content of galena is greater in these deposits than in those of cluster 1. The mineralization in these deposits can either be cogenetic with the Cambrian unit EBG, or younger and of replacement type (section 4.4.2).

Remobilization of the sulphides during deformation is apparent from concentration and thickening of sulphide horizons in the hinge zone of isoclinal folds. For example (Dickie,

1985) at the Spar deposit sulphides are concentrated in an upright slightly asymmetric fold in which sulphide apparent thickness at the crest is twice that on the limbs; similar features are observed in the Lucky Coon (Fig. 4.1). Faults also offset and/or truncate sulphide bearing strata. On a smaller scale, deformation and remobilization of sulphides are outlined by crystal deformation (steel galena, undulatory extinction in quartz), replacement of arsenopyrite by galena and sphalerite, and overgrowth of euhedral pyrite (observed in polished section from samples of the Lucky Coon and Spar deposits). The stratigraphic level of the sulphide horizons in the Nikwikaia syncline (Lucky Coon, Elsie and King Tut) appear equivalent to the Spar deposit (Dickie, 1985) indicating that these deposits may be contemporaneous. The stratiform nature and apparent continuity of the sulphide lenses in the same stratigraphic unit over 8km suggests that these deposits are syngenetic but remobilized by later folding.

Near Sqwaam Bay, close to the lake shore, mineralized carbonate swells are common in chloritic schist (Agate Bay; Table 4.0, Fig. 4.0, Appendix A). Since the isotopic composition of the lead from these swells is similar to the lead from the stratiform deposits in the plateau, the showing probably represents local concentrations of disseminated cogenetic lead. The thrust fault of Schiarizza and Preto



Figure 4.1 Folded mineralized layers, Lucky Coon deposit.

(1984), assumed to pass slightly north of this deposit, has been relocated southward so that all isotopically-related deposits are within similar thrust slices (Fig. 4.0). (Note that the existence of this fault was questioned in section 4.1.1.)

Two other deposits, Sunrise and Red Top (Table 4.0; Fig. 4.0, Appendix A), plot in cluster 2. These deposits consist of semi-conformable lenses and lenticular sheets of sulphide confined to a specific stratigraphic position in unit EBQ (close to quartzitic and limy zones associated with chloritic quartz-schists that are locally graphitic). The mineralization has a discontinuous but conformable distribution. Host unit EBQ is strongly folded around an easterly trending open antiform that is partly disrupted by faulting. The sulphide zones exhibit evidence of remobilization similar to that of the Lucky Coon, Mosquito King and Spar deposits. The Sunrise and Red Top deposits are classified in old reports as replacement deposits related to the emplacement of the Baldy and/or Raft batholiths (Appendix A), implying that the sulphides were introduced by solutions emanating from intrusions. However, if the assigned Cretaceous age for the batholiths is correct then the foregoing conclusion is untenable on the basis of the lead isotope data, because it plots in the Upper Triassic cluster. However any interpretation related to the intrusive age of the Raft batholith is uncertain until new zircon dates establish a more

reliable crystallization age for the batholith.

Vein deposits

The remaining group of data with isotopic composition plotting in cluster 2 is associated with well defined vein deposits (Table 4.0, Appendix A). The lead data from the vein deposits are indistinguishable from the lead of the above stratiform deposits. The occurrence of these veins is not restricted to any particular unit of the Eagle Bay Formation, and is not spatially clustered (Fig. 4.0). However, their distribution is not totally random and can be categorized as follows:

- 1) The Enargite and Fortuna veins (Table 4.0, Fig. 4.0, Appendix A) trend northward and occur close to well defined faults. These faults are associated with two distinct thrusting events of post-Permian to pre-Jurassic age, and of Late Jurassic age (Section 2.3); the bracketed age of the faulting includes the Upper Triassic.
- 2) The Vavenby, PS-75-185, and White Rock veins (Table 4.0, Fig. 4.0, Appendix A) are hosted by the Tshinakin Limestone. The occurrence of veins in the Cambrian Limestone with Triassic model age indicates the occurrence of an epigenetic Triassic pulse of mineralization.
- 3) The Silver King-Queen vein is part of a major vein system cutting rocks of unit EBG. Since this unit also hosts the above

stratiform deposits, it demonstrates the occurrence of different types of mineralization of equivalent age in similar rocks.

4.4.2 Multiple Interpretation of Lead isotope data

Three possible interpretations are examined below in an attempt to reconcile the lead data with the observed geological features. These can be summarized as: 1) the mineralization is syngenetic and Cambrian, but deformation and/or metamorphism reset the lead isotopic system to an Upper Triassic model age; 2) all mineralization is epigenetic, Upper Triassic in age, and related to an epigenetic event; and 3) the mineralization is cogenetic with its host, and unit EBG, or part of it, is Triassic in age.

Remobilization model

Short term growth of radiogenic lead in the host rocks from time of original deposition (assumed to be Cambrian) to subsequent remobilization (in Jurassic time) coupled with an increase in temperature (capable of starting an efficient leaching and homogenizing process) might be responsible for the resetting of the lead system and for the apparent model age obtained for the stratiform deposits. This model requires production of radiogenic components from the uranium present in the rocks. Rock lithologies which have an upper crustal

protolith are enriched in uranium and therefore in situ growth of uranium daughters is to be expected within rocks derived from such source. The production of radiogenic uranium isotopes generates an increase in the $^{206}\text{Pb}/^{204}\text{Pb}$ ratio without substantially affecting the $^{207}\text{Pb}/^{204}\text{Pb}$ ratio. The radiogenic lead produced would be relatively easy to extract due to its loosely held position in defect structure within the mineral lattice.

Post-depositional accumulation of radiogenic lead in unit EBG is possible, but would be limited by the generally intermediate to mafic nature of the volcanics. Furthermore the processes responsible for the leaching and re-transportation of metals would have to be effective over a long period of time to permit substantial extraction of metals and relative homogenization of lead isotopes (Gulson et al., 1983).

Could intense deformation in the Early Jurassic and/or the Cretaceous have caused remobilization of galena lead isotope ? Certainly the present configuration of the sulphide masses within the deposits (see Fig. 4.1) suggests that remobilization deeply affected the ore and controlled their current distribution. Locally derived radiogenic lead may therefore have been added to the sulphides after their initial formation. In general very little is known about the effect of metamorphism

upon lead isotopic composition (Richards et al., 1981) and even if remobilization can account for general behavior, several inconsistencies arise when details are considered. Radiogenic isotopes released from incompatible unfitted lattice sites during metamorphism might move far enough to allow them to become incorporated into surrounding mineral during remobilization (Doe and Hart, 1963). However only a high temperature regime or extensive hydrothermal activity would permit complete homogenization of the ore. Moreover, one would expect that any remobilization mechanism responsible for such homogenization would require recrystallization to such extent that all primary ore textures would have been obliterated (Le Hurray, 1982). Such an intense process did not occur as metamorphism only reached greenschist facies, and intense hydrothermal alteration observed elsewhere (Homestake deposit, Hoy and Goutier, 1986) is not observed in the deposits on the Adams Plateau.

Thus low temperature alteration processes apparently at best would leave the deposits with an inhomogeneous and scattered isotopic composition (Cumming and Gudiurdis, 1973; Slawson, 1983), but analysis of several samples from the same deposit (Appendix B) reveals that the lead isotopic composition of the deposits do not exhibit such variation (section 3.3.2). Alternatively galena lead isotope evolved in the Jurassic from

Cambrian source rocks with variable uranium content fall along a straight line--not close to a point as in cluster 2.

Comparative evidence between major deposits also negates the hypothesis that remobilization processes caused the Triassic model age obtained for the stratiform deposits. It seems reasonable to assume that if a Mesozoic re-homogenization of the lead yielded the Triassic model age assigned to those deposits hosted by the Cambrian unit EBG, it would also have affected the age of the other deposits hosted by pre-Mesozoic units in the Eagle Bay Formation. The Homestake and Rea Gold deposits should therefore also have had their isotopic composition adjusted by the metamorphic event. This is not the case since their model age is Devonian and concordant with the age of the surrounding rocks. Furthermore the lower galena and lead content of Rea Gold and Homestake deposits should have made them more susceptible to resetting since small additions of metamorphic lead would be more easily discernable from the isotopic composition of deposits containing low amounts of lead--especially when a relatively short time interval separates deposition and metamorphism.

Consequently the Triassic model age obtained for the stratiform deposits hosted by unit EBG is probably not an effect of the Early Jurassic deformational and metamorphic event.

Nevertheless this event, did control their spatial distribution.

Epigenetic, Upper Triassic model

An alternative interpretation for the Triassic model age is that all the deposits with lead composition plotting in cluster 2 are epigenetic veins, or replacement lodes emplaced in older units during an Upper Triassic event. If this is the case the sulphides in the stratiform deposits hosted by the Cambrian unit EBG would have been deposited in favorable stratigraphic horizons from solutions that leached and extracted lead from the surrounding volcanic and sedimentary rocks. Recognition of a magmatic and/or mineralizing event affecting the area in Triassic time would be significant because it might indicate a period of active hydrothermal circulation that supplied radiogenic lead to the rocks of unit EBG just before Jurassic remobilization. No direct evidence of such a major event has been identified in the Adams Plateau-Clearwater area. However the vein deposits which cut the Cambrian Tshinakin Limestone and whose lead isotopic composition fall in cluster 2 are examples of epigenetic mineralization of Triassic age. The association of the sulphide rich horizons with particular stratigraphic levels, and the relationship between the ore and the surrounding rocks suggests strongly that the ore masses were originally controlled by the stratigraphy. The association of the sulphide horizons with chemical sediments indicates that they were

probably deposited contemporaneously with their host unit (EBG) even if clearly remobilized later.

Triassic cogenetic deposits

If the mineralization at the Lucky Coon, Mosquito King and Spar deposits is cogenetic with the host rocks, and the lead model age is accommodated, then unit EBG, or part of it, must be Triassic.

Unit EBG, fault bounded on both sides by other units of the Eagle Bay Formation, consists mainly of massive fragmental greenschist of volcanic affinities associated with an heterogeneous meta-sedimentary succession containing Tshinakin Limestone, the major marker of the Eagle Bay Formation. A correlated limestone unit in the Vavenby area contains Archaeocyathids of Early Cambrian age (Norford in Schiarizza, 1986), which have been used to infer a Cambrian age for the entire unit EBG. The Tshinakin Limestone is immediately underlain and overlain by similar sequences of greenschists. Locally the limestone abruptly lenses out; these terminations reflect original margins of the carbonate bank according to Preto et al. (1980). However, despite the fact that this package was mapped as a single unit representing a continuous succession, alternative interpretation are possible given the structural and stratigraphic complexities of the Eagle Bay

Formation.

It is proposed here that the southern part of unit EBG, depicted in Fig. 4.0 as unit T-EBG, is lithologically distinct from the northern part, and represent an additional thrust slice within the Eagle Bay Formation with a bounding thrust fault on the southern side and near the base of the Tshinakin Limestone. This thrust if present would separate the limestone and the greenschist volcanic rocks to the north from the meta-sedimentary sequence to the south. As presently mapped by Schiarizza and Preto (1984), the meta-sedimentary succession, containing both the folded conglomeratic and the phyllitic quartzite member (sub-units EBGcg and EBGq), occurs only on the southern side of the Tshinakin Limestone. Furthermore, the sub-unit EBGp seems restricted to the area north of the limestone. Although the Tshinakin Limestone is interbedded with greenschist in several places, it is never in direct contact with the metasediments. Even though the metasedimentary succession appears to be in stratigraphic contact, and locally is interdigitated with greenschist, the contact relationships have been obscured by folding. Thus the apparent contact between some of these units could be structural rather than stratigraphic (i.e. deformed and transposed contact).

The division between units EBG and T-EBG also is supported

by marked differences in deformational intensity and style between the Tshinakin Limestone the greenschist volcanics, and the meta-sedimentary sequence. Gentle warping of the Tshinakin limestone contrast with the tight Nikwikaia Lake synform, which was formed by the Colombian Orogeny, and which repeats the phyllitic quartzitic beds (sub-unit EBGq, Fig. 4.0). Older structures within unit T-EBG have not been identified and Devonian orthogneiss has not been mapped. Therefore the T-EBG part of the unit EBG does not contain any recognizable pre-Triassic elements.

Implications of the presence of a Triassic unit within the Eagle Bay Formation are numerous. Certainly more detailed mapping and better structural and stratigraphic understanding are required to resolve whether or not two thrust faulted units (EBG and T-EBG) exist within the presently defined thrust slice EBG (Fig. 4.0). Contact relationships between the Eagle Bay Formation and the Sicamous Formation (exposed on the shores of Shuswap Lake, Fig. 2.0), as well as the age of the Sicamous Formation, are further constraints on the Upper Triassic age for unit T-EBG in the Eagle Bay Formation--this is elaborated on below.

The Sicamous Formation until recently was considered Upper Triassic and viewed as a facies equivalent of rocks of the

Slocan assemblage, but there is no direct paleontological evidence to support this correlation (Okulitch, 1979). The contact between the Sicamous and the Eagle Bay Formation therefore was assumed to be a thrust fault which juxtaposed Devono-Mississippian rocks (unit EBA) on Upper Triassic rocks of the Sicamous Formation (Okulitch, 1979). However, recent mapping and drill core from the upper contact between the Sicamous and the Eagle Bay Formation in the Blind Bay area (Daughtry in Preto and Schiarizza, 1985) supports a gradual transition between a limestone member of the Sicamous Formation and a chloritic green calcareous schist of the Eagle Bay Formation. This conformable contact relationship between these two formations has been interpreted in two different ways:

1. The Sicamous Formation underlies Devono-Mississippian unit EBA of the Eagle Bay Formation and is therefore older (i.e. Cambro-Ordovician) than unit EBA. In this case some limestone members of the Sicamous Formation could be correlative with the Index Formation of the Lardeau Group in the Kootenay Arc (Okulitch, pers. comm., 1986).
2. The contact between the Sicamous and the Eagle Bay Formation is gradual, even though not necessarily conformable, and inverted by a synformal structure overturned to the south (Daughtry, pers. comm., 1986). The Sicamous then could be Upper Triassic and part of it could be equivalent to rocks of the Slocan Group or to some black shale of the Nicola Group. These

shales, which may represent a deeper depositional facies of the Sicamous Formation form a more or less continuous band down to the Vernon area where they contains conodonts of Norian age (Daughtry, pers. comm., 1986; Okulitch, 1979). However, because direct paleontological evidence is lacking near Adams Lake, and structural and stratigraphic relationships ambiguous, neither of the two interpretations above can be unequivocally favored or ruled out.

Imbrication of Triassic rock sequences within a succession with peri-cratonic affinities has been documented by Ross et al. (1985) from the Crooked Lake area--100km east of Williams Lake. In this area a Triassic sequence of black phyllites, correlated to the Quesnellia terrane, were mechanically imbricated within the Snowshoe Group, which is part of the Barkerville Terrane. A similar type of imbrication could be possible within the Eagle Bay Formation. However, the lead isotopic composition of the deposits hosted by unit EBG are unlike those hosted elsewhere by Quesnellia rocks (and therefore any Nicola Group related rocks), which have lead isotopic composition that plot below the shale curve (Andrew, 1982) rather than in the position of cluster 2. Correlation of unit T-EBG with a Slocan type assemblage would be better supported by lead isotopic evidence since at least part of the Slocan Group lead was probably derived from cratonic rocks (D. Gosh, in Logan 1985).

4.4.3 Summary

Although model ages for stratiform deposits with lead isotopic composition enclosed by cluster 2 is similar to, or close to, the orogenic and metamorphic Early Jurassic Colombian Orogeny, it is unlikely that the lead isotope composition of the stratiform sulphide ores from the Adams Plateau (hosted by the unit EBG) was affected by metamorphism to the point of complete resetting. The Triassic model age for the stratiform deposits in cluster 2 can be interpreted as follow: 1) the mineralization is of replacement type and related to a Triassic event, in which case cluster 2 can be used to fingerprint that event, or 2) the mineralization is cogenetic with unit EBG and, a structural subdivision of the unit EBG into two separate units of Cambrian and Triassic age is required. Until the origin of these stratiform deposits is more clearly defined or the suggestion that a thrust exists within the unit EBG is tested in the field, these are equally valid.

4.5 LEAD DATA BETWEEN CLUSTER 2 & 3

Model ages for deposits with lead isotopic compositions that plot between cluster 2 and 3 are not interpretable. The random distribution of some of these data probably reflects an highly radiogenic component generated by proximal uranium and thorium mineralization (i.e. Rexspar deposit Table

4.0, Fig. 4.0, Appendix A).

The highly anomalous lead isotopic composition in galena from the Rexspar deposits is associated directly with the high uranium and thorium concentration found there. This deposit, hosted by a tuffaceous trachytic to andesitic member of unit EBA, contains two mineralized zones: an uranium bearing zone composed of abundant pyrite associated with fluorophlogopite, and a fluorite zone containing traces of galena and molybdenite but mainly barren of uranium and thorium. A K-Ar date of 236 ± 8 Ma (Preto, 1977) obtained from fluorophlogopite at Rexspar ruled out the Cretaceous Baldy batholith as a potential source for the mineralization. Preto (1977) therefore proposed that the mineralization was 'syngenetic' with the host rocks. The $^{207}\text{Pb}/^{204}\text{Pb}$ value for the galena at Rexspar (Table 3.3) is much greater than the average value for the other deposits hosted by the Eagle Bay Formation; it consequently plots well above the remodeled curve in Figure 3.3. The $^{206}\text{Pb}/^{204}\text{Pb}$ and $^{208}\text{Pb}/^{204}\text{Pb}$ values (Table 3.3) are not as extreme and fall within the expected range for the deposit of the Eagle Bay Formation, however, since Rexspar is likely cogenetic with the Devono-Mississippian sequence, these values should be lower and within the range of values delimited by the deposits in cluster 1.

The Foghorn, Rouge, Birch Island and Tindal deposits (Table 4.0, Fig. 4.0, Appendix A) are veins in an area dominated by the same felsic volcanic rocks (Devonian unit EBA--trachytic member) that host the Rexspar deposit. The lead data for these epigenetic veins fall to the right of cluster 2. The high lead ratios reflect incorporation in the mineralizing solutions of a highly radiogenic component generated by the in situ decay of uranium and thorium in the surrounding rocks, most of which was probably generated and released from uranium and thorium rich minerals like those in the Rexspar deposit. Model age determinations for these veins is ambiguous and involves consideration of a short term growth of radiogenic lead from a locally uranium and thorium rich environment. Consequently the remodeled curve cannot be used directly to estimate the model age for these veins. Because an increase in radiogenic lead would generate model ages younger than the mineralization event and the lead isotopic composition is less than that associated with the mineralization caused by the Baldy batholith (cluster 3), these veins more likely are related to the Jurassic deformation associated with the Colombian orogeny. However new older dates from the Raft batholith (Jung, pers. comm., 1986) may link the formation of these veins to its intrusion.

The Fluke deposit (Table 4.0, Fig. 4.0, Appendix A) consists of discontinuous sulphide rich layers that are

semi-conformable with the shistosity and compositional layering of host unit EBG. The sulphide zones associated with a carbonate-rich schist member therefore appear to be a true replacement. Proximity of the deposit to granitic intrusions may indicate that the mineralization was concentrated in the limy horizons by lateral circulation of fluids emanating from the intrusion. The lead plots (Fig 3.3 to 3.5) for the Fluke deposit lie between cluster 2 and 3, but it is closest to cluster 3. The slightly lower lead isotopic composition, compared to those from veins of cluster 3, is probably related to a larger component of wallrock lead.

4.6 CLUSTER 3: CRETACEOUS VEINS

The Leemac vein, two unclassified small sized occurrences, and the stratiform Beca deposit plot in cluster 3 (Table 4.0, Fig.4.0, Appendix A).

The Leemac vein, in the Cretaceous Baldy batholith has a lead isotopic composition coincident with the Cretaceous isochron on the remodeled curve (cluster 3; Fig. 3.3 to 3.5). This relationship suggests a genetic link between the intrusion and the mineralization. The fact that the lead isotopic composition of the vein in the batholith plots on the remodeled curve also indicates that the lead of the batholith has evolved

from a similar protolith source as the surrounding rocks of the Eagle Bay Formation. Specifically, the lead isotopic composition reflects the direct influence of an upper crustal basement in the origin and generation of the intrusion; this supports the interpretation that the roots of the batholith are in the adjacent Shuswap Complex (Okulitch, 1979; see section 2.4.4).

Cluster 3, therefore, is the fingerprint for Cretaceous deposits that are cogenetic with the intrusion of the batholith. Accordingly, two small mineralized siliceous zones carrying variable values of lead, zinc and silver, sampled in the vicinity of Lichen Mountain on the Adams Plateau (Red Mineral Claim 1 and 3, Table 4.0, Fig. 4.0, Appendix A) that were previously interpreted as syngenetic exhalative deposits, seems more appropriately related to a small granitic plug in the Scotch Creek area (Fig. 4.0) which is probably a satellite of the Baldy batholith.

Four other showings around Lichen Mountain on Adams Plateau: Pet, Red mineral claim 2, Orell 5P and Silver King-A (Table 4.0, Fig. 4.0, Appendix A) yielded lead isotopic signatures that were distinctly different from the two Cretaceous showings by falling in cluster 2 instead of cluster 3. The spatial relationships between these unclassified

occurrences and the Spar and Mosquito King, coupled with their isotopic composition, indicates that they probably represent local accumulation of cogenetic mineralization similar to the other nearby stratiform deposits. The distinction between two different types of mineralization among these six mineralized occurrences is a good example of the applicability of the lead method for discriminating different ages and origin for otherwise similar looking deposits.

The Sonja vein (Table 4.0, Fig. 4.0, Appendix A) cuts through the Devonian unit EBA near Clearwater. It occurs as a discontinuous silicified zone along the side of a major dyke from geological evidence, and lead data that plots in cluster 3, the mineralization on the Sonja property is epigenetic and Cretaceous.

Another deposit with lead data plotting in cluster 3 is the Beca deposit (Table 4.0, Fig. 4.0, Appendix A). However, in all lead diagrams (Figs. 3.3 to 3.5) Beca plots furthest from the mean value of cluster 3. Interpretation regarding the geological setting of the Beca property is uncertain. The deposit has been classified as a syngenetic volcanogenic deposit (Preto et al., 1985; BCDM Assessment Report no. 7040) because it contains conformable sulphide rich horizons associated with pyritic cherty bands, and because it occurs within the same

Devonian felsic volcanic sequence as the Homestake and Rea Gold deposits (unit EBA). However the lead isotopic signature of the Beca deposit falls in cluster 3, and is markedly distinct from the lead from the Rea Gold, Homestake and Ford deposits. These isotope data indicate that the mineralization is epigenetic and Cretaceous rather than syngenetic and Devonian-Mississippian. Zircons from Beca property (Fig. 4.0), yielded a discordant chord intercepting the concordia curve at points corresponding to 399 and 100Ma (Preto, 1981). The Devonian date is interpreted as the time of crystallization for the volcanics. A subsequent Cretaceous event is advocated to account for lead loss and resulting zircon discordance. It is interesting to note that the Cretaceous age of this subsequent event corresponds to the model age of cluster 3. Therefore lead remobilization and homogenization of the lead in the Cretaceous might have occurred. The Cretaceous intrusion of the Baldy batholith offers greater potential for generation of circulating solutions than does the Jurassic event related to deformation and metamorphism. Nevertheless the same argument against the re-homogenization process (see section 4.2.2) applies here, as the lead isotopic composition of the deposits hosted by the same Devonian unit (the cogenetic deposits of cluster 1) has not been re-homogenized to a Cretaceous age. Unfortunately, the Beca deposit is not located closer than other deposits in the area to the batholith and this cannot be used to justify why its lead

composition could have been more significantly affected by the intrusion. The mineralization might be an epigenetic replacement.

4.7 LEAD DATA BEYOND CLUSTER 3

Mineralization of the June vein is probably late and related to a Tertiary event since its lead data plots close to a Tertiary model age along the remodeled curve. The only uncertainty surrounding this interpretation is that, although it is based on three duplicate analysis from the same deposit, no analysis from any other deposit has a similar lead isotopic composition. Tertiary lamprophyre dykes are widespread in the map area and occur in close vicinity of the Mosquito King, Spar and Fluke deposits. The isotopic signature of lead mineralization from cross-cutting structures, spatially related to these dykes, cannot be statistically distinguished from the lead from the massive sulphide zones (Appendix C). Consequently, the intrusion of these late dykes did not affect the overall lead isotopic composition of those deposits. If the Eocene thermal and deformational event did affected the Eagle Bay Formation, the paucity of lead of Tertiary composition is another argument against remobilization as a common process responsible for variations in the lead isotopic composition of galena.

4.8 SUMMARY

The lead isotopic composition of deposits hosted by the Eagle Bay Formation indicates that three pulses of mineralization were responsible for sulphide concentration within the units of the Formation. The oldest mineralization identified in the Eagle Bay Formation is represented by cluster 1 with a model age of Devonian. This cluster characterized lead from polymetallic deposits which are cogenetic with felsic to intermediate volcanic rocks of Devonian-Mississippian age. Therefore, cluster 1 can be used to fingerprint such type of mineralization occurring in the Eagle Bay Formation.

The second period of mineralization is Upper Triassic, and is represented by cluster 2. This cluster contains almost half of the deposits--mainly veins and stratiform deposits--sampled for this study. The vein deposits indicate that there was a pulse of mineralization occurring during that period that is mainly characterized by infilling of suitable structures. The stratiform deposits within this cluster may be either replacement or cogenetic in origin. If cogenetic, the part of the unit which host these deposits must be Upper Triassic rather than Cambrian as currently mapped (Schiavizza and Preto, 1984) since resetting of the lead isotopic composition by

metamorphism cannot account for the Triassic model age of these deposits. Based upon the upper crustal signature of the Eagle Bay Formation, the Upper Triassic unit would probably be equivalent to rocks of the Slocan Group.

Some deposits, which have their lead isotopic composition falling outside of and to the right of cluster 2, are hosted by an uranium rich member of the formation which is probably the cause for the radiogenic signature. Finally, the last major period of mineralization recorded by the lead isotope data from this study is mid-Cretaceous and represented by cluster 3. This event is related to the intrusion of the Baldy batholith. Lead isotopic compositions, of Tertiary model age, are markedly absent and indicate that even if the Formation was affected by a thermal Tertiary event no important mineralizing processes were associated with it.

5. CONCLUSIONS

This lead isotopic study of 37 mineralized occurrences hosted by the Eagle Bay Formation in the Adams Plateau-Clearwater area allowed evaluation of the applicability of the 'shale' curve of Godwin and Sinclair (1981) to deposits in the Adams Plateau-Clearwater area. The lead isotopic composition of these deposits plot generally along the 'shale' curve indicating that the model is substantially correct. This shows that the lead source is upper crustal in origin, was derived from autochthonous portion of the Canadian Cordillera, and involved Precambrian basement under the Eagle Bay Formation. It also reinforced the correlation of the Eagle Bay Formation with other peri-cratonic successions, particularly in the Kootenay Arc and Barkerville Terranes.

The 'shale' curve was inadequate for precise model age determination from the galena-lead data from the Eagle Bay Formation. Better coincidence of the data was obtained with a remodeled curve using 2.0Ga as departure time from the average growth curve of Stacey and Kramers (1975). This curve has the same u value as the 'shale' curve, but has a lower w value of 45.35. The 2.0Ga departure time approximates the time of formation of the Cordilleran crust, and was chosen because it corresponds to ages determined by others for the Shuswap

Metamorphic Complex (cf. Duncan, 1982).

The lead isotopic composition of galena from the deposits in the Eagle Bay Formation plot in three distinct clusters along the remodeled curve. The Devonian cluster 1 encloses lead isotopic compositions which characterize cogenetic mineralization associated with Devonian-Mississippian volcanic rocks. This cluster therefore can be used to fingerprint polymetallic volcanogenic deposits hosted by the Eagle Bay Formation. Similarly, the mid-Cretaceous cluster 3 can be used to distinguish vein deposits related to the intrusion of the Baldy batholith and of its satellites. The Upper Triassic cluster 2 contains deposits of various types so that a unique interpretation cannot apply to all of the deposits represented. Some of them are epigenetic veins, and their formation might be related to juxtaposition of the Fennell Formation with the Eagle Bay Formation, or to a yet undefined event which affected the area in the Triassic. The stratiform deposits on the Adams Plateau, which also plot in that cluster, also may have formed during such event, however, if the mineralization in these deposits is cogenetic with the Cambrian unit EBG, the interpretation of the lead model age imply stratigraphic reconsideration and the unit EBG should be subdivided into two distinct members of Cambrian (unit EBG), and of Upper Triassic (unit T-EBG) age to accommodate the data.

The galena lead isotope study developed here further illustrates the applicability of the common lead method in categorizing mineral deposits within a given region. Recognition of a lead isotopic field that 'fingerprints' the deposits hosted by the Eagle Bay Formation has important implications for exploration programs by providing a curve from which the age and general genesis of any new mineralized discoveries in the Adams Plateau-Clearwater area can be assessed. The distinction of Triassic unit T-EBG from unit EBG cannot be settled solely by the lead isotopic composition of ore lead. However the lead isotope data presented here provide constraints which any successful interpretation must satisfy.

REFERENCES

- AGGARWAL, P.K., and NESBITT, B.E. 1984. Geology and geochemistry of the Chu Chua massive sulphide deposit, B.C. *Economic Geology*, 79, pp. 815-825.
- ANDREW, A. 1982. A lead isotope study of selected precious metal deposits in British Columbia. Unpublished M.Sc. Thesis, University of British Columbia.
- ARMSTRONG, R.L. 1986. Mesozoic and early Cenozoic magmatic evolution of the Canadian Cordillera. In *Rodgers Symposium Volume*, Geological Society of America, Special Volume, in press.
- ARMSTRONG, R.L., and HEIN, S.M. 1973. Computer simulation of lead and strontium isotopes evolution in the earth's crust and upper mantle. *Geochimica Cosmochimica Acta*, 37, pp. 1-8.
- ARMSTRONG, R.L. 1968. A model for the evolution of strontium and lead isotopes in a dynamic earth. *Review Geophysic*, 6, pp. 175-199.
- BREVART, O., DUPRE, B., and ALLEGRE, C.J. 1982. Metallogenic provinces and the remobilization process studied by lead isotopes: Lead-zinc ore deposits from the southern Massif Central France. *Economic Geology*, 77, pp. 564-575.
- BROCK, R.B. 1934. The metamorphism of the Shuswap Terrane of British Columbia. *Journal of Geology*, 42, pp. 673-699.
- BROWN, R.L., and READ, P.B. 1983. Shuswap terrane of British Columbia: A Mesozoic "core complex". *Geology*, 11, pp. 164-168.
- CANNON, R.S., PIERCE, A.P., and ANTWEITER, J.C. 1971. Suggested uses of lead isotopes in exploration. *Proc. Third Intern. Geoch. Explor. Symp. Canad. Inst. Mining Metallur. Soc. Spec. Vol. 11*, pp. 457-463.

- CAMPBELL, R.B. 1973. Structural cross section and tectonic model of the southeastern Canadian Cordillera. Canadian Journal of Earth Sciences, 10, pp. 1607-1620.
- CAMPBELL, R.B., OKULITCH, A.V. 1973. Stratigraphy and structure of the Mount Ida Group, Vernon (82L), Adams Lake (82M), and Bonaparte (92P) map-areas. Geological Survey of Canada, Report of Activities, Part A, paper 1973-1, pp. 21-23.
- CAMPBELL, R.B., and TIPPER, H.W. 1971. Geology of Bonaparte Lake map area, British Columbia. Geological Survey of Canada, Memoir 363, 100 p.
- COOPER, J.A., REYNOLDS, P.H., RICHARDS, J.R. 1969. Double-spike calibration of the Broken Hill standard lead. Earth and Planetary Science Letters, 6, pp. 467-478.
- COOPER, J.A., RICHARDS, J.R. 1966. Solid-Source lead isotope measurements and isotopic fractionation. Earth and Planetary Science Letters, 1, pp. 58-64.
- CONEY, P.J. 1980. Cordilleran metamorphic core complexes: An overview; in Cordilleran Metamorphic Core Complexes, ed. M.D. Crittenden, J.R. Coney, P.J., Davis, G.H.; Geological Society of America, Memoir 153 pp. 4-34.
- CUMMING, G.L., and RICHARDS, J.R. 1975. Ore lead isotope ratios in a continuously changing earth. Planetary Earth and Science Letters, 28, pp. 155-171.
- CUMMING, G.L., and GUDJURGIS, P.J. 1973. Alteration of trace lead isotopic ratios by post-ore metamorphic and hydrothermal activity. Canadian Journal of Earth Sciences, 10, pp. 1782-1789.
- DALY, R.A. 1915. A geological reconnaissance between Golden and Kamloops, British Columbia, along the Canadian Pacific Railway. Geological Survey of Canada, Mem. 68, 260 p.
- DAWSON, G.M. 1898. Shuswap Sheet map. Geological Survey of Canada.

- DICKIE, G.J. 1985. Exploration for Ag-Pb-Zn sulphide deposits in a multiply-deformed terrain in southern British Columbia. Minequest Exploration Associates Limited. Unpublished report.
- DOE, B.R., and ZARTMAN, R.E. 1979. Plumbotectonics, the phanerozoic, in Barnes H.L., ed., Geochemistry of hydrothermal ore deposits, New York, Wiley Interscience, pp. 20-70.
- DOE, B.R., and STACEY, J.S. 1974. The application of lead isotopes to the problems of ore genesis and prospect evaluation. A review. Economic Geology, 69, pp. 757-777.
- DOE, B.R. 1970. Lead isotopes, minerals, rocks, and inorganic materials. Monograph series of theoretical and experimental studies Nb. 3. Springer-Verlag ed., 137 p.
- DOE, B.R., and HART, S.R. 1963. The effect of contact metamorphism on lead in potassium feldspars near the Eldora stock, Colorado. Journal of Geophysical Research, 68, p. 3521.
- DUNCAN, I.J. 1982. The evolution of the Thor-Odin gneiss dome and related geochronological studies. Unpublished Ph.D. thesis University of British Columbia, 345 p.
- FAURE, G. 1977. Principles of isotope geology. New York, J.Wiley & Sons ed., 464 p.
- FYSON, W.K. 1970. Structural relations in metamorphic rocks, Shuswap Lake area, British Columbia. in Structure of the Southern Canadian Cordillera, ed. J.O. Wheeler; Geological Association of Canada, Special paper 6, pp. 107-122.
- GODWIN, C.I., and SINCLAIR, A.J. 1982. Average lead isotopic growth curves for Shale-hosted Zn-Pb deposits in the Canadian Cordillera. Economic Geology, 77, pp. 675-690.
- GODWIN, C.I., and SINCLAIR, A.J. 1981. Preliminary interpretations of lead from shale-hosted deposits in British Columbia and Yukon Territory. B.C. Ministry of Energy, Mines & Pet. Res.

Geological Fieldwork 1980, paper 1981-1, pp. 185-190.

GOUTIER, F., GODWIN, C.I., and HOY, T. 1985. Mineral deposits of the Birk Creek area: An introduction to a metallogenic study of the Adams Plateau-Clearwater area (82M). B.C. Ministry of Energy, Mines & Pet. Res. Geological Fieldwork 1984, paper 1985-1, pp. 67-76.

GULSON, B.L., PERKINS, W.G., and MIZON, K.J. 1983. Lead isotope studies bearing on the genesis of copper orebodies at Mount Isa, Queensland. *Economic Geology*, 78, pp. 1466-1504.

HART, S.R., and TILTON, T.R. 1963. Geochronology. *Science*, vol 140, Nb. 3565, pp. 357-ss.

HICKSON, C.J. 1986. Quaternary volcanism in the Wells Gray-Clearwater area, east central British Columbia. Unpublished Ph.D thesis, The University of British Columbia.

HOLMES, A. 1946. An estimate of the age of the earth. *Nature*, Vol. 159, p. 127.

HOUTERMANS, F.G. 1946. The isotope ratios in natural lead and the age of uranium. *Naturwissenschaften*, Vol. 33, pp. 185-186.

HOY, T., and GOUTIER, F. 1986. Rea Gold (Hilton) and Homestake volcanogenic sulphide barite deposits. Southeastern British Columbia (82M/4W). B.C. Ministry of Energy, Mines & Pet. Res. Geological Fieldwork 1985, paper 1986-1, pp. 59-68.

HUTCHISON, R.W. 1973. Volcanogenic sulphide deposits and their metallogenic significance. *Economic Geology*, 68, pp. 1223-1246.

JAMES, D.H. 1949. Geology of the Adams Plateau central British Columbia. Unpublished report for Dresser Minerals Canada, 47 p.

JONES, A.G. 1959. Vernon map area, British Columbia. Geological Survey of Canada, Memoir 296.

- JOURNEY, M., AND BROWN, R.L. 1986. Major tectonic boundaries of the Omineca Belt in southern B.C: A progress report. Geological Survey of Canada, Current Research Part A, paper 86-1A, pp. 81-88.
- JUNG, A. 1986. Geochronometry and geochemistry of the Tuya, Takomkane, Raft and Baldy Batholiths, west of the Shuswap Metamorphic Complex, south-central British Columbia. Unpublished BSC thesis, University of British Columbia, 127 p.
- KANASECWICH, E.R. 1968. The interpretation of lead isotopes and their geological significance. Radiometric Dating for geologists. Hamilton & Farquhar ed., pp. 147-223.
- KOPPEL, V., and GRUNENFELDER, M. 1979. Isotope geochemistry of lead. Lecture In Isotope Geology, E.Jager & J.C.Hunziker, Springer Verlag ed., 329 p.
- LAMBERT, I.B., and SATO, T. 1974. The Kuroko and associated ore deposits of Japan: A review of their features and metallogenesis. Economic Geology, 69, pp. 1215-1236.
- LeHURAY, A.P. 1982. Lead isotopic patterns of galena in the Piedmont and Blue Ridge Ore deposits, southern Appalachians. Economic Geology 77, pp. 335-351.
- LOGAN, J.W. 1986. Geochemical constraints on the genesis of AG-PB and ZN deposits, Sardon, British Columbia. Unpublished M.Sc. thesis, University of British Columbia, 178 p.
- McMILLAN, W.C. 1980. CC prospect Shuswap mountain (92P/8E). B.C. Ministry of Energy, Mines & Pet. Res. Geological Fieldwork, 1979, paper 1980-1, pp. 37-48.
- MONGER, J.W.H., BERG, H.C. 1985. Lithotectonic terrane map of western Canada and southeastern Canada.
- MONGER, J.W.H., PRICE, R.A., and TEMPELMAN-KLUIT, D.J. 1982. Tectonic accretion and the origin of the two major metamorphic

and plutonic welts in the Canadian Cordillera. *Geology*, 10, pp. 70-75.

MORTENSEN, J.K., MONTGOMERY, J.M., and FILLIPONE, J.A. in press. U-Pb zircon, monazite and sphene ages for granitic orthogneiss of the Barkerville Terrane, east-central British Columbia. *Canadian Journal of Earth Sciences*.

OKULITCH, A.V. 1984. The role of the Shuswap Metamorphic Complex in Cordilleran tectonism: A review. *Canadian Journal of Earth Sciences*, 21, pp. 1171-1193.

OKULITCH, A.V. 1979. Lithology, stratigraphy, structure and mineral occurrences of the Thompson-Shuswap-Okanagan area British Columbia. Geological Survey of Canada, open file 637.

OKULITCH, A.V., and CAMERON, B.E.B. 1976. Stratigraphic revisions of the Nichola, Cache Creek and Mount Ida Groups based on conodont collections from the Western margin of the Shuswap Metamorphic Complex, south central British Columbia. *Canadian Journal of Earth Sciences*, 13, pp. 44-53.

OKULITCH, A.V. 1975. Stratigraphy and structure of the Western margin of the Shuswap Metamorphic Complex; Vernon (82L) and Seymour Arm (82M) map area British Columbia Geological Survey of Canada, Current Research, Paper 75-1, part A, pp. 27-28.

OKULITCH, A.V., WANLESS, R.K., and LOVERIDGE, W.D. 1975. Devonian plutonism in south central B.C. *Canadian Journal of Earth Sciences*, 12, pp. 1760-1769.

OVERSBY, V.M. 1974. New look at the lead isotope growth curve. *Nature*, 248, pp. 132-133.

OZARD, J.M., and RUSSELL, R.D. 1970. Discrimination in solid source lead isotope abundance measurement. *Earth and Planetary Science Letters*, 8, pp. 331-336.

PALMER, A.R. 1983. The decade of North American Geology 1983 geologic time scale. *Geology*, 11, pp. 503-504.

- PARRISH, R., CARR, S., and PARKINSON, D. 1985. Metamorphic complexes and extensional tectonics, southern Shuswap Complex, southeastern British Columbia. Geological Society of America, Cordilleran Section Guidebook, pp. 12-1 to 12-15.
- PATTERSON, C.C. 1956. Age of meteorites and the earth. *Geochimica Cosmochimica Acta*, 10, pp. 230-237.
- PRETO, V.A., and SCHIARIZZA, P. 1985. Geology and mineral deposits of the Adams Plateau - Clearwater region. Geological Association of America, Cordilleran Section Meeting, guidebook, Field trip 16, pp. 1-11.
- PRETO, V.A. 1981. Barriere Lakes-Adams Plateau area (82M/4,5W; 92P/1E). B.C. Ministry of Energy, Mines & Pet. Res. Geological Fieldwork 1980, paper 1981-1, pp. 15-23.
- PRETO, V.A., McLAREN, G.P., and SCHIARIZZA, P.A. 1980. Barriere lakes- Adams Plateau area (82L/13E; 82M/4,5W; 92P/1E,8E). B.C. Ministry of Energy, Mines & Pet. Res. Geological Fieldwork 1979, paper 1980-1, pp. 28-36.
- PRETO, V.A. 1979. Barriere Lakes-Adams Plateau area (82L/13E; 82M/4,5W; 92P/1E,8E). B.C. Ministry of Energy, Mines & Pet. Res. Geological Fieldwork 1978, paper 1979-1, pp. 31-37.
- PRETO, V.A. 1977. Rexspar (82M/12W). Geology in B.C. 1977-1981 B.C. Ministry of Energy, Mines & Pet. Res. pp. 45-56.
- READ, P.B., and BROWN, R.L. 1981. Columbia river fault zone: southeastern margin of the Shuswap and Monashee Complexes, southern British Columbia. *Canadian Journal of Earth Sciences*, 18, pp. 1127-1145.
- RESSOR, J.E., and MOORE, J.M. 1970. Thor-Odin gneiss dome, Shuswap Metamorphic Complex. Geological Survey of Canada, Bull. 195, 134 p.
- RICE, H.M.A., and JONES, A.G. 1948. Salmon Arm map area, map 48-4A. Geological Survey of Canada, paper 48-4.

- RICHARDS, J.R. 1962. Age of the earth crust and lead model age. *Nature*, 195, p. 65.
- RICHARDS, J.R., FLETCHER, I.R., and BLOCKLEY, J.G. 1981. Pilbara galenas: Precise isotopic assay of the oldest Australian leads; model ages and growth-curve implications. *Mineralium Deposita*, 16, pp. 7-30.
- ROSS, J.V., and FILLIPONE, J.A. in press. Details of a convergent zone associated with accretion of Late Paleozoic to Early Mesozoic allochthons to the western margin of North America, central British Columbia.
- ROSS, J.V. 1974. A Tertiary thermal event in South-Central British Columbia. *Canadian Journal of Earth Science*, 11, pp. 1116-1121.
- RUSSELL, R.D., and FARQUHAR, R.M. 1960. *Lead Isotopes in Geology*. Interscience, New York ed., 243 p.
- SATO, K., and SASAKI, A. 1976. Lead isotopic evidence on the genesis of pre-Cenozoic stratiform sulphide deposits in Japan. *Geochemical Journal*, 10, pp. 197-203.
- SATO, K., DELEVAUX, M.H., and DOE, B.R. 1981. Lead isotope measurements ores, igneous and sedimentary rocks from the Kuroko mineralization area. *Geochemical Journal*, 15, pp. 135-140.
- SCHIARIZZA, P.A. 1986. Geology of the Eagle Bay Formation between the Raft and Baldy Batholiths (82M/5,11,12). B.C. Ministry of Energy, Mines & Pet. Res. Geological Fieldwork 1985, paper 1986-1, pp. 89-94.
- SCHIARIZZA, P.A. 1986b. Geology of the Vavenby area. NTS 82M5,11,12. B.C. Ministry of Energy, Mines & Pet. Res. Open file.
- SCHIARIZZA, P.A., and PRETO, V.A. 1984. Geology of the Adams

Plateau-Clearwater area. B.C Ministry of Energy, Mines & Pet. Res. Map Nb. 56.

SCHIARIZZA, P.A. 1982. Clearwater area (82M/12W; 92P/8E,9E). B.C. Ministry of Energy, Mines & Pet. Res. Geological Field-work 1981, paper 1982-1, pp. 59-67.

SCHIARIZZA, P.A. 1981. Clearwater area (82M/12W; 92P/8E,9E). B.C. Ministry of Energy, Mines & Pet. Res. Geological Field-work 980, paper 1981-1, pp. 159-164.

SLAWSON, W.F. 1983. Isotopic composition of lead from a paleo-island arc: Shasta California. Canadian Journal of Earth Sciences, 20, pp. 1521-1527.

SOLOMON, M. 1976. Volcanic massive sulphide deposits and their host rocks: A review and explanation. in Handbook on strata-bound and stratiform ore deposits, K.H. Wolf ed. Elsevier Amsterdam, Vol. 2, pp. 21-50.

STACEY, J.S., and KRAMERS, J.D. 1975. Approximation of terrestrial lead isotope evolution by a two stage model. Earth and Planetary Sciences Letters, 26, pp. 207-221.

STACEY, J.S., DELEVAUX, M.H., and ULRICH, T.J. 1969. Some triple filament lead isotope ratio measurements and an absolute growth curve for single-stage leads. Earth and Planetary Science Letters, 6, pp. 15-25.

STANTON, R.L., and RUSSELL, R.D. 1959. Anomalous leads and the emplacement of lead sulphide ores. Economic Geology, 54, pp. 588-607.

STEIGER, R.W., and JAGER, E. 1977. Subcommittee on geochronology convention on the use of decay constants in geo and cosmochronology. Earth and Planetary Science Letters, 36, p. 359.

STRUICK, L.C. 1986. Imbricated terranes of the Cariboo gold belt with correlations and implications for tectonics in southern British Columbia. Canadian Journal of Earth Sciences, Vol. 23,

pp. 1047-1061.

TATSUMOTO, M., KNIGHT, J.R., and ALLEGRE C.J. 1973. Time differences in the formation of meteorites as determined from the ratio of lead 207 to lead 206. *Science*, 180, p. 1279.

UGLOW, W.L. 1922. Geology of the north Thompson Valley map-area, British Columbia. Geological Survey of Canada, Summary Report 1921, Part A. pp. 72-106.

WANLESS, R.K., STEVENS, R.D., LACHANCE, G.R., and RIMSAITE, J.Y.H. 1966. Age determinations and geological studies: K-Ar isotopic ages, Report 5. Geological Survey of Canada, paper 65-17, 101 p.

WATSON, P.H. 1981. Genesis and zoning of silver-gold veins in the Beaverdell area, south-central British Columbia. Unpublished M.Sc. thesis University of British Columbia, 156 p.

WHEELER, J.O., and GABRIELES, H. 1972. The Cordilleran structural provinces. In R.A. Price and R.J.W. Douglas ed. Variations in tectonic styles in Canada. Geological Association of Canada Special paper 11, pp. 1-18.

YORK, D. 1969. Least squares fitting of a straight line with correlated errors. *Earth and Planetary Science Letters*, 5, pp. 320-324.

ZARTMAN, R.E. 1974. Lead isotopic provinces in the Cordillera of the western United States and their geologic significance. *Economic Geology*, 69, pp. 792-805.

APPENDIX A

ADAMS PLATEAU-CLEARWATER AREA
DEPOSIT DESCRIPTIONS

The following descriptions constitute a brief summary of literature review on the deposits of the Adams Plateau-Clearwater area augmented by observations, and in some case detailed work, made by the writer in the summers 1984 and 1985. The compilation map of Schiarizza et al. (1984) has been used to assign lithologic names to host units of the deposits. The abbreviated names for these units (and subunits) appear in parentheses. Descriptions of these units and subunits appear on Schiarizza's map (op. cit.) and in BCDM fieldwork papers from Schiarizza and/or Preto on the Adams Plateau Clearwater area between 1978 and 1986.

Table A.1: Mineral deposits in the Adams Plateau-Clearwater Area

Deposit Name	Deposit Type
ADAMS PLATEAU AREA	
Beca	Stratabound
Lucky Coon	Stratiform/Remobilized
Spar	Stratiform/Remobilized
Mosquito king	Stratiform/Remobilized
BC Zn 1	Disseminations
Crowfoot Mtn	Replacement
Ford property	Volcanogenic
Silver king	Vein
Silver king-Queen	Vein
Pet	Vein
Red Mineral Claims	Vein
JOHNSON LAKE AREA	
Agate Bay	Mineralized pods
Twin Mountain	Vein
Art	Vein
Homestake	Volcanogenic/polymetal.
Rea Gold	Volcanogenic/polymetal.
BARRIERE LAKES AREA	
Birk Creek Showings	Stratiform/Volcanogenic
Enargite	Vein
Fortuna	Vein
White Rock	Vein
June/Kajun	Vein
Broken Ridge	Disseminations
Leemac	Vein
VAVENBY-CLEARWATER AREA	
Chu-Chua	Volcanogenic/cyprus
Foghorn	Vein
Rexspar	Volcanogenic/Uranium
Mt McClennan	Replacement
Vaverby	Vein
Ps-75-185	Vein
Sonja	Vein
Birch Island	Vein
Tindal	Vein

ADAMS PLATEAU AREA:

BECA:

Also known as: Quest Group, Lucky Strike, Rhode Island,
Lakeview-Joe, Tom

Minfile number: 082M-054,055

Mineral Inventory number: 82M4-PB4

Map number: 007; Lat. 51.050N long. 119.710W

Production, as listed in Minfile: 5 tonnes of ore (1926):

31 g	Au
2,395 g	Ag
1,496 kg	Pb

Location: The Beca property on the shore of Adams Lake, due east of Squaam Bay is directly accessible by boat. A switchback road dropping 1,800m from Nikwkwia lake on the western edge of the plateau, also leads to the property.

Host rock: The area consists of a repetitive succession of andesitic to rhyolitic volcanic rocks and associated quartzitic and argillaceous meta-sedimentary rocks (EBA). The rocks are metamorphosed to greenschist facies and show a high degree of schistosity that strikes about N85W and dips 25 to 45 degrees north. The more felsic phase has clearly invaded andesitic rocks which are preserved as xenoliths in the felsic rocks. Small granitic intrusions immediately south of the property boundary produced a thermal metamorphic aureole that overprints regional low grade metamorphism. The chemical similarity between the granitic rocks and the felsic volcanic rocks may indicate a comagmatic relationship between these two rock types.

Mineralization: The two mineralized areas found on the property are associated with pyritic cherty bands. The sulphides occur as fine grained conformable lenses containing porphyroblasts of arsenopyrite and local layers of sphalerite. Locally, altered rhyolite is laced with narrow (1 to 25mm), closely spaced quartz veins which are sporadically mineralized with galena and more rarely with sphalerite.

Sample description: Samples are a fine grained mixture of pyrite, chalcopyrite, galena, and sphalerite associated with calcite and minor quartz. The samples were collected from massive sulphide rich layers within the schist beside the old adits near the lake shore.

References: BCDM ASS RPT 6680, 7040.
BCDM GEM 1970 p. 314.

LUCKY COON:

Also known as Mc Gillivary group, Elsie, Speedwell, King Tut.

Minfile number: 082M-012 to 015

Mineral Inventory number: 82M4-PB4 to PB7

Map number: 018; Lat. 51.070N Long. 119.600W

Grades, as listed in Minfile: Total deposit (indicated 1972):

68,040 tonnes, cut off used: 296.0 g/t Ag

7.1 % Pb

4.8 % Zn

Production, as listed in Minfile

: from Lucky Coon, 496 tonnes of ore (1976-1977):

274 g Au

228,669 kg Ag

62,033 kg Pb

41,367 kg Zn

114 kg Cd

: from East Lehmi, 30 tonnes of ore (1956):

31 g Au

35,146 g Ag

8,330 kg Pb

2,393 kg Zn

Location: Lucky Coon is on the Adams Plateau at an elevation of 1,830m. The property is accessible by logging roads either from Scotch Creek across the plateau to the old open pit, or from the south end of Adams Lake to within 2km of the property.

Host Rock: The mineralization is associated with black and dark brown siliceous and graphitic phyllite, and with phyllitic limestone (EBG). Wide bands of fine-grained sericitized quartzite, interlayered with smaller chlorite-calcite rich bands occur close to sulphide-rich horizons. These metasedimentary units are folded by the Nikwikaia Lake synform and are surrounded by greenschists that are derived from mafic flows and tuffs. Quartz feldspar porphyry dykes crosscut part of the southern limb of the synform and show evidence of subsequent folding. Basic dykes are also present but are not well exposed.

Structure: Isoclinal and asymmetric folds, especially well exposed in the northern pit, demonstrate the prominent role of the structure in controlling the distribution of the sulphides. In such folds, sulphide beds 25cm thick on the limbs reach a thickness of 45cm in the hinge zone. Original texture in the sulphide horizons has been obliterated by the deformation.

Mineralization: Silver, lead and zinc sulphides are generally restricted to a specific stratigraphic horizon (siliceous and graphitic phyllites, phyllitic limestones) that is generally continuous along strike for 2000m. In detail, however, the sulphide zones are discontinuous due to remobilization and disruption during folding (Dickie, 1985). The sulphides are fine-grained and occur as bands, from 15cm to 1m wide separated by 30 to 90cm of siliceous phyllite, or as veins in sericitic schists. The mineralization consists of arsenopyrite, pyrite, sphalerite, galena, argentite and a little tetrahedrite. The ratio of the different sulphides throughout the deposit is variable; the arsenopyrite content varies from 1 to 25% (commonly diamond shaped grains are locally extensively replaced by sphalerite and galena). The pyrite can comprise as much as 75% of the sulphide zone but is often embayed and/or replaced by sphalerite and galena; however, euhedral unbroken pyrite crystals (probably formed by recrystallization) do occur. The sphalerite and galena are intimately associated. Embayed islands of sphalerite with cusp-shape borders are common.

Sample description: Massive sulphide samples were collected from the sericitic schist unit in the old pit number 1. The samples consist of small blebs of galena associated with quartz and calcite in a fine-grained matrix composed mainly of sphalerite and pyrite.

References: BCDM ASS. RPT. 11,521.
BCDM MMAR 1936 pp. D41-D43.
BCDM MMAR 1930 pp. A184-A186.
DICKIE, G.J. 1985.

SPAR:

Also known as: Ex 1, Bel

Minfile number: 082M-017, 018

Mineral Inventory number: 82M4-PB2, PB5 to PB7

Map number: 027; Lat. 51.060N Long. 119.540W

Production, as listed in Minfile: 274 tonnes of ore,
(1952, 1953, 1955, 1976):

435 g	Au
249,383 g	Ag
4,953,594 kg	Pb
891,766 kg	Zn
291 kg	Cu

Location: The Spar deposit is on the southeastern edge of the Adams Plateau less than 2km west of the Mosquito King deposit. It is accessible by the logging roads parallel to Scotch Creek.

Host Rock: Mineralization is hosted by folded limy phyllites associated with minor sericite quartzites, limestone and chloritic meta-volcanics (EBGs). The sulphide horizons and the host rocks are enclosed within the same intermediate to mafic volcanic and volcanoclastic sequences encountered at the Mosquito King and Lucky Coon deposits. Mineralization is also cut by small fine-grained diorite and granite porphyry dykes.

Structure: The rocks in the vicinity of the deposit are strongly foliated, have a general east-west strike, and dip gently northward. Strata show dragfolding and crenulation cleavage; fold axes strike S600W with low plunge (the crest plunges 100SW). Two sets of fractures cut the rocks: one dipping steeply north-south and the other dipping more shallowly dipping east-west. The north-south set seems to have acted as a channel way for mineralizing solution since fairly massive fine-grained sphalerite is found in the folded zones directly above such fractures (Dickie, 1985). The east-west set terminates abruptly some mineralized horizons and thus may be part of a late fracturing event.

Mineralization: Stratiform sulphide masses occur as folded elongated bodies (extending over 400m). The mineralization distribution does not appear to be confined to only one layer. However the mineralization is apparently stratabound and was originally deposited within a siliceous unit. This unit has been folded and metamorphosed, resulting in the migration and concentration of the sulphide minerals along the crests of folds or crumpled zones in the enclosing sericitic sequence (Dickie, 1985).

The sulphide horizons are composed of massive layered galena bordered by a fringe zone of galena, sphalerite, pyrite, pyrrhotite and chalcopyrite. Minor amounts of tetrahedrite, arsenopyrite and argentite also occur. The bands of massive mineralization (40cm thick) are separated by sericitized argillite.

Sample description: Samples were collected from the main old adits from which most of the minerals were extracted in the 1950's. Fine-grained galena is associated with sphalerite and pyrite in a quartz carbonate matrix. A vein containing abundant fluorite was also sampled.

References: BCDM MMAR 1953 pp. 102-103.
HAINSWORTH, W.G. 1973. Unpublished report on the Giant Metallic Mines.
JAMES, D.H. 1949.

MOSQUITO KING:

Also known as: Oro, King Tut, Garnet

Minfile number: 082M-016, 140

Mineral Inventory number: 82M4-AG2, CU2

Map number: 025; Lat. 51.060N Long. 119.520W

Reserves, as listed in Minfile 40,824 tonnes @ (Ind. 1981):

1.25	g/t	Au
21.70	g/t	Ag
10.0	%	Pb
8.5	%	Zn

Production, as listed in Minfile 419 tonnes of ore

(1972-73, 1976):

219	g	Au
232,154	g	Ag
22,721	kg	Pb
18,328	kg	Zn

Location: The Mosquito King property is located at an approximate elevation of 1,750m on a ridge on the Adams Plateau. A logging road between Nikwkwain Gold Creek and Kwikoit Creek leads to the property.

Host Rock: Sulphide lenses are enclosed within intensively silicified beds of argillites and quartz sericite rocks. These clastic rocks are part of a predominantly mafic volcanic succession (EBGs). These units have been metamorphosed to greenschist facies and contain abundant chlorite and sericite. Silicification and bleaching is ubiquitous in the limy argillites and in the quartzite, but not in the greenschist. The sequence is cut by andesite and hornblende porphyry dykes which are similar to those occurring on the Lucky Coon property.

Structure: Folds on the property have a predominant east-west trend but axes striking north-south are not uncommon; drag-folding is ubiquitous in most exposures. Joints and small north striking faults seem to control, at least locally, the mineral distribution.

Mineralization: At the main showing mineralization varies in thickness from 60cm to 3.5m (average 1.5m). It consists of several thin, closely spaced beds composed of black sphalerite, galena, pyrite, chalcopyrite and fine-grained pyrrhotite which are more or less concordant with the enclosing host. Lower in the succession, beds have been mineralized with iron sulphides (mainly pyrrhotite) and minor sphalerite. Pyrrhotite and pyrite rich lenses (up to 60cm wide) are extensive in the limy argillites. Disseminated pyrite also occurs along bedding planes and in fractures associated with silicified zones. Mineralized beds can be traced over 915m along a N700E strike

but they are not uniformly or continuously distributed. Veins of galena and sphalerite occur locally in the schists and in the limy beds. Magnetite and secondary copper minerals are locally abundant in the mafic volcanics. Minor mineralization also occurs associated with the porphyry dykes (James, 1949).

Sample description: Well crystallized but deformed galena in a quartz and calcite matrix containing a minor amount of pyrite and sphalerite is characteristic of the main mineralization. The samples come from the main mineralized area of the deposit in the open old workings. Galena was also collected from cross-cutting veins near a dyke.

References: BCDM ASS RPT 45, 7019.
BCDM MMAR 1949 pp. A134-136.
BCDM MMAR 1930 pp. A186-188.
DICKIE, G.J. 1985.
JAMES, D.H. 1949.

BC ZN 1:

Also known as: Cu 1, Cu 5

Minfile number: 082M-138, 139

Mineral Inventory number: 82M4-CU1, ZN2

Map number: 022; Lat. 51.010N Long. 119.520W

Grades, as listed in Minfile:

Indicated:	148,000 tonnes
Possible:	272,000 tonnes @ 0.19 % Cu
Reserves:	326,000 tonnes @ 0.35 % Cu
	38 G/t
	6 % Pb
	2.41 % Zn
	0.19 % Cu
	0.14 % Mo

Location: This mineralized occurrence is about 5.5km south of the Mosquito King deposit near the locally named China Creek. It is accessible from one of the numerous logging roads on the Adams Plateau.

Host Rock: Argillaceous phyllites are intercalated with limy and siliceous horizons interbedded with abundant greenstone derived from mafic volcanics and volcanoclastics (EBG). The sequence is intruded by a series of minor diabasic dykes and sills. One dyke sampled consists of hornblende, quartz, andradite and minor clinopyroxene, clinozoisite, chlorite and plagioclase. Schistosity of the host rock strikes east-northeast and dips moderately to the northwest.

Mineralization: A stratiform zone contains disseminated sphalerite and galena with minor pyrrhotite and locally abundant magnetite. Some zones of high iron content yield good Cu and Au values. One zone may be continuous for over 510m; it has a width of as much as 1.65m.

Sample description: Fine-grained sphalerite and minor galena disseminated in highly chloritic schist is characteristic of the mineralization.

References: BCDM ASS RPT 5132

BCDM GEM 1978, p. E101.

BCDM GEM 1974, p. 95.

CROWFOOT MOUNTAIN:

Also known as: Fluke, Saul

Minfile number: 082M-104, 105

Map number: 032; Lat. 51.060N Long. 119.250W

Grade: composite sample, gross average:	0.34 g/t Au
(From ASS.RPT.)	170.0 g/t Ag
	0.1 % Cu
	5.0 % Pb
	8.0 % Zn
	0.18 % Sn

Location: The Fluke claims on Crowfoot Mountain are approximately 16km north of Magma Bay on the north shore of Shuswap Lake, and are accessible by forestry roads.

Host Rock: Mineralization is hosted by phyllitic marble and altered limestone associated with phyllite, quartzite and greenstone similar to those found in the other deposits on the Plateau (EBG). These rocks are strongly foliated and lineated. The area is intruded by an enormous number of dykes, sills and small irregular bodies of granitic and diabasic rocks. Silicification is extensive in the vicinity of the sulphide rich zones.

Structure: Intense drag folding, disruption of limy horizons and greenschist facies in the meta-volcanic rocks are indications that the area has the same deformational characteristics as the rest of the Adams Plateau. Structural details of the deformation in the vicinity of the deposit are not known.

Mineralization: Mineralization has been described as sulphide replacement in bands of limestone and marble. On a large scale the sulphides are confined to horizons within the limestone, but the distribution of the sulphides is highly erratic. Galena and sphalerite occur in pods as well as in disseminations throughout the rock. Sulphides are also found in veins cutting chloritic schist. These veins strike in the same direction as the main foliation (striking N400N and dipping moderately northwestward) but dip in the opposite direction. Veins are unevenly mineralized with galena, pyrite, sphalerite and chalcopyrite.

Sample description: Blebs of calcite, pyrite, galena and sphalerite plus minor quartz in laminated but contorted and discontinuous limestone lenses were sampled on the property. Vein mineralization close to a lamprophyre dyke was also sampled.

References: BCDM ASS RPT 609, 3821, 4031, 6230, 6857.

FORD PROPERTY:

Map number: 038; Lat. 51.000N Long. 119.600W

Location: The Ford property is centred near the head of Woolford Creek. Access is facilitated by a network of logging roads.

Host Rock: The main rock types in the area are sericite quartz phyllite and sericite felspar quartz phyllite containing abundant medium to fine-grained angular clasts (unit EBA). It is likely that these rocks are altered intermediate to felsic tuffs. The units have a fragmental and porphyroblastic appearance due to metamorphism. A graphitic limestone containing unfoliated white quartz sandstone also occurs in the area. All these rocks have undergone greenschist facies regional metamorphism and locally contain abundant chlorite. Post metamorphic intrusion of diorite and lamprophyre dykes, cut through the rocks of the property.

Structure: The contact between the different units appear in several places to be planar but not continuous along strike. The well developed foliation, parallel to sub-parallel with the lithologies, is gently warped; this probably indicates the presence of a large open fold plunging to the north across the property. Steeply dipping north-northeasterly trending faults truncate and offset some of the units.

Mineralization: The property is the probable host of stratiform massive sulphide deposits as four zones contain mineralization: 1) a series of five lenses (5 to 20cm thick) of massive sulphide containing mainly pyrrhotite and small amounts of sphalerite and chalcopyrite associated with abundant silica (the mineralized lenses are conformable to the foliation), 2) a series of narrow layers (1 to 3cm thick) of massive pyrite within a chloritic quartz phyllite unit, 3) pyrite rich meta-rhyolite that may be a metamorphic equivalent of a quartz-pyrite exhalative unit, and 4) a narrow (1 to 3cm thick) silver rich, galena-chalcopyrite-quartz-calcite vein cutting through sericitic chlorite quartz schist. An alteration zone consisting of secondary quartz, muscovite, biotite and actinolite is present in the lower part of the section. This zone has characteristics similar to a thermal metamorphic aureole and is interpreted by Robinson (1986) to have been generated by an intrusive at depth.

Sample Description: Samples collected consist of fine grained massive sulphides containing galena associated with abundant pyrrhotite and minor sphalerite.

Reference ROBINSON, C. 1986. Geology of the Ford property Adams Plateau, south central British Columbia. Unpublished BSc Thesis, University of British Columbia.

SILVER KING-A:

Minfile number: 082M-129

Mineral Inventory number: 82M4-AG3

Map number: 036; Lat. 50.950N Long. 119.480W

Location: This small showing is less than 500m north of the Spar deposit along the logging road leading to the Lucky Coon deposit.

Description: Mineralization occurs in altered limestone in close proximity to brecciated rock containing fragments of argillite (fresh and partially replaced) cemented by sugary quartz. The sulphides do not occur directly in the breccia and seem restricted to the surrounding limestone. Zones rich in calcite, fluorite and porcelaneous quartz occur adjacent to the sulphides.

Sample description: Small seams of fine grained galena mixed with coarser sphalerite grains in a calcitic gangue are characteristic of the sampled specimens.

Reference: BCDM GEM 1971, p. 436.

SILVER KING-SILVER QUEEN:

Also known as: King James

Minfile number: 082L-NW044

Map number: 045; Lat. 50.950N Long. 119.480W

Location: A large exposure of this vein occurs on the east side of Scotch Creek 8km north of the post office of Scotch Creek along the logging road that follows the power line.

Description: Mineralization occurs in a vein system which is about 30m wide and strikes northwesterly through the chloritic schist and calcareous phyllite of unit EBG. The vein contains pockets of coarse grained galena and sphalerite in quartz-calcite gangue.

References: BCDM GEM 1977, p. E85.
BCDM GEM 1975, p. E55.

PET:

Minfile number: 082M-143

Map number: 026; Lat. 51.050N Long. 119.530W

Location: This showing is exposed in a trench, about 1km south of the main workings of the Spar deposit.

Description: Small amounts of galena and sphalerite (marmate) occurs as dissemination in chloritic schist.

Sample description: No description is available. Data used came from analyses by the GSC (GSC number: G79PE).

References: BCDM ASS RPT 5919.

BCDM GEM 1976, p. E59.

RED MINERAL CLAIMS:

Also known as: Fox, Deer, Fir, Pat, Joe

Minfile number: 82M-154

Map numbers: 033	Lat. 51.080N	Long. 119.380W
034	51.100N	119.380W
035	51.070N	119.380W
037	51.050N	119.540W

Location: The mineralized showings are clustered around Lichen Mountain, located northwest of the Mosquito King deposit, about 3km east-southeast of the junction of Cross and Kwikwit Creeks.

Host Rock: The mineralization is mostly found in carbonate layers associated with argillites and meta-volcanics (EBG). Locally manganese rich bands occur near the mineralized zones. The rocks are folded and metamorphosed, as are their equivalents elsewhere on the Adams Plateau. The main foliation in the rocks strikes northeast and dips north.

Mineralization: These mineral occurrences are of small size, outcrop on surface, and do not have any known underground extent. Quartz veins containing argentiferous galena cut through both volcanic rocks and limestone. The mineralization has been described as conformable lenses of cylindrical shape; but this geometry could not be confirmed in the field.

Sample description: All the collected samples contain coarse galena in quartz gangue associated with variable amounts of sphalerite and pyrite. The galena from the occurrence number 033, above, clearly shows evidence of deformation.

References: BCDM Open File.

BCDM Exploration in BC 1979

JOHNSON LAKE AREA:**AGATE BAY:**

Also known as: Try Me, Rankin Group, Karen, Joe

Minfile number: 082M-053

Map number: 006; Lat. 51.080N Long. 119.750W

Location: The showing is exposed at the shore line near the northern end of Squaam Bay.

Host Rock: Fine-grained quartz-sericite schists are interbedded with chloritic schist (EBAa). These greenstones are highly altered and contain swells of carbonates (calcite and ankerite). This unit, mapped as part of the felsic package of the Eagle Bay Formation, bear more resemblance to the more mafic sequence (unit EBG) found to the north, and on the other side of Adams Lake.

Structure: The mineralization occurs within a highly altered schist package. The main foliation strikes in average at N70W and dips from 22° to 55° northeast. Abundant small faults cut the schist.

Mineralization: Low grade Pb-Zn-Cu occurs in quartz veins. Two types of veins cut the host rocks: 1) narrow (1 to 3cm thick) closely spaced veins more or less conformable to the schistosity, 2) discontinuous larger veins (8 to 40cm thick) scattered through the schists, as pods or lenses. All the vein-like masses pinch and swell erratically and are truncated by faults. In both types of occurrences, the sulphides are erratically distributed and consist of pyrite and sphalerite with traces of galena and chalcopyrite in a quartz, calcite and ankerite gangue. Tourmaline has been reported in these veins (BCDM, 1961).

Sample description: Euhedral galena grains in quartz-calcite veins cutting altered greenstone.

References: BCDM ASS RPT 4135.

BCDM MMAR 1961 pp. 53-55.

TWIN MOUNTAIN:

Also known as: Star, Max, Hope

Minfile number: 082M-020

Mineral Inventory number: 82M4-PB3

Map number: 019; Lat. 51.13ON Long. 119.80OW

Grade: Subjective average value of 11 samples considered to be representative of the mineralized zone (BCDM ASS RPT 9882) are:

0.170	g/t Au
8.84	g/t Ag
0.90	% Pb
2.15	% Zn
0.18	% Cu

Barite is also present in quantities sufficient to be of possible economic interest.

Location: The showing occurs on the south-east flank of Samatosum Mountain at an elevation of 1,200 to 1,500m. The old workings are accessible via logging roads.

Host Rock: Two conformable mineralized zones or veins are hosted by greenschist and chlorite schist derived from mafic to intermediate volcanic and volcanoclastic rocks (EBGq). These rocks contain abundant thin carbonaceous layers and fracture fillings, and show remnant pillow structures. Tuffaceous and more siliceous horizons occur within the greenschist. This package of rocks is overlain by the Tshinakin Limestone.

Structure: Rocks in the area are moderately contorted and in places exhibit kink banding. The main foliation strikes N40OW and dips 43ONW.

Mineralization: The veins or mineralized zones contain pyrite, chalcopyrite, sphalerite and galena in a carbonate gangue with minor quartz, and barite; the zones locally are azurite stained. Mineralized zones range in width from 20cm to over 1m. An apparently unrelated vein lacking visible mineralization contains up to an estimated 30 percent barite.

Sample description: The analysed samples are from an open trench close to the old adits. They contain blobs of sphalerite, pyrite and galena in a calcitic matrix.

References: BCDM ASS RPT 9882, 2093.
BCDM MMAR 1936, p. D39.

Art:

Minfile number: 082M-124

Map number: 017; Lat. 51.100N Long. 119.950W

Location: This showing is adjacent to the road between Louis Creek and Squaam Bay, near the east end of Forest Lake.

Host Rock: Mineralization is hosted by a spotted quartz muscovite schist containing limy quartzitic pods. This schist is part of the subunit EBSS characterized by phyllitic sandstone, grit, phyllite, chlorite schist, and quartzite with a small amount of limestone.

Mineralization: Quartz carbonate veins containing minor pyrite and galena cut the schist. Traces of fuchsite are also present.

Sample description: Quartz veins in the schist contain pods of galena associated with minor carbonates.

References: BCDM Minfile number 082M-124.

HOMESTAKE:

Minfile number: 082M-025

Mineral inventory number: 82M4-AG1

Map number: 011; Lat. 51.11°N Long. 119.83°W

Reserve: proven (The Financial Post, Jan. 1973) are
1,010,800.0 tonnes of ore:

240.0 g/t	Ag
2.5 %	Pb
4.0 %	Zn
0.6 %	Cu
28.0 %	barite

Production, as listed in Minfile: 6,965 tonnes of ore
(between 1935 to 1941):

12,400 g	Au
9,565,900 g	Ag
11,080 kg	Cu
171,325 kg	Pb
426,520 kg	Zn

Location: Access to the property is by a switchback road that leaves the main road 5km northwest of Squam Bay.

Host Rock: The mineralized barite lenses are overlain by sideritic phyllite that contain interbedded argillite, and by a tuffaceous chloritic schist unit (EBAA). A wide zone of altered rock occurs below the mineralized lens. Regional metamorphism and local hydrothermal alteration have obscured the primary composition of the host rocks; consequently, the following unit descriptions are based on mineral assemblages (Table).

A poorly exposed chlorite phyllite (unit 1) occurs in the southern part of the map area (Fig. A.1). It is a thinly laminated brownish green chlorite phyllite that is noticeably less foliated than the overlying schists.

Unit 2 comprises dominantly sericite-quartz schist with abundant disseminated pyrite throughout. Unit 2a is a more massive phase of the "paper" schist of unit 2b and contains lenticular, silica-rich segregations up to 6 cm in length. Unit 2b, referred to as a sericite-quartz "paper" schist, is the most conspicuous unit in the map area. In outcrop, the paper schist unit is easily discernible by its fissile appearance and by its weathered coating of yellow ferric sulphate. It is the host and the footwall to the barite- sulphide lenses and is interpreted to be a highly altered, predominantly felsic tuff unit. A number of quartz veins up to a metre thick are found within the paper schist below the barite

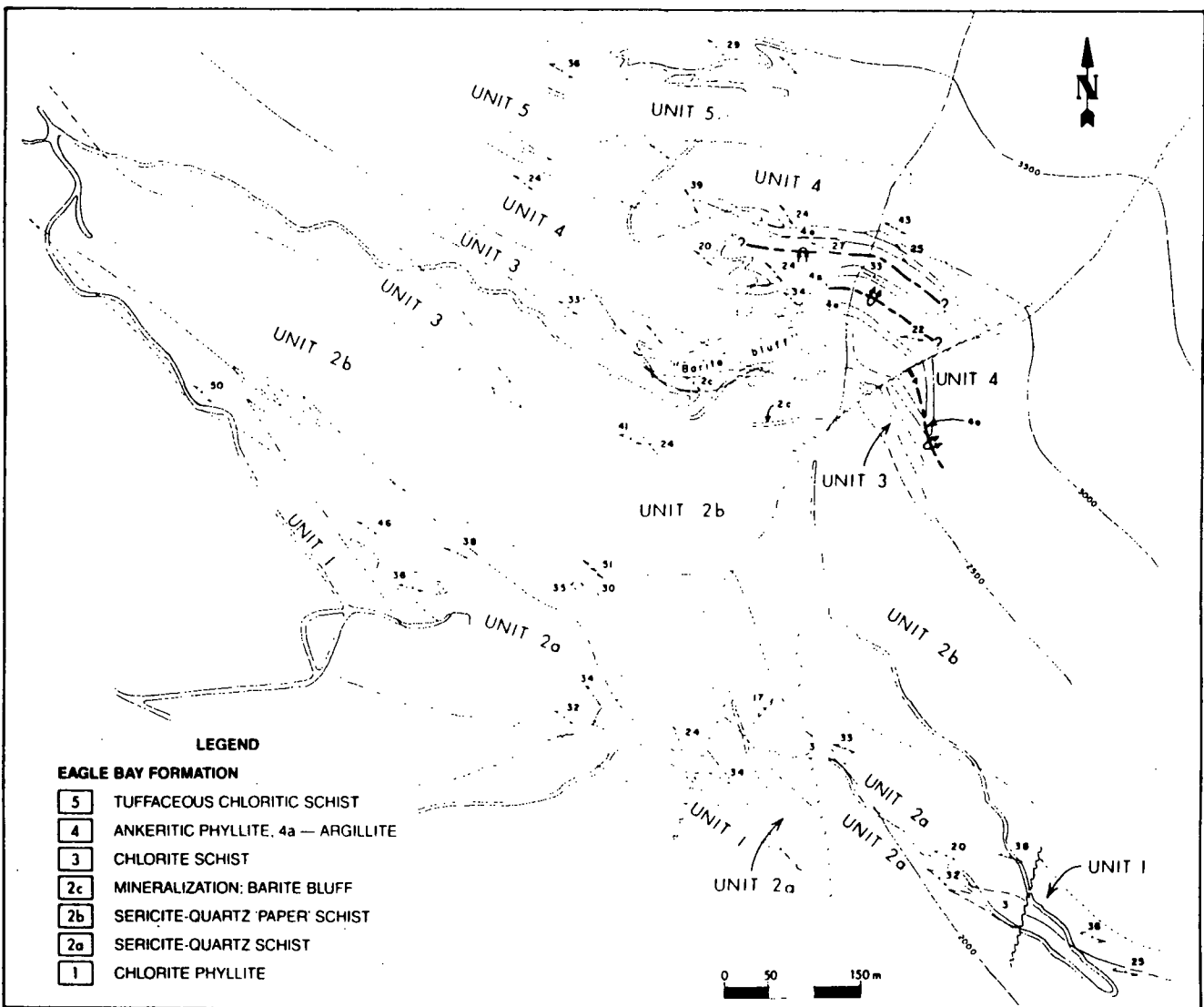


Figure A.1 Map of the Homestake property showing geology and access roads (from Hoy and Goutier, 1986).

lenses; they contain pyrite but are generally barren of other sulphides.

A dark green laminated chlorite schist (unit 3) occurs stratigraphically above and laterally west of unit 2b. It consists of carbonate phenocrysts within a fine-grained chlorite-feldspar matrix. These phenocrysts, which may be pseudomorphic after plagioclase, are rimmed and partially replaced by chlorite. This unit is probably altered andesite tuff; its contact with unit 2b is in part an interfingering of felsic and intermediate tuffs but may also reflect an irregular pervasive potassic and silicic alteration boundary.

A fine-grained ankeritic phyllite (unit 4) composed of interbedded layers of ankerite-bearing chloritic phyllite occurs above units 2b and 3. In outcrop limonitic pseudomorphs after iron-rich carbonate give the rocks a characteristic brown tinge. Some fine-grained pyritic argillites within the phyllite package are the most continuous and reliable marker units at Homestake. These argillite layers contain elongated quartz eyes and augen-shaped clasts up to 0.8 mm in diameter. The quartz eyes have cores of euhedral pyrite crystals and are set in a fine-grained pyritic carbonaceous matrix of phyllosilicates, quartz, and feldspar. Unit 4 is interpreted to be largely a sedimentary clastic rock with interbedded chloritic tuff layers.

A tuffaceous chlorite schist (unit 5) occurs on the steep cliffs in the upper, northern portion of the Homestake area. The rock contains massive and tuffaceous zones composed of chlorite and carbonate (probably developed from regional metamorphism of rocks of intermediate composition such as andesite). Relict flattened felsic clasts imply a pyroclastic origin for at least part of this unit. Pyritic quartz veins and calcite stringers occur throughout the schist, and in several places cut the foliation. Locally, cherty pods and argillite layers are interbedded with the schist. This unit is overlain by a thick greenstone sequence (V.A. Preto, pers. comm., 1985).

Structure: A well defined penetrative mineral foliation is ubiquitous throughout the Homestake area. The foliation is outlined by the preferred orientation of platy minerals such as sericite and chlorite, and lenticular silica-rich segregations in unit 2. Foliation plotted on a stereonet (Fig. A.2), has a reasonably tight cluster around a maximum that strikes 120 degrees and dips 30 degrees northeast.

Original compositional layering generally is difficult to see. Except within the argillite bands of unit 4, it has been largely obscured by either metamorphism or the intense deformation. In general, however, it strikes between 120 and 160 degrees with

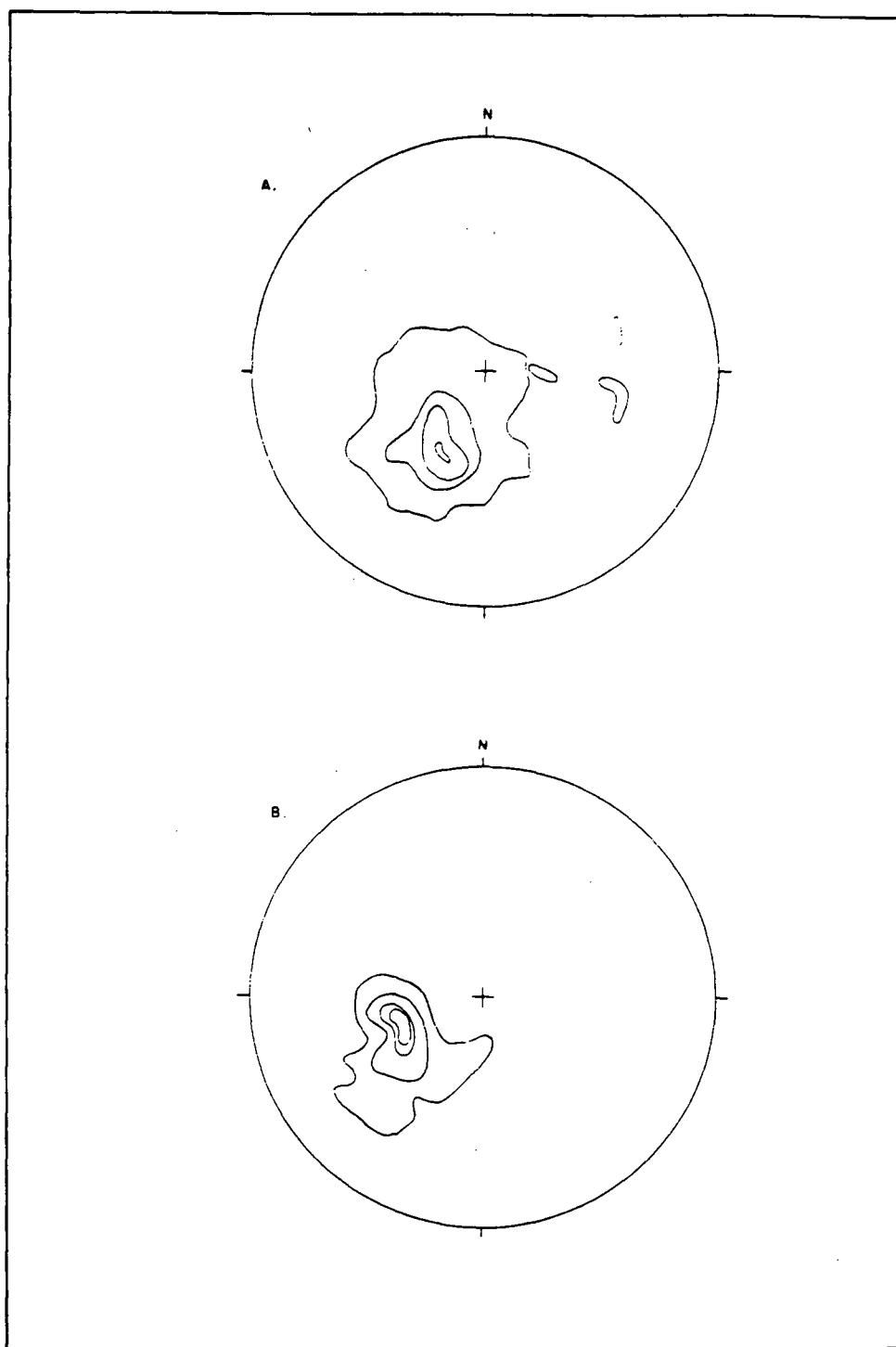


Figure A.2. Lower hemisphere equal area projections of structural elements Homestake deposit area:
A- Poles (92) to foliation, maximum concentration-30%
B- Poles (15) to compositional layering, maximum concentration -33%. Contour intervals-1, 10 (from Hoy and Goutier, 1986).

an average dip of 35 degrees northeast (Fig. A.2). The similarity between foliation and bedding attitudes indicates either tight or isoclinal folding or a constant facing direction.

No large folds have been identified in the chlorite or sericite phyllites beneath the barite lenses. Nearly all bedding-cleavage intersections in these phyllites have a common vergence. Therefore, the succession could be a homoclinal, non-folded sequence on the lower, upright limb of a tight syncline. However, rootless tight to isoclinal minor folds throughout the succession and the presence of large folds outlined by argillite beds in overlying rocks (unit 4) suggest that larger folds also occur within the phyllites. These folds would be asymmetric, essentially confined to a single unit, with shortened or sheared-out overturned folds limbs. On a regional scale the Homestake property is located on the southern limb of a large overturned syncline (Schiarizza and Preto 1984; Preto and Schiarizza, 1985). Evidence in the Homestake area, including fold closures and vergences obtained from bedding-cleavage intersections, supports a synclinal fold closure to the northeast.

Mineralization: A number of barite sulphide lenses with variable amounts of sulphide occur within the upper part of unit 2b. They are described in detail in early Ministry of Mines Annual Reports (1927, 1936) and are briefly reviewed here. At least three lenses, separated by sericite schist, are recognized. They range in thickness from less than a metre to at least 10 metres; underground some have been traced several hundred metres. Metallic minerals within these lenses include tetrahedrite, galena, sphalerite, pyrite, chalcopyrite, argentite, minor native silver, and trace ruby silver and native gold.

The lenses may consist either of massive to banded barite with only scattered metallic minerals throughout, or interlayered barite, schist, and sulphides. Two lenses are exposed on surface. The largest, referred to as the "barite bluff" (unit 2c), has an exposed thickness of 5 to 6 metres. It pinches out rapidly along strike, has a sharp hangingwall contact with sericite schist, and grades downward into massive sericitic chert. A smaller lens, 1 to 2 metres thick, occurs below the "barite bluff" unit; it is banded but contains only minor sulphides.

Sample description: Samples were collected from the barite bluff and are composed of erratically distributed medium grained pyrite, spalerite and galena. Galena sample from quartz vein material was also analysed.

References: HOY, T., and GOUTIER, F. 1986.

REA GOLD:

Also known as: Hilton

Minfile number: 082M-091

Map number: 015; Lat. 51.130N Long. 119.810W

Published drill indicated reserves: 120,000 tonnes of ore.

18.2	gt	Au
141.2	gt	Ag
0.85	%	Cu
4.11	%	Zn
3.67	%	Pb

Location: The Rea Gold property is located west of Samatsum mountain and is accessible via logging road from Squaam Bay.

Host Rock: The deposit description is from Hoy and Goutier (1986). The deposit includes two thin, laterally continuous lenses that lie stratigraphically above a highly altered sequence of dominantly mafic and minor felsic tuffs (Fig. A.3). Stratigraphically above these lenses is a thin mafic tuff sequence and a thicker sequence of argillite, siltstone, and grits (EBFf). The succession is inverted; hence, the "footwall alteration zone" or "stockwork feeder zone" now forms the hangingwall of the lenses.

Rock Units: The oldest unit within the deposit area comprises predominantly mafic tuff (unit 1) that lies at the structural top of the succession. This tuff unit includes ash, crystal, and lapilli tuffs with variable amounts of disseminated pyrite. They are strongly foliated, producing green phyllites and schists; more massive "greenstone" units may be derived from mafic flows. There are thin chert bands and a noticeable increase in sericite content toward the contact with unit 2. In general, this contact is gradational and reflects, in part, an increase in alteration in the stratigraphic footwall of the deposit.

Unit 2 is the footwall alteration or stockwork feeder zone of the sulphide lenses. It is very extensive in the hangingwall of the more northerly of the two lenses, but is only a few metres thick in the hangingwall of RG8, the southern lens. It includes extensively altered mafic tuffs, otherwise similar to those of unit 1, chert layers, and thin more felsic (dacite?) ash tuff layers. These units now appear as pale tan to pale green siliceous phyllites and schists interbedded with pure to sericitic chert. Alteration increases dramatically toward the contact with the sulphide lenses. It includes: a) silicification through introduction of silica in the form of quartz veins, and of thin to relatively thick chert layers, discontinuous chert lamellae, and fragmental chert;

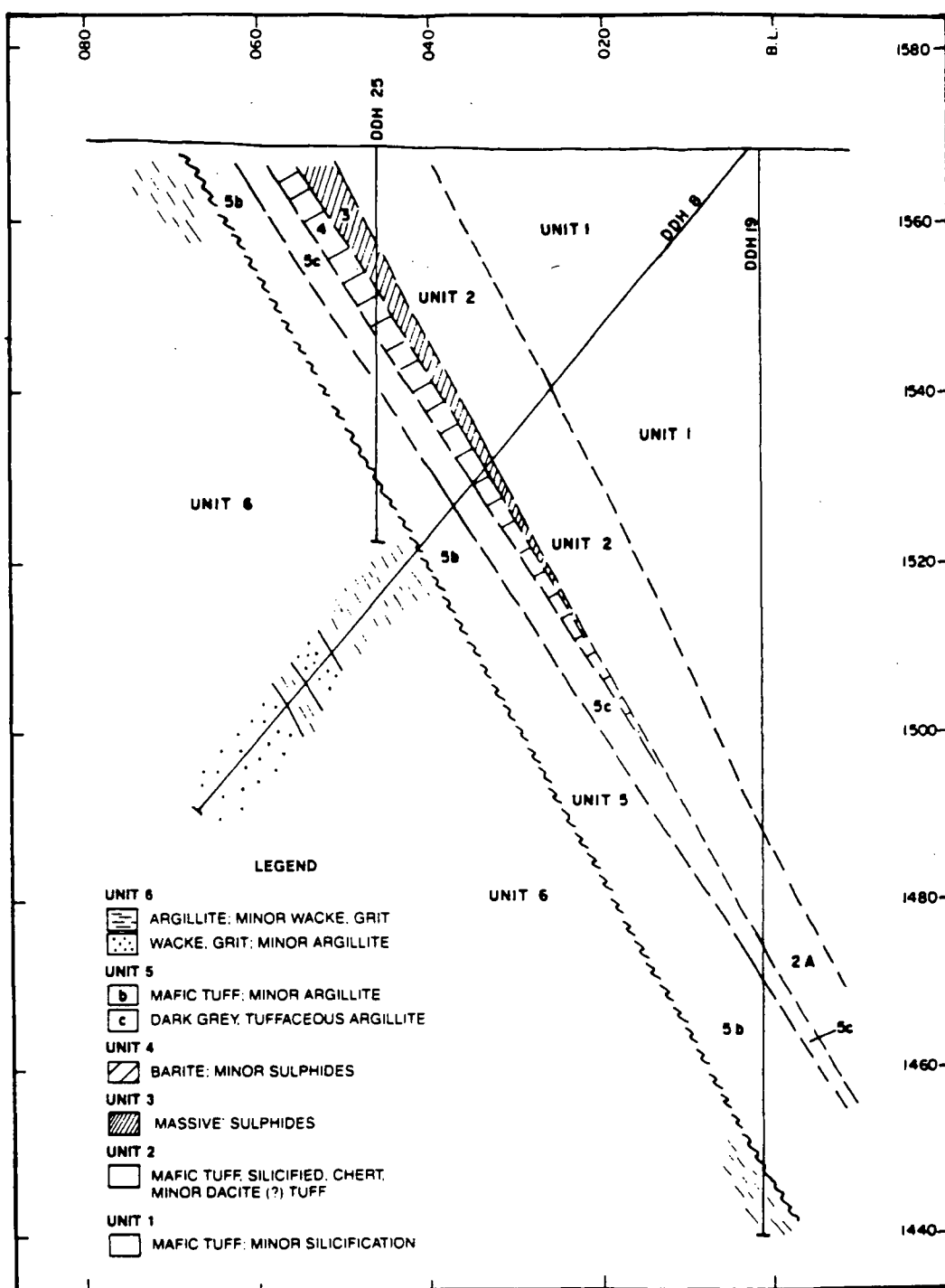


Figure A.3 Vertical section (97+00) through the RG 8 sulphide barite lens, Rea Gold deposit (from Hoy and Goutier, 1986).

b) pyrite, which is disseminated, in veins, and in discontinuous streaks; it increases from 1 to 2 per cent in unit 1 to commonly 10 to 20 per cent near the stratigraphic top of unit 2; and c) sericite which becomes ubiquitous within unit 2. White (1985) noted both local soda enrichment (as massive albite and paragonite) and carbonization (as dolomite, iron-rich magnesite, and calcite).

Stratigraphically overlying the sulphide or sulphide-barite lenses is a thin sequence of predominantly mafic tuffs (unit 5) that grades up into argillites. These tuffs are pale grey to brown-weathering thin-bedded chlorite phyllites. Silicified zones occur only locally and pyrite content is generally low. A dark grey tuffaceous "argillite" (unit 5c) with high Ba content (I. Pirie, pers. comm., 1985) occurs in the intermediate footwall of the RG8 lens, at the stratigraphic base of unit 5. Unit 5 is generally in fault contact with unit 6, but in some drill intersections it grades through an interval of interbedded green phyllite and argillite (Fig.).

A sequence of metaclastic rocks (unit 6) at the structural base of the succession are the youngest rocks in the deposit area. They comprises grey laminated argillite, siltstone, wacke, and local pebble conglomerate with both volcanic and sedimentary clasts. Bedding and graded beds are well preserved. Thin mafic ash tuff layers occur in the basal part of unit 6.

Structure: The deposit and host rocks are within a northwest-trending, northeast-dipping homoclinal succession that has been structurally inverted. A pronounced mineral schistosity largely masks primary bedding except in structural footwall rocks where well-bedded and commonly graded metaclastic rocks occur. The observed bedding is sub-parallel to the schistosity (Fig. A.4), indicating tight to isoclinal folding. Changes in the vergence of the bedding-schistosity intersections and the many small, rootless isoclinal folds indicate, however, that the succession is folded. Folding is asymmetrical in style and individual folds are confined to specific units since repetition of the major lithologic subdivisions is not apparent. Within unit 2, cleavage-bedding intersections indicate a synformal axis located to the northeast.

Relationships between the massive sulphide, barite, and alteration zone indicate that the deposit is inverted; this suggests that the observed schistosity and associated folds are second generation structures superimposed on a previously inverted panel. Within more competent structural footwall rocks (unit 6), these folds are relatively open and the location of fold hinges can be defined. A late southeast-trending crenulation cleavage, associated with minor open folds, is superimposed on the earlier schistosity. Faults parallel to schistosity are common but only the largest

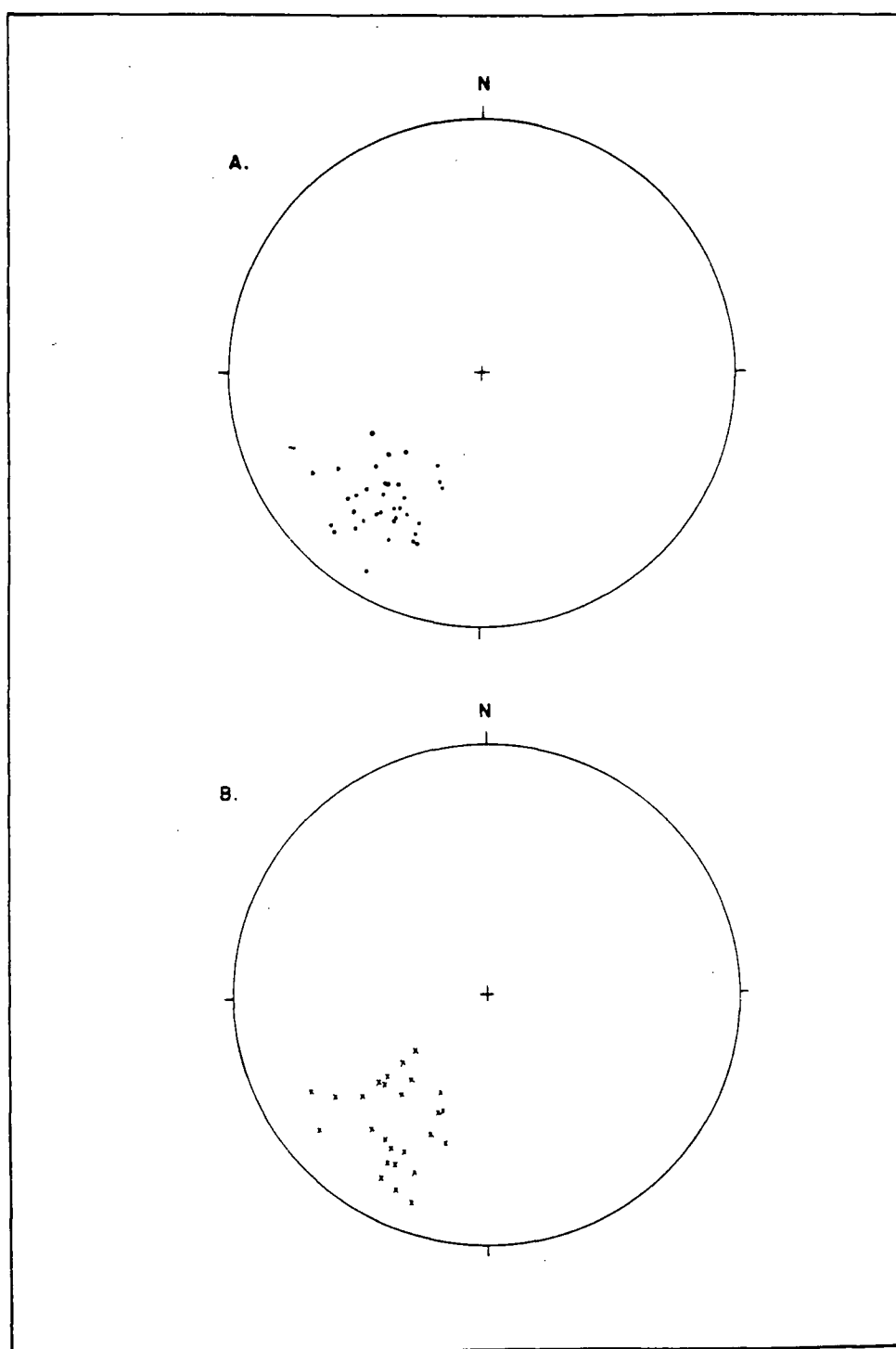


Figure A.4 Equal area projections onto lower hemisphere of structural elements Rea Gold deposit:
A- Poles to foliation
B- Poles to compositional layering
(from Hoy and Goutier, 1986).

are shown on the map. The most prominent fault strikes northwest, juxtaposing unit 5 against unit 6. The displacement on the fault is probably not large as there does not appear to be much loss of stratigraphy across it; the fault cuts locally up into unit 5 leaving a normal stratigraphic contact between units 5 and 6.

Mineralization: The sulphides, within this volcanogenic sulphide-barite bearing deposit, are contained in two main lenses. The more southern, the RG8 lens, appears to be at a slightly higher stratigraphic level than the L100 lens. It has a less extensive footwall alteration zone, and is "capped" by massive barite. Description of these sulphide lenses are based on visual examination of drill core and mapping of trenches.

The RG8 lens is well exposed in two trenches. It has a relatively sharp contact with altered "footwall" rocks of unit 2 and grades stratigraphically up into massive barite of unit 4. However it is in sharp contact with tuffaceous muds or mafic tuffs of unit 5 at its fringes. The barite "cap" consists of grey to white, massive or faintly banded barite with variable amounts of disseminated sulphides. The sulphide content of the barite generally decreases away from the underlying massive sulphide (Fig. A.3).

The L100 lens has a surface strike length of approximately 50 metres and a down dip projection of at least 120 metres. A thick zone of intense silica alteration stratigraphically below the lens is abruptly overlain by mafic tuffs of unit 5a. It does not have a barite "cap".

Sulphide mineralogy in both lenses includes pyrite, arsenopyrite, sphalerite, galena, chalcopyrite, and tetrahedrite-tennantite (White, 1985). Sulphides are fine-grained and massive, crudely laminated or brecciated. Gold occurs mainly in the massive sulphides but is also found in barite, in footwall stockwork, and in fault gouge (I. Pirie, pers. comm., 1985). Silver is associated with both barite and massive sulphides, while zinc, lead, and copper occur primarily in massive sulphides.

Sample description: The sample was collected from the massive sulphide zone occurring on surface and is composed of extremely fine-grained sulphide ore containing essentially pyrite, arsenopyrite, and sphalerite, with only minor galena. Vein samples containing coarser galena was also analysed.

References: HOY, T., and GOUTIER, F. 1986.

BARRIERE LAKES AREA:

BIRK CREEK SHOWINGS:

Also Known as: Anaconda, Lynx, Rainbow, Copper Cliff,
 Minfile number: 082M-067, (059, 131)
 Mineral Inventory number: 82M5-CU3
 Map number: 008; Lat. 51.33ON Long. 119.90OW

Location: The area is situated 3km west of North Barriere Lake. The showings are accessible by trail that follows the north-east side of Birk Creek.

Host Rock: The area is underlain by sericite schist, chlorite schist, black phyllite, and some recrystallized limestone (unit EBAA). Two stratigraphic sections; A-A', B-B' and a longitudinal section D-D' crossing the section C-C', are shown on the Figures, and are described in the following paragraphs.

Section A-A'

A cliff section is exposed from an elevation of 970m at the creek to 1,102m up section. It consists dominantly of quartz-eye sericite schist. The strike of the foliation varies from 265 to 290 degrees and dips 5 to 20 degrees to the north. The overall minimum thickness (perpendicular to foliation, which is approximately coincident with bedding) is 175m (Fig. A.5). At the base of the section the schists contain 15 per cent phenocrysts (maximum size 2mm) of quartz and plagioclase in a quartz-muscovite-plagioclase matrix. The plagioclase is altered to calcite but up section this alteration is not apparent because the plagioclase content decreases. Autolithic fragmental units (average fragment size 1.5mm), occur locally. Disseminated pyrite with an average grain size of 0.5mm, constitutes up to 8 per cent of the rock. Trace amounts of interstitial chalcopryrite are present with the pyrite. No markedly sulphide-rich horizons were observed.

Section B-B'

This section (Fig. A.5) passes close to several old workings. Exposure is limited to one or two outcrops and the collars of two slumped adits. A well-developed foliation, parallel to compositional layering, trends 265 to 275 degrees and dips gently north (3 to 20 degrees). Observable bedrock is composed of quartz-sericite and chlorite schist with limonite altered pyrite-rich layers, and minor laminated black phyllites. Thin sections of the schists show zones with elongated fragments (up to 3mm) of polycrystalline quartz grains. Disseminated pyrite is present throughout much of the section. Silicified massive pyrite lenses with minor chalcopryrite were observed within an 8-metre section near the old adits. The pyrite is euhedral, but fragmented, and associated with chalcopryrite which generally is located at the borders of the pyrite grains. Material observed on a dump in the immediate area contains

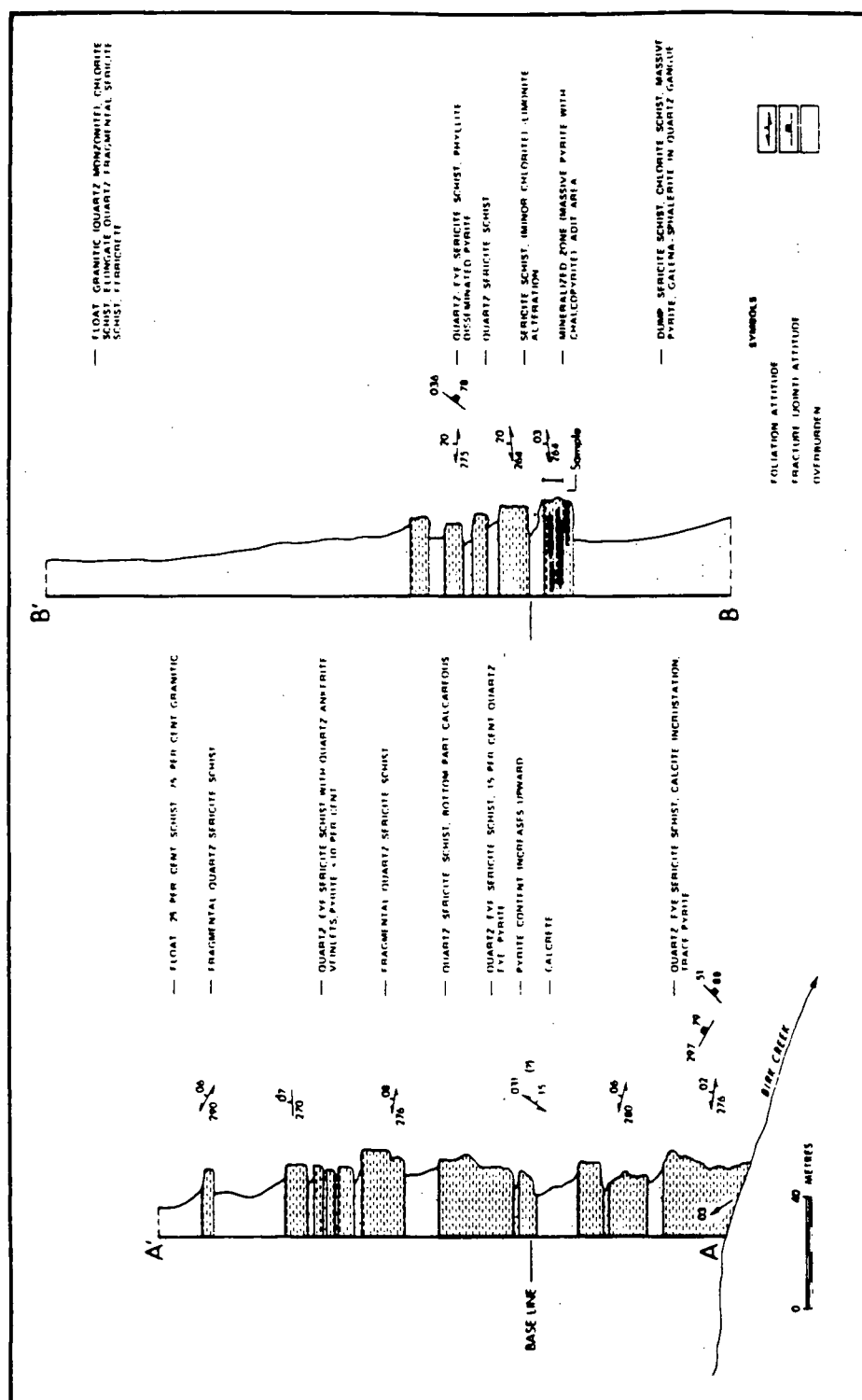


Figure A.5 Detailed sections A-A' and B-B' from the north side of Birk Creek--sections about 350m apart (from Goutier et al., 1985).

similar mineralization, as well as a few blocks of vein quartz with blebs of sphalerite and galena. The latter type of mineralization was not observed in outcrop.

Sections C-C' and D-D'

Sections C-C' and D-D' cross a major showing along a cliff section on the south side of Birk Creek. Three short accessible adits, about 9 metres long are parallel to a major joint direction (012 degrees). Other workings in the immediate vicinity have been flooded by the creek and are observable when water levels are low (V. Preto, pers. comm., 1984). This section is composed of sulphide-rich sericite schist in fault contact with an impure limestone unit.

Structure: A well developed foliation parallel to bedding strikes east-west and dips variably to the south and north. A superimposed north striking, shallowly east-dipping crenulation cleavage is pronounced on outcrops near the creek. Early mesoscopic recumbent isoclinal folds with axial planes parallel to the pronounced schistosity and axes plunging parallel to the mineral lineation, probably indicate a large structure which controls the distribution of the stratiform mineralized zones (Preto, pers. comm., 1984).

Mineralization: Mineral occurrences are stratiform massive pyrite deposits with minor chalcopyrite sphalerite and galena. Sulphides occur as massive pods (up to 1m thick), as layers (up to 10cm thick) and as fragments in silicified breccia. Sulphide mineralization is composed mainly of well-formed but disrupted pyrite grains (average size 2.5mm across) with minor chalcopyrite in an ankeritic quartz matrix. This unit looks like a pyrite-silica exhalite. Locally the sulphide horizons are well layered (layers are 8cm thick over an exposed thickness of 3.5m). Attitudes of layering and coincident foliation are the same as those observed in the limestone. Most mineralization appears to be stratabound and syngenetic with the host felsic schists.

Sample description: Collected samples consist of fine grained galena disseminated through massive iron sulphide horizons. Vein material, also analysed, contains coarser galena and sphalerite in quartz gangue.

Reference: GOUTIER et al, 1985.

ENARGITE:

Also known as: North Star, Ace

Minfile number: 082M-064, 065

Map number: 004; Lat. 51.35ON Long. 119.99OW

Production as listed in Minfile:

From the south showing 31 tonnes of ore (1954):

280 g Ag
1,561 kg Cu

From the north showing 5 tonnes of ore (1972):

3,452 g AG
1,341 kg Pb
651 kg Zn

Location: The property at the head of Birk Creek is at the summit between the valley of Barriere Creek and the North Thompson River.

Host rock: The Enargite vein occurs at, or adjacent to, the contact between a fine grained meta-sedimentary package of the Eagle Bay Formation (composed of phyllite, slate, interbedded siltstone and sandstone, and various limestone horizons, subunit EBPl), and the meta-basalt of the Fennell Formation (lFu).

Structure: The vein strikes N15OW and dips 45OW. The rocks in the area strike almost vertically; near the vein the host rocks are highly disturbed.

Mineralization: The sulphides are hosted by a strong quartz vein (45cm wide) bordered by gouge material probably related to a fault between the two formations above. The sulphides, mainly galena, are irregularly distributed and occur in pockets. Locally disseminated sulphides occur in the adjacent carbonate host rocks.

Sample description: Coarse galena in quartz vein was sampled; no other sulphides were present in the sample.

References: BCDM EXPL. IN BC. 1978, pp. E108.
BCDM GEM 1974, p. 97.
BCDM MMAR 1927, p. 190.

FORTUNA:

Also known as: Kuno

Minfile number: 082M-070 to 072

Map number: 013; Lat. 51.37°N Long. 119.93°W

Location: The property is on the flank of Fortuna hill. The aluminium roof of an old cabin on the property is visible from great distance and can be used to guide access to the workings along old trails.

Host rock: Quartz lenses (or vein segments) cut through light to dark green chloritic phyllites, silstone, limestone and quartzite (EBU). The schists close to these lenses are very altered and in places silicified.

Structure: The foliation in the host rocks strikes at N45°W and dips 24° to the southwest. The overall strike of the mineralized bodies parallels the foliation.

Mineralization: Scattered pockets of galena occur in the quartz. The various mineralized zones are more or less parallel to each other, and although they occur at several places on the slope of the hill, their continuity has not been determined.

Sample description: Well crystallized galena associated with minor amounts of pyrite was sampled from one of these bodies occurring near the old workings.

References: BCDM MMAR 1927, p. 190.

WHITE ROCK:

Minfile number: 082M-066

Mineral Inventory number: 82M5-PB1

Map number: 028; Lat. 51.30°N Long. 119.91°W

Grade as listed in BCDM MMAR 1950:

Composite sample: 0.34 g/t Au

91.80 g/t Ag

2.2 % Pb

0.8 % Zn

Location: The deposit is approximately 1.6km east, and 500 to 800 metres above Barriere River at the south end of North Barriere Lake.

Host Rock: The mineralization is hosted by the Tshinakin limestone (EBGt) which occurs interdigitated with green calcareous chloritic schist (EBG).

Structure: The main fracture system which hosts the veins strikes northeasterly and cuts the limestone at high angles. These fractures have been interrupted by late faults both along and across the plane of the infilling veins (BCDM, 1950). A large number of small veins, exposed on surface, are of irregular width and of unknown length. These veins generally strike N10°E and dip steeply to the east.

Mineralization: Quartz veins, clots and stringers, carrying mainly argentiferous galena, occur in a series of fractures which are probably related to the main fault zone along the Barriere River valley. In several places the contact of the limestone and the surrounding schist is also well mineralized. The veins are of irregular length; widths vary from 5cm to 45cm.

Sample description: Concentric galena blebs surrounded by a quartz-calcite gangue was sampled from a vein on the property.

References: ECONOMIC GEOLOGY SERIES NO. 8, GSC 1930, p. 302.
BCDM MMAR 1950, pp. 111-112.
BCDM MMAR 1928, p. 212.
BCDM MMAR 1927, p. 189.

JUNE KAJUN:

Also known as: Rennings, Kajun.

Minfile number: 082M-058

Map number: 021; Lat. 51.260N Long. 119.800W

Location: A large north-south trench (120m long) exposed a mineralized vein on the southeast side of East Barriere Lake at the mouth of Deadfall Creek.

Host rock: A folded mineralized vein is hosted by grey to white limestone (EBG1) associated with black graphitic phyllite. A large fault, near the base of the exposure in the trench, is underlain by black siliceous and limy gouge and by unconsolidated breccia. Above the vein, the limestone is not disturbed and strikes from N200W to 450W with dips near 400E.

Structure: The mineralized vein is associated with a possible fault indicated by the presence of gouge material. The vein strikes N700W and dips 650SW. In several places mineralization is concentrated in the crests of small drag folds.

Mineralization: In the crest of a open large fold a mineralized zone, approximately 7m long by 4m high, is composed of siliceous calcitic and dolomitic gangue contain sections up to 1.3m thick which are mineralized with galena, sphalerite and minor chalcopyrite. Patches and streaks of sphalerite, galena, chalcopyrite and pyrite extend locally into the surrounding limestone.

Sample Description: Well crystallized but fine grained galena associated with pyrite and sphalerite was sampled from the exposed quartz mass. The samples were collected both adjacent to and 5m away from the gouge rich zone.

References: BCDM ASS. RPT. 2232, 2230.

LEEMAC:

Also known as: Boomac.

Minfile number: 082M-056

Map number: 046; Lat. 51.35ON Long. 119.70OW

Location: The Leemac group of claims are accessible by logging roads from the east side of the town of Barriere. The claims are along Fennell Creek.

Host rock: The vein occur within the Cretaceous Baldy batholith. Near the vein the intrusion is porphyritic, reddish in color and nearly devoid of mafic minerals. Sericite is locally abundant in the vicinity of the vein structure. Narrow mafic dykes (striking parallel to the mineralized vein and dipping to the north) occur throughout the batholith.

Structure: The vein strikes N25OE with a moderate dip to the northwest. It is bordered on both sides by fault gouge, indicating that the vein has been subjected to movement or that it fills a shear zone related to a faulting event.

Mineralization: The mineralization is hosted by a well delineated quartz vein having an average width of 90cm. The sulphides, pyrite, sphalerite and galena, are coarse and well crystallized. This mineralized vein is surrounded by a subsidiary vein system mostly barren of sulphide minerals.

References: BCDM ASS. RPT. 5939.

BROKEN RIDGE:

Also known as: May.

Minfile number: 082M-130

Map number: 009; Lat. 51.35ON Long. 119.88OW

Location: The mineralized zone occurs on Harper Creek 2km northwest of the west end of North Barriere Lake.

Description: Lenses and blebs of pyrite and pyrrhotite with minor amounts of chalcopyrite, sphalerite and trace of galena occur semi-conformably with the foliation in the chloritic member of the quartz-sericite schist unit EBA. Numerous iron gossans in the area are related to abundant iron sulphides (pyrite and pyrrhotite) in the schist.

Sample description: The data used come from analyses made by the Geological survey of Canada, analyse no. G79BN-001.

References: BCDM EXPL. in BC 1976, p. E62
BCDM GEM 1971, p. 440.

BIRCH ISLAND-CLEARWATER AREA:**CHU-CHUA:**

Minfile number: 092P-140

Map number: 003; Lat. 51.38°N Long. 120.07°W

Location: The Chu-Chua property is approximately 20km north-northwest from the town of Barriere, on the ridge east of Chu-Chua mountain.

Host Rock: The deposit is hosted in the upper structural division of the Fennell Formation (ufb) composed mainly of basalt with alkalic affinities (Aggarwall et al., 1984), in which primary textures and pillows (1 to 3m across) are still visible. The margins of the pillows are slightly chilled and are chloritized or bleached. Massive talc zones and siliceous rocks are locally abundant within this package, particularly near the sulphide rich zones. Chert and/or tuffite overlie the mineralization and are believed to be exhalative in origin (Aggarwall et al., 1984).

Structure: Rocks of the Fennell Formation are generally not highly foliated. The schistosity, where developed, is axial planar to early, generally northeast plunging isoclinal folds. Two generations of later folds (easterly and northwesterly trending, Schiarizza, 1980) refolded the main schistosity and may be responsible for repetition of the mineralized horizons.

Mineralization: The basalt contains two major (eastern and western), and two minor lenticular bodies of massive sulphides that appear to be stratabound. In general the deposits trend north-south, dip steeply west, and plunge gently south. The sulphides are in sharp contact with the hangingwall rocks, but the extension of the bodies down dip are irregular and in several places lens out into cherty rocks (McMillan, 1980). The mineralized zones are associated with massive talc magnetite lenses, and are composed mainly of pyrite and chalcopyrite with minor sphalerite, cubannite, stannite, and quartz and calcite. Bedding is not common and occurs only locally where it is outlined by chalcopyrite-rich layers or by alternating layers of pyrite of different sizes. The massive sulphides are cut by quartz-talc veins and, in one hole, by molybdenite stringers (McMillan, 1980).

The Chu-Chua deposit is believed by Aggarwall et al. (1984) to represent deposition from saturated solution on the sea floor and/or nearby seamounts. The different lenses formed from different vent sources. The associated magnetite and talc rich zones probably represent areas where a higher component of sea-water was involved in alteration and mineralization. Similarly the apparent lack of footwall alteration is most likely due to a lack of significant interaction between the hydrothermal solution and the host rocks.

Sample description: Lead data referred to in the present study are from Aggarwall and Nesbitt (1984). Their analysed lead was extracted from pyrite and chalcopyrite rather than galena and the data are only used here on a comparative basis.

References: AGGARWALL, P.K., and NESBITT, B.E. 1984.
AGGARWALL, P.K., FUJJI, T., and NESBITT, B.E. 1984.
MCMILLAN, W.C. 1980.

FOGHORN:

Also known as: Gopher, Shamrock

Minfile number: 082M-008, 029, 030, 040, 108

Mineral Inventory number: 82M12-Cu2, Ag1

Map number: 005; Lat. 51.540N Long. 119.930W

Production as listed in Minfile: Foghorn 73 tonnes of ore
(1916-17)

88,364 g Ag

57,276 kg Pb

Location: The property is at approximately 2,000m elevation on Foghorn Mountain, 6.5km south of Birch Island.

Host Rock: The property is underlain by rusty weathered feldspar-chlorite schist and sericitic quartzites (EBFq), but the mineralized veins are hosted by siliceous and limy schists. The Baldy batholith, exposed in the southern part of the property at Granite Mountain, is surrounded by fine to medium grained biotite quartz gneiss with interlayered amphibolite and pelitic hornfels. Felsic porphyry dykes occur near the mineralized zones and may be responsible for both the silicification of the host rocks and for the sulphide veins.

Structure: The Foghorn showings are located on the northern limb of an east-west striking antiform in very close proximity to a major northerly striking thrust fault. The northeasterly strike of the vein is at a high angle to the thrust fault. Small scale structures, drag folds for example, indicate that original bedding has been deformed and probably transposed into tight isoclinal folds now seen as foliation (striking N30°E and dipping 80°W).

Mineralization: Quartz vein segments occur throughout the schist; their distribution is not continuous and may therefore represent a system of small veins rather than a major single discontinuous vein. These vein segments are locally heavily mineralized with galena, sphalerite and pyrite. In places chalcopyrite also occurs but only in minor amounts (disseminated chalcopyrite is found in greater amounts in the nearby Lydia prospect). The width of the vein segments is approximately 35cm; they strike about N35°E and dip in various directions --some of them are vertical.

Sample Description: Samples were collected from the old workings. The galena occurs with minor amounts of sphalerite and pyrite in quartz gangue specimens.

References: BCDM ASS. RPT. 11381, 3820.
BCDM OPEN FILE.

REXSPAR:

Also known as: Smuggler, Spar, Black Diamond

Minfile number: 082M-021

Mineral Inventory number: 082M12-U1, FSP1

Map number; 016 Lat. 51.57°N Long. 119.90°W

Reserves as listed in Minfile: Rexspar,
total deposit (dec. 1976): 1,114,000 tonnes
@ 1.55% U cut off used.

Location: The Rexspar deposit 5km, south of Birch Island, is on the south slope of the North Thompson valley between Lute and Foghorn Creeks.

Host Rock: Mineralization at Rexspar is directly associated with the trachytic member of the felsic unit EBA. The trachyte is massive or brecciated and strongly foliated. The surrounding rocks, chlorite sericite schist and silvery sericite-quartzite, contain exposures of clearly recognizable dacitic and andesitic volcanic breccia.

Structure: The rocks of the trachyte suite exhibit brecciation, cataclasis and mylonitization structures. The foliation in the rocks strikes north-easterly with a 300 dip to the northwest. The mineralized zones are deformed and are near to several faults and thrusts.

Mineralization: The two main mineralized zones present at Rexspar are: 1) an uranium rich zone confined to tuffaceous and argillitic lenses containing abundant pyrite associated with aggregates of uranium bearing fluorophlogopite. The lenses are discontinuous, average 20cm in thickness, and are conformable with the schistosity of the host trachyte.

2) a fluorite zone, barren of both thorium and uranium, is mineralized with celestite, pyrite, trace of galena and molybdenite.

The mineralization at Rexspar has been interpreted by Preto (1978, in BCDM Geology) as resulting from deposition from a late stage deuteric volatile rich fluid evolved from the highly differentiated intrusive-extrusive igneous suite. However, because CO₂ apparently played an important role in the transport and deposition of uranium associated with hydrothermal solutions (Morton, 1978), then the uranium and thorium mineralization could be syngenetic with the trachyte unit.

Sample description: No samples were collected from the Rexspar deposit by the writer. The data referred to here came from analyses by the Geological Survey of Canada (sample number G79SA-001).

References: GSC paper 78-1B, pp. 137-140.
BCDM Geology in BC 1977-1981, pp. 44-56
CIM Bull., 71, 1978, pp. 82.
MORTON, R.D., AUBUT, A., GANDHI, S.S. 1978. Rexspar Deposit. Geological Survey of Canada, Current Research, paper 78-1B, pp. 137-140.

MT MCCLENNAN AREA

Deposit names: Red Top, Mt McClennan, Sunrise (Naomi).

Also known as: Mimsic Claims

Minfile number: 082M-044, 046

Mineral Inventory number: 82M12-PB1

Map numbers: 531, 539, 541; **Lat.** 51.640N **Long.** 119.780W

Location: This area comprises three old prospects near the summit of the McClennan Mountain located about 7.5km northeast of Birch Island. All the showings are accessible via forestry roads.

Host Rock: The mineralized occurrences of the Mt McClennan area are hosted by greenschist and by calcareous chloritic and graphitic schist intercalated with minor quartzite siliceous schist and carbonate (EBQ). Granitic rocks crop out about 2km north of the showings; the contact between the intrusion and the schists is marked by the development of hornfelsic rocks and by skarn zones in carbonate-rich horizons. Lamprophyre dykes occur in the western end of the area.

Structure: Rocks in the vicinity of McClennan Mountain are highly foliated and are folded around a strong easterly trending open antiform plunging 150E. The south limb of the antiform has been dislocated by faulting and granitic intrusion.

Mineralization: Pb-Zn-Ag and Cu occurrences are widespread in the area, the three old workings sampled for the present study are:

1) the eastern area that comprised the old Sunrise group and Naomi claims. The mineralization consists of pyrrhotite and pyrite with galena and sphalerite occurring in quartzitic rocks as lenticular sheets traceable on surface over a distance of 125m along strike. The sheets vary in thickness from .3 to 1.2m and are not totally conformable with the enclosing host.

2) the central area hosts the MT McClennan (Snow) showing. This showing contains massive and semi-massive heavily oxidized pyrite with galena, sphalerite and minor amounts of chalcopyrite in impure limy horizons. The sulphide rich layers are up to 50cm thick and parallel the schistosity and compositional layering of the schists. A magnetite bearing skarn is developed below an adjacent prominent bed of crystalline limestone.

3) the western area hosts the Red Top showing which consists of galena and sphalerite associated with silicified pyritic zones occurring along bedding in limestone. Chalcopyrite fills many gash-like openings. The sulphides have an erratic distribution along strike, occurring in blows and seams. Nevertheless they are stratabound to a definite stratigraphic horizon composed of calcareous quartz sericite schist adjacent to an horizon that varies from skarn to clear crystalline limestone.

In general these mineralized bodies appear to occur as discontinuous lenses (more or less conformable with the schistosity) or as erratic swellings formed by limestone replacement and/or skarn development due to metasomatism probably related to the intrusion of the Raft batholith.

Samples description:

1) eastern area (Sunrise): Fine grained highly altered sample containing sphalerite and galena associated with abundant pyrite.

2) central area (Mt McClennan): Coarse and fine grained galena from disseminations from an altered limy horizon.

3) western area (Red Top): Seams of fine grained sulphides disseminated in chloritic schist.

References: BCDM ASS. RPT. 6931, 6603, 5813, 436.
BCDM Geology in BC 1977-81, pp. 44-56.

VAVENBY:

Map number: 042; Lat. 51.580N Long. 119.750W

Description: Quartz vein containing narrow sulphides seam (5cm wide) cut through the Tshinakin Limestone (EBGt). The vein is mineralized with galena and contains abundant calcite material. A syenite dyke occurs in the vicinity of the mineralized vein.

References: Paul Schiarizza, pers. comm., 1985.

PS-75-185:

Map number: 048; Lat. 51.580N Long. 119.750W

Description: Galena and sphalerite occur in a narrow quartz vein cutting the Tshinakin Limestone, 4km east of the fossil occurrence near Vavenby.

References: Paul Schiarizza, pers. comm., 1985.

SONJA:

Also known as: LSD, Valentine.

Minfile number: 092P-049

Map number: 044; Lat. 51.590N Long. 120.010W

Location: This small mineralized showing occurs on the south bank of the North Thompson River, 1km east of the Clearwater railway station.

Description: Discontinuous silicified lenses or veins carry crystalline galena and anglesite. The mineralized masses occur within a quartz sericitic schist wedge of the Eagle Bay Formation close to the contact with the Fennell Formation. The mineralization appears to follow the east side of a major dyke (3.5 to 13m wide) which cuts the rocks of the Eagle Bay formation.

References: BCDM EXPL. in BC 1976, p. E132.
BCDM GEM 1969, p. 230.

BIRCH ISLAND:

Minfile number: 082M-023

Mineral Inventory number: 82M12-PB2

Map Number: 040; Lat. 51.560N Long. 119.900W

Production as listed in Minfile: 14 tonnes of ore (1926):

6,566 g Ag

3,362 kg Pb

Location: The old workings are located along Foghorn Creek road south of Birch Island.

Description: Erratic galena mineralization occurs in a fissure vein cutting through a quartzitic member of the felsic unit (EBA). The fissure, striking north and dipping steeply west, is bordered by a zone in which pyrite, siderite and calcite are locally abundant. The presence of manganese ore was also reported from this area (1931).

References: BCDM MMAR 1931, p. 107.

BCDM MMAR 1929, p. C224.

TINDAL:

Map number: 043; Lat. 51.600N Long. 119.780W

Description: Galena was collected in an old adit from a quartz vein cutting quartz sericite schist of the Eagle Bay Formation.

References: none available

APPENDIX B

LABORATORY PROCEDURES FOR GALENA LEAD ISOTOPE ANALYSIS

B.1 GALENA LEAD SAMPLE PREPARATION

Galena crystals selected from rock or ore samples are stored in plastic vials. Approximately 10 mg of grains of clean galena are picked out, using a needle and a binocular microscope, and put into a disposable 10 ml polypropylene beaker. A clean glass beaker (10 ml) is weighed, then the galena grains are emptied into the glass beaker and the container is reweighed. The weight of the sample indicates the amount of water that must be added to the lead chloride crystals prior to loading.

Approximately 8 ml 2N HCl is added to the sample in the glass beaker, which is then left overnight on a hotplate. The lead sulphide is converted to lead chloride with the production of hydrogen sulphide. The dry PbCl_2 crystals are rinsed in 4N HCl three times. Most of the impurities are readily dissolved in 4N HCl, but PbCl_2 is least soluble at this normality. Cleaned lead chloride crystals are dried by returning the beaker to the hotplate for a few minutes. A solution containing 1 ug Pb per 2 ul aqueous solution is prepared by adding a calculated amount of quartz distilled water allowing for the loss of 30% of the sample due to non-dissolution of some of the galena and loss of lead chloride during rinsing.

B.2 PREPARATION AND LOADING OF FILAMENTS

Pre-cleaned rhenium ribbon 1.5 cm long is spot-welded to single filament posts. A micropipette with disposable tips is used to load 2 ul of sample onto each filament, using a new tip for each sample. Samples are dried at 1 Amp. 4 ul of silica gel-phosphoric acid solution is loaded on top of the dry sample. This is left to dry at 1.1 Amp, then the current is gradually increased until the load dissolves and reprecipitates. When recrystallization is complete, the current is slowly increased until white smoke is given off and the load turns white. The current can then be turned up to 2 Amps or higher to allow the load to glow gently for a few seconds, then off.

B.3 MASS SPECTROMETRIC PROCEDURES

All the reported analyses were done by Francoise Goutier in the Geochronology Laboratory at the University of British Columbia using a VG Isotopes Isomass 54R mass spectrometer linked to a HP-85 microcomputer.

Samples were loaded into the mass spectrometer, six at a time, and heated to 11500-12500. The isotopic composition is measured using 'UBCGPB' programs. Due to the uncertainty in measuring ^{204}Pb peak, this program measured the $^{204}\text{Pb}/^{207}\text{Pb}$ ratio twice as often as the other two ratios, improving the statistics on the ratio.

Raw data is converted to the $^{206}\text{Pb}/^{204}\text{Pb}$, $^{207}\text{Pb}/^{204}\text{Pb}$ and $^{208}\text{Pb}/^{204}\text{Pb}$ ratios, then normalized to absolute values using correction factors determined by repeated analyses of the Broken Hill Standard (Table 3.1). Each analysis is reported with an associated error based on a combination of the fractionation variation between runs, the uncertainty in mass fractionation factors, and within-run precision.

References: Andrew, A. Ph.D Thesis in preparation, University of British Columbia.

APPENDIX C

Adams Plateau: Lead Isotope Data

Sample No	Deposit/Sample Name	Mt	Anl	Qual	Pb6/4	%6/4	Pb7/4	%7/4	Pb8/4	%8/4	Pb6/7	%6/7	Pb6/8	%6/8
30504-001	ENARGITE	GL	FG	GOOD	19.101	0.01	15.692	0.01	38.993	0.02	1.21720	0.01	0.489849	0.01
30504-00102	ENARGITE	GL	FG	GOOD	19.090	0.03	15.688	0.03	38.981	0.03	1.21687	0.00	0.489732	0.00
30504-AVG	ENARGITE N=2	GL	FG	GOOD	19.096	0.02	15.690	0.02	38.987	0.05	1.21704	0.01	0.489791	0.01
30504/00101	ENARGITE	GL	FG	FAIR	19.079	0.06	15.664	0.04	38.875	0.07	1.21799	0.04	0.490772	0.04
30505-002	FOGHORN (SAMPLE 011)	GL	FG	GOOD	19.190	0.03	15.708	0.03	39.140	0.04	1.22164	0.01	0.490291	0.02
30505-00201	FOGHORN (SAMPLE 011)	GL	FG	GOOD	19.202	0.03	15.693	0.03	39.077	0.03	1.22356	0.01	0.491389	0.01
30505-003	FOGHORN (VEIN 007)	GL	FG	GOOD	19.225	0.04	15.713	0.03	39.146	0.05	1.22355	0.03	0.491108	0.03
30505-00301	FOGHORN (VEIN 007)	GL	FG	FAIR	19.213	0.12	15.728	0.12	39.189	0.12	1.22156	0.01	0.490262	0.01
30505-AVG2	FOGHORN N=2 (SAMPLE 011)	GL	FG	GOOD	19.196	0.03	15.701	0.03	39.109	0.03	1.22260	0.01	0.490840	0.02
30505-AVG3	FOGHORN N=2 (VEIN 007)	GL	FG	GO/FR	19.219	0.08	15.721	0.08	39.168	0.08	1.22260	0.02	0.490685	0.02
30505-AVG	FOGHORN N=4	GL	FG	GO/FR	19.208	0.05	15.711	0.05	39.138	0.06	1.22258	0.02	0.490763	0.02
30505/001	FOGHORN (SAMPLE 007)	GL	FG	POOR	18.915	0.41	15.516	0.41	38.537	0.42	1.21908	0.07	0.490829	0.08
30505/00101	FOGHORN (SAMPLE 007)	GL	FG	FAIR	19.073	0.21	15.680	0.20	38.959	0.21	1.21643	0.05	0.489572	0.04
30506-001	AGATE BAY	GL	FG	GOOD	19.148	0.02	15.703	0.02	38.927	0.04	1.21938	0.01	0.491889	0.04
30506-00101	AGATE BAY	GL	FG	FAIR	19.148	0.05	15.705	0.02	38.916	0.10	1.21916	0.05	0.492018	0.08
30506-00102	AGATE BAY	GL	FG	FAIR	19.134	0.05	15.695	0.05	38.885	0.05	1.21912	0.01	0.492084	0.01
30506-AVG	AGATE BAY N=3	GL	FG	FAIR	19.143	0.04	15.701	0.03	38.909	0.06	1.21922	0.02	0.491997	0.04
30506/00103	AGATE BAY	GL	FG	FAIR	19.033	0.06	15.633	0.06	38.681	0.06	1.21749	0.02	0.492044	0.02
30507-001	BECA (TOM)	GL	FG	GOOD	19.334	0.02	15.668	0.02	38.979	0.02	1.23393	0.01	0.496001	0.01
30507-00101	BECA (TOM)	GL	FG	GOOD	19.344	0.02	15.687	0.01	39.042	0.02	1.23317	0.01	0.495474	0.01
30507-00102	BECA (TOM)	GL	FG	FAIR	19.339	0.01	15.684	0.01	39.026	0.01	1.23300	0.01	0.495531	0.00
30507-AVG	BECA N=3	GL	FG	GO/FR	19.339	0.02	15.680	0.02	39.016	0.02	1.23338	0.01	0.495669	0.01
30507/00103	BECA (TOM)	GL	FG	POOR	19.322	0.03	15.703	0.03	39.056	0.03	1.23049	0.01	0.494725	0.02
30508-001	BIRK CREEK (SECTION X DUMP)	GL	FG	GOOD	18.948	0.02	15.718	0.02	38.861	0.03	1.20548	0.01	0.487575	0.01
30508-00101	BIRK CREEK (SECTION X DUMP)	GL	FG	FAIR	18.947	0.08	15.741	0.08	38.856	0.08	1.20368	0.01	0.487617	0.01
30508-002	BIRK CREEK (SECTION X)	GL	FG	GOOD	18.904	0.03	15.710	0.01	38.791	0.03	1.20328	0.03	0.487321	0.01
30508-00201	BIRK CREEK (SECTION X)	GL	FG	GOOD	18.882	0.03	15.699	0.03	38.751	0.03	1.20275	0.01	0.487256	0.01
30508-00301	BIRK CREEK (SECTION 012)	GL	FG	POOR	19.026	0.39	15.798	0.39	39.027	0.39	1.20433	0.01	0.487514	0.02
30508-004	BIRK CREEK (VEIN SECT. 012)	GL	FG	GOOD	18.896	0.02	15.705	0.01	38.755	0.02	1.20319	0.02	0.487565	0.01
30508-00401	BIRK CREEK (VEIN SECT. 012)	GL	FG	POOR	18.949	0.14	15.741	0.05	38.987	0.16	1.20384	0.13	0.486037	0.07
30508-005	BIRK CREEK (NEAR BRIDGE)	GL	FG	GOOD	18.893	0.01	15.721	0.01	38.829	0.01	1.20174	0.01	0.486577	0.00
30508-506	BIRK CREEK (G798A-001)	GL	BR	FAIR	18.878	0.06	15.708	0.13	38.893	0.18	1.20182	0.00	0.486224	0.00
30508-50601	BIRK CREEK (G798A-002)	GL	BR	FAIR	18.869	0.08	15.722	0.16	38.834	0.18	1.20018	0.00	0.486737	0.00
30508-AVG1	BIRK CREEK N=2 (SECT. DUMP)	GL	FG	GO/FR	18.948	0.05	15.730	0.05	38.859	0.05	1.20458	0.01	0.487448	0.01
30508-AVG2	BIRK CREEK N=2 (SECT. X)	GL	FG	GOOD	18.893	0.03	15.705	0.02	38.771	0.03	1.20302	0.02	0.487289	0.01
30508-AVG4	BIRK CREEK N=2 (SECT. X)	GL	FG	GO/PR	18.923	0.08	15.723	0.03	38.871	0.09	1.20352	0.08	0.486801	0.04
30508-AVG6	BIRK CREEK (G798A-AVG)	GL	BR	FAIR	18.874	0.07	15.715	0.08	38.863	0.18	1.20100	0.00	0.486477	0.00
30508-AVG	BIRK CREEK N=10	GL	G/R	GO/FR	18.907	0.06	15.716	0.05	38.848	0.09	1.20304	0.05	0.486692	0.05
30508/003	BIRK CREEK (SECTION 012)	GL	FG	FAIR	18.901	0.02	15.691	0.01	38.744	0.02	1.20454	0.01	0.487849	0.01
30509-501	BROKEN RIDGE (G798N-001)	GL	BR	FAIR	19.249	0.06	15.697	0.11	39.253	0.13	1.22630	0.00	0.491221	0.00
30511-001	HOMESTAKE	GL	FG	FAIR	18.776	0.05	15.696	0.05	38.574	0.05	1.19619	0.01	0.486742	0.01
30511-002	HOMESTAKE	GL	FG	FAIR	18.887	0.05	15.693	0.05	38.681	0.06	1.20350	0.00	0.488279	0.02
30511-00201	HOMESTAKE	GL	FG	GOOD	18.900	0.04	15.705	0.02	38.717	0.05	1.20341	0.04	0.488150	0.01
30511-502	HOMESTAKE (KAMAD 70)	GL	GSC	FAIR	18.827	0.00	15.719	0.00	38.621	0.00	1.19773	0.00	0.488325	0.00
30511-501	HOMESTAKE (361-G798Q-001)	GL	GSC	FAIR	18.878	0.08	15.687	0.17	38.533	0.18	1.20343	0.12	0.490766	0.12
30511-AVG2	HOMESTAKE N=2	GL	FG	FAIR	18.894	0.05	15.699	0.03	38.699	0.06	1.20346	0.02	0.488215	0.01
30511-AVG	HOMESTAKE N=5	GL		FR/GO	18.854	0.06	15.700	0.10	38.626	0.12	1.20085	0.07	0.488452	0.07
30511/00101	HOMESTAKE	GL	FG	POOR	18.869	0.19	15.770	0.19	38.779	0.19	1.19652	0.04	0.486569	0.02
30513-001	FORTUNA	GL	FG	GOOD	19.118	0.02	15.716	0.01	39.000	0.02	1.21643	0.01	0.490196	0.01
30513-00101	FORTUNA	GL	FG	GOOD	19.132	0.02	15.726	0.02	39.035	0.02	1.21657	0.01	0.490128	0.01
30513-AVG	FORTUNA N=2	GL	FG	GOOD	19.125	0.02	15.721	0.02	39.018	0.02	1.21650	0.01	0.490162	0.01
30515-001	REA GOLD (MASS. SULPH. HORZ.)	GL	FG	FAIR	18.859	0.04	15.709	0.04	38.766	0.05	1.20052	0.02	0.486467	0.02
30515-002	REA GOLD (VEIN)	GL	FG	GOOD	18.852	0.01	15.680	0.01	38.687	0.02	1.20228	0.01	0.487299	0.02

Adams Plateau: Lead Isotope Data

Sample No	Deposit/Sample Name	Mt	Anl	Qual	Pb6/4	%6/4	Pb7/4	%7/4	Pb8/4	%8/4	Pb6/7	%6/7	Pb6/8	%6/8
30515-00201	REA GOLD (VEIN)	GL	FG	GOOD	18.862	0.02	15.688	0.01	38.742	0.03	1.20232	0.02	0.486872	0.03
30515-003	REA GOLD (BARITE HORZ.)	GL	FG	GOOD	18.893	0.03	15.706	0.03	38.823	0.03	1.20292	0.01	0.486640	0.01
30515-AVG2	REA GOLD N=2 (VEIN)	GL	FG	GOOD	18.857	0.02	15.684	0.01	38.715	0.02	1.20232	0.02	0.487086	0.03
30515-AVG	REA GOLD N=3	GL	FG	GOOD	18.869	0.03	15.699	0.03	38.755	0.03	1.20192	0.03	0.486879	0.03
30515/00101	REA GOLD (MASS. SULPH. HORZ.)	GL	FG	POOR	18.804	0.24	15.661	0.24	38.904	0.24	1.20066	0.03	0.483341	0.01
30515/00301	REA GOLD (BARITE HORZ.)	GL	FG	POOR	18.776	0.50	15.702	0.50	38.708	0.50	1.19577	0.04	0.485070	0.05
30516-101	REXSPAR (G79SA-001)	GL	BR	FAIR	19.177	0.10	15.911	0.20	38.986	0.20	1.20528	0.00	0.492734	0.00
30517-001	ART	GL	FG	FAIR	19.079	0.10	15.750	0.08	39.185	0.11	1.21132	0.06	0.486886	0.04
30517-00101	ART	GL	FG	GOOD	19.040	0.01	15.724	0.01	39.109	0.01	1.21088	0.01	0.486848	0.00
30517-AVG	ART N=2	GL	FG	GD/FR	19.060	0.05	15.737	0.04	39.147	0.06	1.21110	0.03	0.486867	0.02
30518-001	LUCKY COON	GL	FG	FAIR	19.123	0.04	15.688	0.01	38.847	0.05	1.21897	0.04	0.492258	0.03
30518-00101	LUCKY COON	GL	FG	GOOD	19.140	0.01	15.699	0.01	38.896	0.03	1.21924	0.00	0.492096	0.02
30518-002	LUCKY COON (PIT 1)	GL	FG	FAIR	19.163	0.10	15.696	0.01	38.958	0.10	1.22084	0.10	0.491874	0.03
30518-AVG1	LUCKY COON N=2	GL	FG	GD/FR	19.132	0.03	15.694	0.01	38.872	0.04	1.21911	0.04	0.492177	0.03
30518-AVG	LUCKY COON N=3	GL	FG	GD/FR	19.142	0.07	15.694	0.01	38.900	0.07	1.21968	0.06	0.492076	0.03
30519-001	TWIN MOUNTAIN (FALCB.SAMPLE)	GL	FG	FAIR	19.013	0.05	15.704	0.02	38.837	0.06	1.21066	0.04	0.489554	0.02
30519-00101	TWIN MOUNTAIN (FALCB.SAMPLE)	GL	FG	FAIR	19.012	0.04	15.691	0.04	38.813	0.05	1.21166	0.01	0.489843	0.01
30519-501	TWIN MOUNTAIN (G79TM-001)	GL	BR	FAIR	19.057	0.07	15.716	0.18	38.846	0.05	1.21260	0.00	0.491415	0.00
30519-AVG1	TWIN MOUNTAIN (FALCB.SAMPLE)	GL	FG	FAIR	19.013	0.05	15.698	0.03	38.825	0.06	1.21116	0.03	0.489699	0.02
30519-AVG	TWIN MOUNTAIN N=2	GL	FAIR	19.035	0.06	15.707	0.10	38.836	0.06	1.21188	0.03	0.490557	0.02	
30521-001	JUNE KAJUN	GL	FG	GOOD	19.472	0.02	15.724	0.02	39.525	0.02	1.23837	0.01	0.492647	0.01
30521-00101	JUNE KAJUN	GL	FG	FAIR	19.469	0.05	15.725	0.02	39.513	0.05	1.23809	0.04	0.492718	0.03
30521-00102	JUNE KAJUN	GL	FG	FAIR	19.442	0.07	15.707	0.07	39.473	0.07	1.23782	0.01	0.492534	0.01
30521-AVG	JUNE KAJUN N=3	GL	FG	FR/GD	19.461	0.05	15.719	0.04	39.504	0.05	1.23809	0.02	0.492633	0.01
30521/101	JUNE KAJUN (G79JU-001)	GL	BR	FAIR	19.441	0.04	15.676	0.14	39.396	0.00	1.24019	0.00	0.494320	0.00
30522-001	9C (ZN 1)	GL	FG	FAIR	18.294	0.01	15.552	0.01	38.309	0.01	1.17631	0.00	0.477523	0.01
30522-00103	9C (ZN 1)	GL	FG	FAIR	18.282	0.06	15.554	0.06	38.337	0.07	1.17539	0.02	0.476889	0.03
30522-AVG	9C (ZN 1)N=2	GL	FG	FAIR	18.288	0.03	15.553	0.03	38.331	0.04	1.17585	0.01	0.477206	0.02
30522/00101	9C (ZN 1)	GL	FG	FAIR	18.403	0.02	15.578	0.02	38.412	0.03	1.18137	0.00	0.479100	0.01
30522/00102	9C (ZN 1)	GL	FG	POOR	18.245	0.30	15.516	0.30	38.243	0.30	1.17594	0.02	0.477093	0.02
30523-501	KING TUT (G79LU-001)	GL	BR	FAIR	19.095	0.08	15.688	0.18	38.835	0.16	1.21718	0.00	0.492547	0.00
30524-501	ELSIE (G79LU-002)	GL	BR	FAIR	19.142	0.08	15.700	0.18	38.975	0.09	1.21925	0.00	0.491974	0.00
30525-001	MOSQUITO KING	GL	FG	GOOD	19.075	0.01	15.692	0.01	38.835	0.02	1.21552	0.02	0.491163	0.01
30525-002	MOSQUITO KING (VEIN)	GL	FG	GOOD	19.071	0.02	15.692	0.02	38.827	0.03	1.21532	0.01	0.491186	0.02
30525-00201	MOSQUITO KING (VEIN)	GL	FG	GOOD	19.124	0.02	15.694	0.02	38.877	0.03	1.21854	0.02	0.491907	0.01
30525-AVG2	MOSQUITO KING N=2 (VEIN)	GL	FG	GOOD	19.098	0.02	15.693	0.02	38.852	0.03	1.21693	0.02	0.491547	0.02
30525-AVG	MOSQUITO KING N=2	GL	FG	GOOD	19.090	0.02	15.693	0.02	38.846	0.03	1.21648	0.02	0.491419	0.02
30526-501	PET (G79PE-001)	GL	BR	FAIR	19.126	0.06	15.732	0.15	38.980	0.11	1.21575	0.00	0.491512	0.00
30527-001	SPAR	GL	FG	GOOD	19.133	0.01	15.692	0.01	38.902	0.06	1.21928	0.01	0.491821	0.06
30527-00101	SPAR	GL	FG	GOOD	19.126	0.04	15.687	0.04	38.859	0.04	1.21926	0.01	0.492191	0.01
30527-002	SPAR (FLUORINE SHOWING)	GL	FG	POOR	19.150	0.28	15.671	0.28	38.864	0.28	1.22197	0.05	0.492745	0.03
30527-AVG1	SPAR N=2	GL	FG	GOOD	19.130	0.03	15.690	0.03	38.881	0.05	1.21927	0.01	0.492006	0.03
30528-001	WHITE ROCK	GL	FG	GOOD	19.151	0.04	15.722	0.04	39.048	0.04	1.21810	0.01	0.490461	0.01
30528/00101	WHITE ROCK	GL	FG	POOR	19.227	0.64	15.801	0.62	39.198	0.65	1.21684	0.14	0.490511	0.15
30531-001	RED TOP	GL	FG	FAIR	19.142	0.05	15.719	0.02	38.938	0.06	1.21781	0.04	0.491608	0.04
30531-002	RED TOP (TRENCH)	GL	FG	GOOD	19.159	0.09	15.737	0.09	38.974	0.10	1.21748	0.01	0.491598	0.04
30531-00201	RED TOP (TRENCH)	GL	FG	FAIR	19.136	0.07	15.710	0.00	38.905	0.07	1.21808	0.01	0.491880	0.01
30531-AVG2	RED TOP N=2 (TRENCH)	GL	FG	GD/FR	19.148	0.08	15.724	0.04	38.940	0.08	1.21778	0.01	0.491739	0.03
30531-AVG	RED TOP N=2	GL	FG	GD/FR	19.146	0.06	15.721	0.04	38.939	0.07	1.21779	0.03	0.491695	0.03
30532-001	FLUKE	GL	FG	GOOD	19.219	0.02	15.702	0.02	39.366	0.06	1.22398	0.01	0.488203	0.06
30532-00101	FLUKE	GL	FG	GOOD	19.227	0.05	15.704	0.05	39.356	0.05	1.22433	0.01	0.488550	0.02
30532-AVG	FLUKE N=2	GL	FG	GOOD	19.223	0.03	15.703	0.03	39.361	0.05	1.22416	0.01	0.488377	0.04
30533-001	ORELL 1D (RED MINERAL)	GL	FG	GOOD	19.362	0.02	15.715	0.02	39.401	0.04	1.23213	0.01	0.491419	0.04

Adams Plateau: Lead Isotope Data

Sample No	Deposit/Sample Name	Mt	Anal	Qual	Pb6/4	%6/4	Pb7/4	%7/4	Pb8/4	%8/4	Pb6/7	%6/7	Pb6/8	%6/8
30533-00101	ORELL 1D (RED MINERAL)	GL	FG	FAIR	19.327	0.07	15.682	0.07	39.318	0.07	1.23245	0.01	0.491567	0.01
30533-002	ORELL 1E (RED MINERAL)	GL	FG	GOOD	19.355	0.02	15.705	0.02	39.377	0.03	1.23237	0.01	0.491516	0.02
30533-AVG	ORELL 1D N=3 (RED MINERAL)	GL	FG	GD/FR	19.345	0.04	15.699	0.04	39.360	0.05	1.23229	0.01	0.491493	0.02
30534-001	ORELL 2G (RED MINERAL)	GL	FG	GOOD	19.121	0.02	15.705	0.02	39.044	0.03	1.21749	0.01	0.489721	0.01
30534-00101	ORELL 2G (RED MINERAL)	GL	FG	GOOD	19.140	0.03	15.722	0.02	39.093	0.04	1.21744	0.02	0.489604	0.03
30534-AVG	ORELL 2G N=2 (RED MINERAL)	GL	FG	GOOD	19.131	0.03	15.714	0.02	39.069	0.04	1.21747	0.02	0.489663	0.02
30535-001	ORELL 3K (RED MINERAL)	GL	FG	FAIR	19.354	0.05	15.706	0.03	39.383	0.05	1.23228	0.04	0.491420	0.02
30536-001	ORELL 4N (SILVER KING, A)	GL	FG	GOOD	19.081	0.04	15.708	0.04	38.899	0.04	1.21471	0.01	0.490516	0.01
30537-001	ORELL 5P	GL	FG	GOOD	19.128	0.01	15.689	0.01	38.879	0.01	1.21923	0.01	0.491982	0.00
30537-00101	ORELL 5P	GL	FG	FAIR	19.128	0.05	15.694	0.05	38.891	0.05	1.21881	0.02	0.491834	0.02
30537-AVG	ORELL 5P N=2	GL	FG	GD/FR	19.128	0.03	15.692	0.03	38.885	0.03	1.21902	0.02	0.491908	0.01
30538-001	UTAH PROSPECT (FORD)	GL	FG	GOOD	18.893	0.02	15.704	0.02	38.699	0.02	1.20308	0.00	0.488201	0.01
30538-00101	UTAH PROSPECT (FORD)	GL	FG	GOOD	18.864	0.07	15.702	0.07	38.696	0.08	1.20267	0.01	0.488007	0.03
30538-00102	UTAH PROSPECT (FORD)	GL	FG	GOOD	18.875	0.01	15.691	0.01	38.659	0.02	1.20287	0.01	0.488240	0.01
30538-00103	UTAH PROSPECT (FORD)	GL	FG	GOOD	18.880	0.03	15.695	0.03	38.651	0.05	1.20292	0.01	0.488468	0.05
30538-AVG	UTAH PROSPECT N=4	GL	FG	GOOD	18.863	0.03	15.698	0.03	38.676	0.04	1.20289	0.01	0.488229	0.03
30539-001	MT McLENNAN (X-CUTTING VEIN)	GL	FG	FAIR	19.249	0.05	15.680	0.05	38.932	0.06	1.22757	0.02	0.494426	0.03
30539-002	MT McLENNAN	GL	FG	FAIR	19.288	0.04	15.715	0.04	39.001	0.06	1.22736	0.01	0.494536	0.05
30539-AVG	MT McLENNAN N=2	GL	FG	FAIR	19.269	0.05	15.698	0.05	38.967	0.06	1.22747	0.02	0.494481	0.04
30540-501	BIRCH ISLAND (HL P45 KQ78-36)	GL	GSC	FAIR	19.335	0.00	15.820	0.00	39.235	0.00	1.22200	0.00	0.493642	0.00
30541-001	SUNRISE	GL	FG	FAIR	19.086	0.07	15.681	0.07	38.806	0.08	1.21715	0.03	0.491827	0.03
30541-002	SUNRISE	GL	FG	GOOD	19.123	0.03	15.711	0.01	38.892	0.04	1.21717	0.03	0.491691	0.02
30541-AVG	SUNRISE N=2	GL	FG	FR/GD	19.105	0.05	15.696	0.04	38.849	0.06	1.21716	0.03	0.491759	0.03
30542-001	VAVENBY	GL	FG	GOOD	19.127	0.03	15.703	0.03	38.889	0.03	1.21804	0.01	0.491833	0.01
30542-00101	VAVENBY	GL	FG	FAIR	19.055	0.14	15.703	0.13	38.802	0.16	1.21344	0.05	0.491074	0.08
30542-AVG	VAVENBY N=2	GL	FG	GD/FR	19.091	0.08	15.703	0.08	38.846	0.09	1.21574	0.03	0.491454	0.05
30543-001	TINDALL (ADIT DUMP)	GL	FG	GOOD	19.251	0.02	15.714	0.02	39.080	0.05	1.22509	0.01	0.492605	0.02
30544-001	SONJA	GL	FG	FAIR	19.356	0.06	15.691	0.06	39.251	0.06	1.23353	0.00	0.493132	0.01
30545-001	SILVER KING-SILVER QUEEN	GL	FG	GOOD	19.098	0.07	15.681	0.05	38.977	0.08	1.21788	0.05	0.489971	0.02
30545-00101	SILVER KING-SILVER QUEEN	GL	FG	FAIR	19.110	0.06	15.685	0.06	38.979	0.06	1.21826	0.01	0.490261	0.02
30545-AVG	SILVER KING-SILVER QUEEN N=2	GL	FG	GD/FR	19.104	0.07	15.684	0.06	38.978	0.07	1.21807	0.03	0.490116	0.02
30546-001	LEEMAC	GL	FG	FAIR	19.406	0.04	15.741	0.04	39.375	0.04	1.23287	0.02	0.492849	0.01
30546-00101	LEEMAC	GL	FG	GOOD	19.375	0.03	15.717	0.03	39.297	0.04	1.23271	0.01	0.493036	0.01
30546-AVG	LEEMAC N=2	GL	FG	FR/GD	19.391	0.04	15.729	0.04	39.336	0.04	1.23279	0.02	0.492943	0.01
30547-001	ROUGE	GL	FG	GOOD	19.267	0.01	15.750	0.00	39.172	0.03	1.22329	0.01	0.491845	0.03
30547-00101	ROUGE	GL	FG	GOOD	19.253	0.00	15.738	0.00	39.139	0.00	1.22331	0.00	0.491910	0.00
30547-AVG	ROUGE N=2	GL	FG	GOOD	19.260	0.01	15.744	0.00	39.156	0.02	1.22330	0.01	0.491878	0.02
30548-001	PS-85-175	GL	FG	GOOD	19.180	0.00	15.725	0.00	38.696	0.00	1.21977	0.00	0.492194	0.00
30548-0101	PS-85-175	GL	FG	GOOD	19.174	0.00	15.717	0.00	38.955	0.00	1.21997	0.00	0.492212	0.00
30548-AVG	PS-85-175 N=2	GL	FG	GOOD	19.177	0.00	15.721	0.00	38.962	0.00	1.21987	0.00	0.492203	0.00